

25.2 Using the higher-order terms in the series (25.3.23), show that the input impedance $Z_{\text{in}} = R + jX$ of a small dipole is given as follows to order $(kl)^4$, where $L = \ln(2a/l)$:

$$R = \frac{\eta}{2\pi} \left[\frac{1}{12} (kl)^2 + \frac{1}{360} (kl)^4 \right], \quad X = \frac{\eta}{2\pi} \left[\frac{4(1+L)}{kl} - \frac{1}{3} \left(L + \frac{2}{3} \right) (kl) - \frac{1}{180} \left(L - \frac{11}{30} \right) (kl)^3 \right]$$

25.3 Consider a small dipole with a linear current given by Eq. (25.3.25). Determine the radiation vector, and the radiated electric and magnetic fields at a far distance r from the dipole. Calculate the radiated power P_{rad} by integrating the radial Poynting vector over a large sphere. Then identify the radiation resistance R through the definition:

$$P_{\text{rad}} = \frac{1}{2} R |I_0|^2$$

and show R is the same as that given by Eq. (25.3.24)

A. Physical Constants

We use SI units throughout this text. Simple ways to convert between SI and other popular units, such as Gaussian, may be found in Refs. [123–126].

The Committee on Data for Science and Technology (CODATA) of NIST maintains the values of many physical constants [112]. The most current values can be obtained from the CODATA web site [1823]. Some commonly used constants are listed below:

quantity	symbol	value	units
speed of light in vacuum	c_0, c	299 792 458	m s^{-1}
permittivity of vacuum	ϵ_0	$8.854 187 817 \times 10^{-12}$	F m^{-1}
permeability of vacuum	μ_0	$4\pi \times 10^{-7}$	H m^{-1}
characteristic impedance	η_0, Z_0	376.730 313 461	Ω
electron charge	e	$1.602 176 462 \times 10^{-19}$	C
electron mass	m_e	$9.109 381 887 \times 10^{-31}$	kg
Boltzmann constant	k	$1.380 650 324 \times 10^{-23}$	JK^{-1}
Avogadro constant	N_A, L	$6.022 141 994 \times 10^{23}$	mol^{-1}
Planck constant	h	$6.626 068 76 \times 10^{-34}$	J/Hz
Gravitational constant	G	$6.672 59 \times 10^{-11}$	$\text{m}^3 \text{kg}^{-1} \text{s}^{-2}$
Earth mass	M_\oplus	5.972×10^{24}	kg
Earth equatorial radius	a_e	6378	km

In the table, the constants c, μ_0 are taken to be exact, whereas ϵ_0, η_0 are derived from the relationships:

$$\epsilon_0 = \frac{1}{\mu_0 c^2}, \quad \eta_0 = \sqrt{\frac{\mu_0}{\epsilon_0}} = \mu_0 c$$

The energy unit of electron volt (eV) is defined to be the work done by an electron in moving across a voltage of one volt, that is, $1 \text{ eV} = 1.602 176 462 \times 10^{-19} \text{ C} \cdot 1 \text{ V}$, or

$$1 \text{ eV} = 1.602 176 462 \times 10^{-19} \text{ J}$$

In units of eV/Hz, Planck's constant h is:

$$h = 4.135\,667\,27 \times 10^{-15} \text{ eV/Hz} = 1 \text{ eV}/241.8 \text{ THz}$$

that is, 1 eV corresponds to a frequency of 241.8 THz, or a wavelength of 1.24 μm .

B. Electromagnetic Frequency Bands

The ITU[†] divides the radio frequency (RF) spectrum into the following frequency and wavelength bands in the range from 30 Hz to 3000 GHz:

RF Spectrum				
band designations		frequency	wavelength	
ELF	Extremely Low Frequency	30-300 Hz	1-10	Mm
VF	Voice Frequency	300-3000 Hz	100-1000	km
VLF	Very Low Frequency	3-30 kHz	10-100	km
LF	Low Frequency	30-300 kHz	1-10	km
MF	Medium Frequency	300-3000 kHz	100-1000	m
HF	High Frequency	3-30 MHz	10-100	m
VHF	Very High Frequency	30-300 MHz	1-10	m
UHF	Ultra High Frequency	300-3000 MHz	10-100	cm
SHF	Super High Frequency	3-30 GHz	1-10	cm
EHF	Extremely High Frequency	30-300 GHz	1-10	mm
	Submillimeter	300-3000 GHz	100-1000	μm

An alternative subdivision of the low-frequency bands is to designate the bands 3-30 Hz, 30-300 Hz, and 300-3000 Hz as extremely low frequency (ELF), super low frequency (SLF), and ultra low frequency (ULF), respectively.

Microwaves span the 300 MHz-300 GHz frequency range. Typical microwave and satellite communication systems and radar use the 1-30 GHz band. The 30-300 GHz EHF band is also referred to as the millimeter band.

The 1-100 GHz range is subdivided further into the subbands shown on the right.

Microwave Bands		
band	frequency	
L	1-2	GHz
S	2-4	GHz
C	4-8	GHz
X	8-12	GHz
Ku	12-18	GHz
K	18-27	GHz
Ka	27-40	GHz
V	40-75	GHz
W	80-100	GHz

Some typical RF applications are as follows. AM radio is broadcast at 535-1700 kHz falling within the MF band. The HF band is used in short-wave radio, navigation, amateur, and CB bands. FM radio at 88-108 MHz, ordinary TV, police, walkie-talkies, and remote control occupy the VHF band.

Cell phones, personal communication systems (PCS), pagers, cordless phones, global positioning systems (GPS), RF identification systems (RFID), UHF-TV channels, microwave ovens, and long-range surveillance radar fall within the UHF band.

[†]International Telecommunication Union.

The SHF microwave band is used in radar (traffic control, surveillance, tracking, missile guidance, mapping, weather), satellite communications, direct-broadcast satellite (DBS), and microwave relay systems. Multipoint multichannel (MMDS) and local multipoint (LMDS) distribution services, fall within UHF and SHF at 2.5 GHz and 30 GHz.

Industrial, scientific, and medical (ISM) bands are within the UHF and low SHF, at 900 MHz, 2.4 GHz, and 5.8 GHz. Radio astronomy occupies several bands, from UHF to L-W microwave bands.

Beyond RF, come the infrared (IR), visible, ultraviolet (UV), X-ray, and γ -ray bands. The IR range extends over 3-300 THz, or 1-100 μm . Many IR applications fall in the 1-20 μm band. For example, optical fiber communications typically use laser light at 1.55 μm or 193 THz because of the low fiber losses at that frequency. The UV range lies beyond the visible band, extending typically over 10-400 nm.

band	wavelength	frequency	energy
infrared	100-1 μm	3-300 THz	
ultraviolet	400-10 nm	750 THz-30 PHz	
X-Ray	10 nm-100 pm	30 PHz-3 EHz	0.124-124 keV
γ -ray	< 100 pm	> 3 EHz	> 124 keV

The CIE[†] defines the visible spectrum to be the wavelength range 380-780 nm, or 385-789 THz. Colors fall within the following typical wavelength/frequency ranges:

Visible Spectrum		
color	wavelength	frequency
red	780-620 nm	385-484 THz
orange	620-600 nm	484-500 THz
yellow	600-580 nm	500-517 THz
green	580-490 nm	517-612 THz
blue	490-450 nm	612-667 THz
violet	450-380 nm	667-789 THz

X-ray frequencies fall in the PHz (petahertz) range and γ -ray frequencies in the EHz (exahertz) range.[‡] X-rays and γ -rays are best described in terms of their energy, which is related to frequency through Planck's relationship, $E = hf$. X-rays have typical energies of the order of keV, and γ -rays, of the order of MeV and beyond. By comparison, photons in the visible spectrum have energies of a couple of eV.

The earth's atmosphere is mostly opaque to electromagnetic radiation, except for three significant "windows", the visible, the infrared, and the radio windows. These three bands span the wavelength ranges of 380-780 nm, 1-12 μm , and 5 mm-20 m, respectively.

Within the 1-10 μm infrared band there are some narrow transparent windows. For the rest of the IR range (1-1000 μm), water and carbon dioxide molecules absorb infrared radiation—this is responsible for the Greenhouse effect. There are also some minor transparent windows for 17-40 and 330-370 μm .

[†]Commission Internationale de l'Eclairage (International Commission on Illumination.)

[‡]1 THz = 10^{12} Hz, 1 PHz = 10^{15} Hz (petahertz), 1 EHz = 10^{18} Hz (exahertz).

Beyond the visible band, ultraviolet and X-ray radiation are absorbed by ozone and molecular oxygen (except for the ozone holes.)

C. Vector Identities and Integral Theorems

Algebraic Identities

$$|A|^2|B|^2 = |A \cdot B|^2 + |A \times B|^2 \quad (C.1)$$

$$(A \times B) \cdot C = (B \times C) \cdot A = (C \times A) \cdot B \quad (C.2)$$

$$A \times (B \times C) = B(A \cdot C) - C(A \cdot B) \quad (\text{BAC-CAB rule}) \quad (C.3)$$

$$(A \times B) \cdot (C \times D) = (A \cdot C)(B \cdot D) - (A \cdot D)(B \cdot C) \quad (C.4)$$

$$(A \times B) \times (C \times D) = [(A \times B) \cdot D]C - [(A \times B) \cdot C]D \quad (C.5)$$

$$A = \hat{n} \times (A \times \hat{n}) + (\hat{n} \cdot A)\hat{n} = A_{\perp} + A_{\parallel} \quad (C.6)$$

where \hat{n} is any unit vector, and A_{\perp} , A_{\parallel} are the components of A perpendicular and parallel to \hat{n} . Note also that $\hat{n} \times (A \times \hat{n}) = (\hat{n} \times A) \times \hat{n}$. A three-dimensional vector can equally well be represented as a column vector:

$$\mathbf{a} = a_x \hat{x} + a_y \hat{y} + a_z \hat{z} \quad \Leftrightarrow \quad \mathbf{a} = \begin{bmatrix} a_x \\ a_y \\ a_z \end{bmatrix} \quad (C.7)$$

Consequently, the dot and cross products may be represented in matrix form:

$$\mathbf{a} \cdot \mathbf{b} \quad \Leftrightarrow \quad \mathbf{a}^T \mathbf{b} = [a_x, a_y, a_z] \begin{bmatrix} b_x \\ b_y \\ b_z \end{bmatrix} = a_x b_x + a_y b_y + a_z b_z \quad (C.8)$$

$$\mathbf{a} \times \mathbf{b} \quad \Leftrightarrow \quad \mathbf{A} \mathbf{b} = \begin{bmatrix} 0 & -a_z & a_y \\ a_z & 0 & -a_x \\ -a_y & a_x & 0 \end{bmatrix} \begin{bmatrix} b_x \\ b_y \\ b_z \end{bmatrix} = \begin{bmatrix} a_y b_z - a_z b_y \\ a_z b_x - a_x b_z \\ a_x b_y - a_y b_x \end{bmatrix} \quad (C.9)$$

The cross-product matrix A satisfies the following identity:

$$A^2 = \mathbf{a} \mathbf{a}^T - (\mathbf{a}^T \mathbf{a}) I \quad (C.10)$$

where I is the 3×3 identity matrix. Applied to a unit vector \hat{n} , this identity reads:

$$I = \hat{n} \hat{n}^T - \hat{N}^2, \quad \text{where} \quad \hat{n} = \begin{bmatrix} \hat{n}_x \\ \hat{n}_y \\ \hat{n}_z \end{bmatrix}, \quad \hat{N} = \begin{bmatrix} 0 & -\hat{n}_z & \hat{n}_y \\ \hat{n}_z & 0 & -\hat{n}_x \\ -\hat{n}_y & \hat{n}_x & 0 \end{bmatrix}, \quad \hat{n}^T \hat{n} = 1 \quad (C.11)$$

This corresponds to the matrix form of the parallel/transverse decomposition (C.6). Indeed, we have $\mathbf{a}_{\parallel} = \hat{n}(\hat{n}^T \mathbf{a})$ and $\mathbf{a}_{\perp} = (\hat{n} \times \mathbf{a}) \times \hat{n} = -\hat{n} \times (\hat{n} \times \mathbf{a}) = -\hat{N}(\hat{N} \mathbf{a}) = -\hat{N}^2 \mathbf{a}$. Therefore, $\mathbf{a} = I \mathbf{a} = (\hat{n} \hat{n}^T - \hat{N}^2) \mathbf{a} = \mathbf{a}_{\parallel} + \mathbf{a}_{\perp}$.

Differential Identities

$$\nabla \times (\nabla \psi) = 0 \quad (C.12)$$

$$\nabla \cdot (\nabla \times \mathbf{A}) = 0 \quad (C.13)$$

$$\nabla \cdot (\psi \mathbf{A}) = \mathbf{A} \cdot \nabla \psi + \psi \nabla \cdot \mathbf{A} \quad (C.14)$$

$$\nabla \times (\psi \mathbf{A}) = \psi \nabla \times \mathbf{A} + \nabla \psi \times \mathbf{A} \quad (C.15)$$

$$\nabla (\mathbf{A} \cdot \mathbf{B}) = (\mathbf{A} \cdot \nabla) \mathbf{B} + (\mathbf{B} \cdot \nabla) \mathbf{A} + \mathbf{A} \times (\nabla \times \mathbf{B}) + \mathbf{B} \times (\nabla \times \mathbf{A}) \quad (C.16)$$

$$\nabla \cdot (\mathbf{A} \times \mathbf{B}) = \mathbf{B} \cdot (\nabla \times \mathbf{A}) - \mathbf{A} \cdot (\nabla \times \mathbf{B}) \quad (C.17)$$

$$\nabla \times (\mathbf{A} \times \mathbf{B}) = \mathbf{A}(\nabla \cdot \mathbf{B}) - \mathbf{B}(\nabla \cdot \mathbf{A}) + (\mathbf{B} \cdot \nabla) \mathbf{A} - (\mathbf{A} \cdot \nabla) \mathbf{B} \quad (C.18)$$

$$\nabla \times (\nabla \times \mathbf{A}) = \nabla(\nabla \cdot \mathbf{A}) - \nabla^2 \mathbf{A} \quad (C.19)$$

$$A_x \nabla B_x + A_y \nabla B_y + A_z \nabla B_z = (\mathbf{A} \cdot \nabla) \mathbf{B} + \mathbf{A} \times (\nabla \times \mathbf{B}) \quad (C.20)$$

$$B_x \nabla A_x + B_y \nabla A_y + B_z \nabla A_z = (\mathbf{B} \cdot \nabla) \mathbf{A} + \mathbf{B} \times (\nabla \times \mathbf{A}) \quad (C.21)$$

$$(\hat{n} \times \nabla) \times \mathbf{A} = \hat{n} \times (\nabla \times \mathbf{A}) + (\hat{n} \cdot \nabla) \mathbf{A} - \hat{n}(\nabla \cdot \mathbf{A}) \quad (C.22)$$

$$\begin{aligned} \psi(\hat{n} \cdot \nabla) E - E(\hat{n} \cdot \nabla \psi) &= [(\hat{n} \cdot \nabla)(\psi E) + \hat{n} \times (\nabla \times (\psi E)) - \hat{n} \nabla \cdot (\psi E)] \\ &\quad + [\hat{n} \psi \nabla \cdot E - (\hat{n} \times E) \times \nabla \psi - \psi \hat{n} \times (\nabla \times E) - (\hat{n} \cdot E) \nabla \psi] \end{aligned} \quad (C.23)$$

With $\mathbf{r} = x\hat{x} + y\hat{y} + z\hat{z}$, $r = |\mathbf{r}| = \sqrt{x^2 + y^2 + z^2}$, and the unit vector $\hat{\mathbf{r}} = \mathbf{r}/r$, we have:

$$\nabla r = \hat{\mathbf{r}}, \quad \nabla r^2 = 2\mathbf{r}, \quad \nabla \frac{1}{r} = -\frac{\hat{\mathbf{r}}}{r^2}, \quad \nabla \cdot \mathbf{r} = 3, \quad \nabla \times \mathbf{r} = 0, \quad \nabla \cdot \hat{\mathbf{r}} = \frac{2}{r} \quad (C.24)$$

Integral Theorems for Closed Surfaces

The theorems involve a volume V surrounded by a closed surface S . The divergence or Gauss' theorem is:

$$\boxed{\int_V \nabla \cdot \mathbf{A} dV = \oint_S \mathbf{A} \cdot \hat{n} dS} \quad (\text{Gauss' divergence theorem}) \quad (C.25)$$

where \hat{n} is the *outward* normal to the surface. Green's first and second identities are:

$$\int_V [\varphi \nabla^2 \psi + \nabla \varphi \cdot \nabla \psi] dV = \oint_S \varphi \frac{\partial \psi}{\partial n} dS \quad (C.26)$$

$$\int_V [\varphi \nabla^2 \psi - \psi \nabla^2 \varphi] dV = \oint_S \left(\varphi \frac{\partial \psi}{\partial n} - \psi \frac{\partial \varphi}{\partial n} \right) dS \quad (C.27)$$

where $\frac{\partial}{\partial n} = \hat{\mathbf{n}} \cdot \nabla$ is the directional derivative along $\hat{\mathbf{n}}$. Some related theorems are:

$$\int_V \nabla^2 \psi dV = \oint_S \hat{\mathbf{n}} \cdot \nabla \psi dS = \oint_S \frac{\partial \psi}{\partial n} dS \quad (C.28)$$

$$\int_V \nabla \psi dV = \oint_S \psi \hat{\mathbf{n}} dS \quad (C.29)$$

$$\int_V \nabla^2 \mathbf{A} dV = \oint_S (\hat{\mathbf{n}} \cdot \nabla) \mathbf{A} dS = \oint_S \frac{\partial \mathbf{A}}{\partial n} dS \quad (C.30)$$

$$\oint_S (\hat{\mathbf{n}} \times \nabla) \times \mathbf{A} dS = \oint_S [\hat{\mathbf{n}} \times (\nabla \times \mathbf{A}) + (\hat{\mathbf{n}} \cdot \nabla) \mathbf{A} - \hat{\mathbf{n}} (\nabla \cdot \mathbf{A})] dS = 0 \quad (C.31)$$

$$\int_V \nabla \times \mathbf{A} dV = \oint_S \hat{\mathbf{n}} \times \mathbf{A} dS \quad (C.32)$$

Using Eqs. (C.23) and (C.31), we find:

$$\begin{aligned} \oint_S \left(\psi \frac{\partial \mathbf{E}}{\partial n} - \mathbf{E} \frac{\partial \psi}{\partial n} \right) dS = \\ = \oint_S [\hat{\mathbf{n}} \psi \nabla \cdot \mathbf{E} - (\hat{\mathbf{n}} \times \mathbf{E}) \times \nabla \psi - \psi \hat{\mathbf{n}} \times (\nabla \times \mathbf{E}) - (\hat{\mathbf{n}} \cdot \mathbf{E}) \nabla \psi] dS \end{aligned} \quad (C.33)$$

The vectorial forms of Green's identities are [1293,1289]:

$$\int_V (\nabla \times \mathbf{A} \cdot \nabla \times \mathbf{B} - \mathbf{A} \cdot \nabla \times \nabla \times \mathbf{B}) dV = \oint_S \hat{\mathbf{n}} \cdot (\mathbf{A} \times \nabla \times \mathbf{B}) dS \quad (C.34)$$

$$\int_V (\mathbf{B} \cdot \nabla \times \nabla \times \mathbf{A} - \mathbf{A} \cdot \nabla \times \nabla \times \mathbf{B}) dV = \oint_S \hat{\mathbf{n}} \cdot (\mathbf{A} \times \nabla \times \mathbf{B} - \mathbf{B} \times \nabla \times \mathbf{A}) dS \quad (C.35)$$

Integral Theorems for Open Surfaces

Stokes' theorem involves an open surface S and its boundary contour C :

$$\boxed{\int_S \hat{\mathbf{n}} \cdot \nabla \times \mathbf{A} dS = \oint_C \mathbf{A} \cdot d\mathbf{l}} \quad \text{(Stokes' theorem)} \quad (C.36)$$

where $d\mathbf{l}$ is the tangential path length around C . Some related theorems are:

$$\int_S [\psi \hat{\mathbf{n}} \cdot \nabla \times \mathbf{A} - (\hat{\mathbf{n}} \times \mathbf{A}) \cdot \nabla \psi] dS = \oint_C \psi \mathbf{A} \cdot d\mathbf{l} \quad (C.37)$$

$$\int_S [(\nabla \psi) \hat{\mathbf{n}} \cdot \nabla \times \mathbf{A} - ((\hat{\mathbf{n}} \times \mathbf{A}) \cdot \nabla) \nabla \psi] dS = \oint_C (\nabla \psi) \mathbf{A} \cdot d\mathbf{l} \quad (C.38)$$

$$\int_S \hat{\mathbf{n}} \times \nabla \psi dS = \oint_C \psi d\mathbf{l} \quad (C.39)$$

$$\int_S (\hat{\mathbf{n}} \times \nabla) \times \mathbf{A} dS = \int_S [\hat{\mathbf{n}} \times (\nabla \times \mathbf{A}) + (\hat{\mathbf{n}} \cdot \nabla) \mathbf{A} - \hat{\mathbf{n}} (\nabla \cdot \mathbf{A})] dS = \oint_C d\mathbf{l} \times \mathbf{A} \quad (C.40)$$

$$\int_S \hat{\mathbf{n}} dS = \frac{1}{2} \oint_C \mathbf{r} \times d\mathbf{l} \quad (C.41)$$

Eq. (C.41) is a special case of (C.40). Using Eqs. (C.23) and (C.40) we find:

$$\begin{aligned} \int_S \left(\psi \frac{\partial \mathbf{E}}{\partial n} - \mathbf{E} \frac{\partial \psi}{\partial n} \right) dS + \oint_C \psi \mathbf{E} \times d\mathbf{l} = \\ = \int_S [\hat{\mathbf{n}} \psi \nabla \cdot \mathbf{E} - (\hat{\mathbf{n}} \times \mathbf{E}) \times \nabla \psi - \psi \hat{\mathbf{n}} \times (\nabla \times \mathbf{E}) - (\hat{\mathbf{n}} \cdot \mathbf{E}) \nabla \psi] dS \end{aligned} \quad (C.42)$$

Stokes and Divergence Theorems in 2-D

$$\int_S \left(\frac{\partial A_y}{\partial x} - \frac{\partial A_x}{\partial y} \right) dS = \oint_C (A_x dx + A_y dy) \quad \text{(Stokes)} \quad (C.43)$$

$$\int_S \hat{\mathbf{z}} \cdot \nabla_{\perp} \times \mathbf{A} dS = \oint_C \mathbf{A} \cdot d\mathbf{l}$$

where, $\mathbf{A} = \hat{\mathbf{x}} A_x + \hat{\mathbf{y}} A_y$, $d\mathbf{l} = \hat{\mathbf{x}} dx + \hat{\mathbf{y}} dy$, and $\nabla_{\perp} = \hat{\mathbf{x}} \partial_x + \hat{\mathbf{y}} \partial_y$, and taking S to lie on the xy plane. Replacing $\mathbf{A} = \hat{\mathbf{z}} \times \mathbf{B}$, or, setting, $B_x = A_y$, $B_y = -A_x$, and noting that $d\mathbf{l} \times \hat{\mathbf{z}} = \hat{\mathbf{n}} d\mathbf{l}$, where $\hat{\mathbf{n}}$ is the outward normal to C ,

$$\int_S \left(\frac{\partial B_x}{\partial x} + \frac{\partial B_y}{\partial y} \right) dS = \oint_C (B_x dy - B_y dx) \quad \text{(divergence)} \quad (C.44)$$

$$\int_S \nabla_{\perp} \cdot \mathbf{B} dS = \oint_C \mathbf{B} \cdot \hat{\mathbf{n}} d\mathbf{l}$$

and as consequence of (C.44), we have for a scalar ψ ,

$$\int_S \nabla_{\perp} \psi dS = \oint_C \psi \hat{\mathbf{n}} d\mathbf{l} \quad \begin{array}{c} \hat{\mathbf{n}} \\ \nearrow \\ \text{---} S \text{---} \\ \searrow \\ C \end{array} \quad (C.45)$$

D. Green's Functions

The Green's functions for the three-dimensional Laplace and Helmholtz equations, and for the one-dimensional Helmholtz equation, are listed below (the two-dimensional case is discussed at the end of this section):

$$\nabla^2 g(\mathbf{r}) = -\delta^{(3)}(\mathbf{r}) \quad \Rightarrow \quad g(\mathbf{r}) = \frac{1}{4\pi r} \quad (D.1)$$

$$(\nabla^2 + k^2) G(\mathbf{r}) = -\delta^{(3)}(\mathbf{r}) \quad \Rightarrow \quad G(\mathbf{r}) = \frac{e^{-jkr}}{4\pi r} \quad (D.2)$$

$$(\partial_z^2 + k^2)G(z) = -\delta(z) \quad \Rightarrow \quad G(z) = \frac{e^{-jk|z|}}{2jk} \quad (\text{D.3})$$

where $r = |\mathbf{r}| = \sqrt{x^2 + y^2 + z^2}$. Eqs. (D.2) and (D.3) are appropriate for describing *outgoing* waves. We considered other versions of (D.3) in Sec. 24.3. A more general identity satisfied by the Green's function $g(\mathbf{r})$ of Eq. (D.1) is as follows (for a proof, see Refs. [143,144]):

$$\partial_i \partial_j g(\mathbf{r}) = -\frac{1}{3} \delta_{ij} \delta^{(3)}(\mathbf{r}) + \frac{3x_i x_j - r^2 \delta_{ij}}{r^4} g(\mathbf{r}) \quad i, j = 1, 2, 3 \quad (\text{D.4})$$

where $\partial_i = \partial/\partial x_i$ and x_i stands for any of x, y, z . By summing the i, j indices, Eq. (D.4) reduces to (D.1). Using this identity, we find for the Green's function $G(\mathbf{r}) = e^{-jkr}/4\pi r$:

$$\partial_i \partial_j G(\mathbf{r}) = -\frac{1}{3} \delta_{ij} \delta^{(3)}(\mathbf{r}) + \left[\left(jk + \frac{1}{r} \right) \frac{3x_i x_j - r^2 \delta_{ij}}{r^3} - k^2 \frac{x_i x_j}{r^2} \right] G(\mathbf{r}) \quad (\text{D.5})$$

This reduces to Eq. (D.2) upon summing the indices. For any fixed vector \mathbf{p} , Eq. (D.5) is equivalent to the vectorial identity:

$$\nabla \times \nabla \times [\mathbf{p} G(\mathbf{r})] = \frac{2}{3} \mathbf{p} \delta^{(3)}(\mathbf{r}) + \left[\left(jk + \frac{1}{r} \right) \frac{3\hat{\mathbf{r}}(\hat{\mathbf{r}} \cdot \mathbf{p}) - \mathbf{p}}{r^2} + k^2 \hat{\mathbf{r}} \times (\mathbf{p} \times \hat{\mathbf{r}}) \right] G(\mathbf{r}) \quad (\text{D.6})$$

The second term on the right is simply the left-hand side evaluated at points away from the origin, thus, we may write:

$$\nabla \times \nabla \times [\mathbf{p} G(\mathbf{r})] = \frac{2}{3} \mathbf{p} \delta^{(3)}(\mathbf{r}) + \left[\nabla \times \nabla \times [\mathbf{p} G(\mathbf{r})] \right]_{\mathbf{r} \neq \mathbf{0}} \quad (\text{D.7})$$

Then, Eq. (D.7) implies the following integrated identity, where ∇ is with respect to \mathbf{r} :

$$\nabla \times \nabla \times \int_V \mathbf{p}(\mathbf{r}') G(\mathbf{r} - \mathbf{r}') dV' = \frac{2}{3} \mathbf{p}(\mathbf{r}) + \int_V \left[\nabla \times \nabla \times [\mathbf{p}(\mathbf{r}') G(\mathbf{r} - \mathbf{r}')] \right]_{\mathbf{r}' \neq \mathbf{r}} dV' \quad (\text{D.8})$$

and \mathbf{r} is assumed to lie within V . If \mathbf{r} is outside V , then the term $2\mathbf{p}(\mathbf{r})/3$ is absent.

Technically, the integrals in (D.8) are *principal-value* integrals, that is, the limits as $\delta \rightarrow 0$ of the integrals over $V - V_\delta(\mathbf{r})$, where $V_\delta(\mathbf{r})$ is an excluded small sphere of radius δ centered about \mathbf{r} . The $2\mathbf{p}(\mathbf{r})/3$ term has a different form if the excluded volume $V_\delta(\mathbf{r})$ has shape other than a sphere or a cube. See Refs. [1419,499,511,638] and [138-142] for the definitions and properties of such principal value integrals.

Another useful result is the so-called *Weyl representation* or plane-wave-spectrum representation [22,26,1419,27,555] of the outgoing Helmholtz Green's function $G(\mathbf{r})$:

$$G(\mathbf{r}) = \frac{e^{-jkr}}{4\pi r} = \int_{-\infty}^{\infty} \int_{-\infty}^{\infty} \frac{e^{-j(k_x x + k_y y)} e^{-jk_z |z|}}{2jk_z} \frac{dk_x dk_y}{(2\pi)^2} \quad (\text{D.9})$$

where $k_z^2 = k^2 - k_\perp^2$, with $k_\perp = \sqrt{k_x^2 + k_y^2}$. In order to correspond to either outgoing waves or decaying evanescent waves, k_z must be defined more precisely as follows:

$$k_z = \begin{cases} \sqrt{k^2 - k_\perp^2}, & \text{if } k_\perp < k, \quad (\text{propagating modes}) \\ -j\sqrt{k_\perp^2 - k^2}, & \text{if } k_\perp > k, \quad (\text{evanescent modes}) \end{cases} \quad (\text{D.10})$$

The propagating modes are important in radiation problems and conventional imaging systems, such as Fourier optics [1422]. The evanescent modes are important in the new subject of *near-field optics*, in which objects can be probed and imaged at nanometer scales improving the resolution of optical microscopy by factors of ten. Some near-field optics references are [534-554,1339-1342,1350-1353].

To prove (D.9), we consider the 2D spatial Fourier transform of $G(\mathbf{r})$ and its inverse. Indicating explicitly the dependence on the coordinates x, y, z , we must have:

$$\begin{aligned} \hat{G}(k_x, k_y, z) &= \int_{-\infty}^{\infty} \int_{-\infty}^{\infty} G(x, y, z) e^{j(k_x x + k_y y)} dx dy = \frac{e^{-jk_z |z|}}{2jk_z} \\ G(x, y, z) &= \int_{-\infty}^{\infty} \int_{-\infty}^{\infty} \hat{G}(k_x, k_y, z) e^{-j(k_x x + k_y y)} \frac{dk_x dk_y}{(2\pi)^2} \end{aligned} \quad (\text{D.11})$$

Writing $\delta^{(3)}(\mathbf{r}) = \delta(x)\delta(y)\delta(z)$ and using the inverse Fourier transform:

$$\delta(x)\delta(y) = \int_{-\infty}^{\infty} \int_{-\infty}^{\infty} e^{-j(k_x x + k_y y)} \frac{dk_x dk_y}{(2\pi)^2},$$

we find from Eq. (D.2) that $\hat{G}(k_x, k_y, z)$ must satisfy the one-dimensional Helmholtz Green's function equation (D.3), with $k_z^2 = k^2 - k_x^2 - k_y^2 = k^2 - k_\perp^2$, that is,

$$(\partial_z^2 + k_z^2) \hat{G}(k_x, k_y, z) = -\delta(z) \quad (\text{D.12})$$

whose outgoing/evanescent solution is $\hat{G}(k_x, k_y, z) = e^{-jk_z |z|}/2jk_z$, from (D.3).

A more direct proof of (D.9) is to use cylindrical coordinates, $k_x = k_\perp \cos \psi$, $k_y = k_\perp \sin \psi$, $x = \rho \cos \phi$, $y = \rho \sin \phi$, where $k_\perp^2 = k_x^2 + k_y^2$ and $\rho^2 = x^2 + y^2$. It follows that $k_x x + k_y y = k_\perp \rho \cos(\phi - \psi)$. Setting $dx dy = \rho d\rho d\phi = r dr d\phi$, the latter following from $r^2 = \rho^2 + z^2$, we obtain from Eq. (D.11) after replacing $\rho = \sqrt{r^2 - z^2}$:

$$\begin{aligned} \hat{G}(k_x, k_y, z) &= \iint \frac{e^{-jkr}}{4\pi r} e^{j(k_x x + k_y y)} dx dy = \iint \frac{e^{-jkr}}{4\pi r} e^{jk_\perp \rho \cos(\phi - \psi)} r dr d\phi \\ &= \frac{1}{2} \int_{|z|}^{\infty} dr e^{-jkr} \int_0^{2\pi} \frac{d\phi}{2\pi} e^{jk_\perp \rho \cos(\phi - \psi)} = \frac{1}{2} \int_{|z|}^{\infty} dr e^{-jkr} J_0(k_\perp \sqrt{r^2 - z^2}) \end{aligned}$$

where we used the integral representation (18.9.2) of the Bessel function $J_0(x)$. Looking up the last integral in the table of integrals [1791], we find:

$$\hat{G}(k_x, k_y, z) = \frac{1}{2} \int_{|z|}^{\infty} dr e^{-jkr} J_0(k_\perp \sqrt{r^2 - z^2}) = \frac{e^{-jk_z |z|}}{2jk_z} \quad (\text{D.13})$$

where k_z must be defined exactly as in Eq. (D.10). A direct consequence of (D.11) is the following result:

$$\int_{-\infty}^{\infty} \int_{-\infty}^{\infty} e^{-j(k_x x' + k_y y')} G(\mathbf{r} - \mathbf{r}') dx' dy' = e^{-j(k_x x + k_y y)} \frac{e^{-jk_z |z - z'|}}{2jk_z} \quad (\text{D.14})$$

One can also show the integral:

$$\int_0^\infty e^{-jk'_z z'} \frac{e^{-jk_z |z-z'|}}{2jk_z} dz' = \begin{cases} \frac{e^{-jk'_z z}}{k'_z{}^2 - k_z^2} - \frac{e^{-jk_z z}}{2k_z(k'_z - k_z)}, & \text{for } z \geq 0 \\ -\frac{e^{jk_z z}}{2k_z(k'_z + k_z)}, & \text{for } z < 0 \end{cases} \quad (\text{D.15})$$

The proof is obtained by splitting the integral over the sub-intervals $[0, z]$ and $[z, \infty)$. To handle the limits at infinity, k'_z must be assumed to be slightly lossy, that is, $k'_z = \beta_z - j\alpha_z$, with $\alpha_z > 0$. Eqs. (D.14) and (D.15) can be combined into:

$$\int_{V_+} e^{-j\mathbf{k}' \cdot \mathbf{r}'} G(\mathbf{r} - \mathbf{r}') dV' = \begin{cases} \frac{e^{-j\mathbf{k}' \cdot \mathbf{r}}}{k'^2 - k^2} - \frac{e^{-j\mathbf{k} \cdot \mathbf{r}}}{2k_z(k'_z - k_z)}, & \text{for } z \geq 0 \\ -\frac{e^{-j\mathbf{k} \cdot \mathbf{r}}}{2k_z(k'_z + k_z)}, & \text{for } z < 0 \end{cases} \quad (\text{D.16})$$

where V_+ is the half-space $z \geq 0$, and $\mathbf{k}, \mathbf{k}_-, \mathbf{k}'$ are wave-vectors with the same k_x, k_y components, but different k_z s:

$$\begin{aligned} \mathbf{k} &= k_x \hat{\mathbf{x}} + k_y \hat{\mathbf{y}} + k_z \hat{\mathbf{z}} \\ \mathbf{k}_- &= k_x \hat{\mathbf{x}} + k_y \hat{\mathbf{y}} - k_z \hat{\mathbf{z}} \\ \mathbf{k}' &= k_x \hat{\mathbf{x}} + k_y \hat{\mathbf{y}} + k'_z \hat{\mathbf{z}} \end{aligned} \quad (\text{D.17})$$

where we note that $k'^2 - k^2 = (k_x^2 + k_y^2 + k_z'^2) - (k_x^2 + k_y^2 + k_z^2) = k_z'^2 - k_z^2$.

The Green's function results (D.8)-(D.17) are used in the discussion of the Ewald-Oseen extinction theorem in Sec. 15.6.

A related Weyl-type representation is obtained by differentiating Eq. (D.9) with respect to z . Assuming that $z \geq 0$ and interchanging differentiation and integration (and multiplying by -2), we obtain the identity:

$$\boxed{-2 \frac{\partial}{\partial z} \left(\frac{e^{-jkr}}{4\pi r} \right) = \int_{-\infty}^\infty \int_{-\infty}^\infty e^{-jk_x x} e^{-jk_y y} e^{-jk_z z} \frac{dk_x dk_y}{(2\pi)^2}, \quad z \geq 0} \quad (\text{D.18})$$

This just means that the left-hand side is the two-dimensional inverse Fourier transform of $e^{-jk_z z}$ with k_z given by Eq. (D.10). Replacing \mathbf{r} by $\mathbf{r} - \mathbf{r}'$, and r by $R = |\mathbf{r} - \mathbf{r}'|$, and noting that $\partial_{z'} = -\partial_z$, we also obtain:

$$\boxed{2 \frac{\partial}{\partial z'} \left(\frac{e^{-jkR}}{4\pi R} \right) = \int_{-\infty}^\infty \int_{-\infty}^\infty e^{-jk_x(x-x')} e^{-jk_y(y-y')} e^{-jk_z(z-z')} \frac{dk_x dk_y}{(2\pi)^2}, \quad z \geq z'} \quad (\text{D.19})$$

This result establishes the equivalence between the Rayleigh-Sommerfeld diffraction formula and the plane-wave spectrum representation as discussed in Sec. 19.2. For the vector diffraction case, we also need the derivatives of G with respect to the transverse coordinates x, y . Differentiating (D.9) with respect to x (or with respect to y), we have:

$$\boxed{-2 \frac{\partial}{\partial x} \left(\frac{e^{-jkr}}{4\pi r} \right) = \int_{-\infty}^\infty \int_{-\infty}^\infty \frac{k_x}{k_z} e^{-jk_x x} e^{-jk_y y} e^{-jk_z z} \frac{dk_x dk_y}{(2\pi)^2}, \quad z \geq 0} \quad (\text{D.20})$$

Setting $z = 0$ in (D.18), we also obtain the special result,

$$\boxed{-2 \frac{\partial}{\partial z} \left(\frac{e^{-jkr}}{4\pi r} \right) \Big|_{z=0} = \int_{-\infty}^\infty \int_{-\infty}^\infty e^{-jk_x x} e^{-jk_y y} \frac{dk_x dk_y}{(2\pi)^2} = \delta(x) \delta(y)} \quad (\text{D.21})$$

This can also be derived by integrating Eq. (D.2) with respect to z over the interval $-\epsilon \leq z \leq \epsilon$ and taking the limit as $\epsilon \rightarrow 0$, invoking the continuity of $G(r)$ (but not $\partial G/\partial z$) with respect to z ,

$$\begin{aligned} (\partial_x^2 + \partial_y^2 + k^2) \int_{-\epsilon}^\epsilon G(r) dz + \frac{\partial G}{\partial z} \Big|_{z=-\epsilon}^{z=\epsilon} &= -\delta(x) \delta(y) \int_{-\epsilon}^\epsilon \delta(z) dz, \quad \text{or,} \\ 2 \frac{\partial G}{\partial z} \Big|_{z=0} &= -\delta(x) \delta(y) \end{aligned}$$

Two-Dimensional Green's functions

The Green's function for the two-dimensional Helmholtz equation will be needed in our discussion of line sources and one-dimensional apertures, such as narrow slits or strips. In order to develop the corresponding 2-D version of the plane-wave spectrum Weyl representation, we will assume that the one-dimensional line source is along the x direction, the propagation is perpendicularly to x towards the z direction, and that there is no dependence on the y coordinate. Because of our assumed $e^{j\omega t}$ time dependence, the outgoing Green's function of the 2-D Helmholtz equation will be:[†]

$$\boxed{(\partial_x^2 + \partial_z^2 + k^2) G(x, z) = -\delta(x) \delta(z) \Rightarrow G(x, z) = -\frac{j}{4} H_0^{(2)}(kr)} \quad (\text{D.22})$$

where $r = \sqrt{x^2 + z^2}$ and $H_0^{(2)}(kr)$ is the order-0 Hankel function of second kind. For definitions and properties of Bessel and Hankel functions, see [1790] or [1822]. Several properties of Hankel functions were also discussed in Sec. 10.15 and 10.19.

The outgoing Green's function of the Helmholtz equation must satisfy the *Sommerfeld radiation condition* for outgoing waves, which reads in d -dimensions,

$$\boxed{\lim_{r \rightarrow \infty} \left[r^{-(d-1)/2} \left(\frac{\partial G}{\partial r} + jkG \right) \right] = 0} \quad (\text{Sommerfeld radiation condition}) \quad (\text{D.23})$$

This condition is easily verified for Eq. (D.2) in the 3D-case ($d = 3$). In the 2D-case ($d = 2$), it follows from the asymptotic behavior of the Hankel function $H_0^{(2)}(kr)$,

$$H_0^{(2)}(kr) \simeq \sqrt{\frac{2}{\pi kr}} e^{-j(kr - \frac{\pi}{4})}, \quad \text{for large } r \quad (\text{D.24})$$

To show (D.22), we consider the 1-D Fourier transform of $G(x, z)$ with respect to the variable x ,

$$\hat{G}(k_x, z) = \int_{-\infty}^\infty G(x, z) e^{jk_x x} dx \Leftrightarrow G(x, z) = \int_{-\infty}^\infty \hat{G}(k_x, z) e^{-jk_x x} \frac{dk_x}{2\pi} \quad (\text{D.25})$$

[†]for $e^{-j\omega t}$ time dependence, we must choose, $G(x, z) = \frac{j}{4} H_0^{(1)}(kr)$.

Transforming the 2-D Helmholtz equation (D.22), we obtain the following 1-D Helmholtz equation that has the same propagating/evanescent Green's function as (D.12),

$$(-k_x^2 + \partial_z^2 + k^2)\hat{G}(k_x, z) = (\partial_z^2 + k_z^2)\hat{G}(k_x, z) = -\delta(z) \Rightarrow \hat{G}(k_x, z) = \frac{e^{-jk_z|z|}}{2jk_z} \quad (D.26)$$

where $k_z^2 = k^2 - k_x^2$, with k_z given by the evanescent square-root,

$$k_z = \begin{cases} \sqrt{k^2 - k_x^2}, & \text{if } |k_x| < k \\ -j\sqrt{k_x^2 - k^2}, & \text{if } |k_x| > k \end{cases} \quad (D.27)$$

Thus, to find $G(x, z)$ we need to find the inverse Fourier transform of (D.26). But we note that the Hankel function $H_0^{(2)}(k\sqrt{x^2 + z^2})$, considered as a function of x , has the following forward and inverse 1-D Fourier transform,

$$\int_{-\infty}^{\infty} H_0^{(2)}(k\sqrt{x^2 + z^2})e^{jk_x x} dx = \frac{2e^{-jk_z|z|}}{k_z} \quad (D.28)$$

$$H_0^{(2)}(k\sqrt{x^2 + z^2}) = \int_{-\infty}^{\infty} \frac{2e^{-jk_x x} e^{-jk_z|z|}}{k_z} \frac{dk_x}{2\pi}$$

where k_z is defined exactly as in (D.27). The transform pair (D.28) can be looked up in Bateman [1640]—see pair #42 and its erratum in Sect.1.13, p.56, of Ref. [1640], or from the combination of pairs #35 and #41, together with the following definitions of the half-integer-order Hankel and modified Bessel functions,

$$H_{-1/2}^{(2)}(u) = \sqrt{\frac{2}{\pi u}} e^{-ju}, \quad K_{-1/2}(u) = \sqrt{\frac{\pi}{2u}} e^{-u} \quad (D.29)$$

Multiplying both sides of (D.28) by $-j/4$, we then obtain $G(x, z)$ and its plane-wave spectrum or Weyl representation,

$$G(x, z) = -\frac{j}{4} H_0^{(2)}(kr) = \int_{-\infty}^{\infty} \frac{e^{-jk_x x} e^{-jk_z|z|}}{2jk_z} \frac{dk_x}{2\pi} \quad (2D \text{ Weyl representation}) \quad (D.30)$$

with $r = \sqrt{x^2 + z^2}$. This is analogous to (D.9), but without the dk_y integration. The 2-D versions of the differentiated Weyl representations (D.18) and (D.20) are as follows and will be used to develop the 2-D versions of the Rayleigh-Sommerfeld diffraction formulas,

$$-2 \frac{\partial G(x, z)}{\partial z} = \int_{-\infty}^{\infty} e^{-jk_x x} e^{-jk_z z} \frac{dk_x}{2\pi} \quad \text{for } z \geq 0 \quad (D.31)$$

$$-2 \frac{\partial G(x, z)}{\partial x} = \int_{-\infty}^{\infty} \frac{k_x}{k_z} e^{-jk_x x} e^{-jk_z z} \frac{dk_x}{2\pi}$$

A quicker way of deriving (D.30) is to start with the 3-D Green's function (D.2), denoted here by $G_3(x, y, z) = e^{-jkR}/(4\pi R)$, $R = \sqrt{x^2 + y^2 + z^2} = \sqrt{r^2 + y^2}$, where $r = \sqrt{x^2 + z^2}$, and define the 2-D Green's function by integrating out the y -variable,

$$G(x, z) = \int_{-\infty}^{\infty} G_3(x, y, z) dy = \int_{-\infty}^{\infty} \frac{e^{-jkR}}{4\pi R} dy \quad (D.32)$$

Integrating over y both sides of the 3-D Helmholtz equation for $G_3(x, y, z)$, we have,

$$(\partial_x^2 + \partial_y^2 + \partial_z^2 + k^2)G_3(x, y, z) = -\delta(x)\delta(y)\delta(z)$$

$$(\partial_x^2 + \partial_z^2 + k^2) \int_{-\infty}^{\infty} G_3(x, y, z) dy + \left[\partial_y G_3(x, y, z) \right]_{y=-\infty}^{y=\infty} = -\delta(x)\delta(z) \int_{-\infty}^{\infty} \delta(y) dy$$

and since, $\partial_y G_3(x, y, z)|_{y=\pm\infty} = 0$,[†] we obtain,

$$(\partial_x^2 + \partial_z^2 + k^2)G(x, z) = -\delta(x)\delta(z) \quad (D.33)$$

The plane-wave spectrum representation of $G(x, z)$ can be derived by inserting the Weyl representation for $G_3(x, y, z)$ into the definition (D.32),

$$G(x, z) = \int_{-\infty}^{\infty} G_3(x, y, z) dy = \int_{-\infty}^{\infty} \int_{-\infty}^{\infty} \int_{-\infty}^{\infty} \frac{e^{-jk_x x} e^{-jk_y y} e^{-jk_z|z|}}{2jk_z} \frac{dk_x dk_y}{(2\pi)^2} dy \quad (D.34)$$

$$= \int_{-\infty}^{\infty} \int_{-\infty}^{\infty} \frac{e^{-jk_x x} e^{-jk_z|z|}}{2jk_z} (2\pi)\delta(k_y) \frac{dk_x dk_y}{(2\pi)^2} = \int_{-\infty}^{\infty} \frac{e^{-jk_x x} e^{-jk_z|z|}}{2jk_z} \frac{dk_x}{2\pi}$$

where we used the delta-function representation,

$$\int_{-\infty}^{\infty} e^{-jk_y y} dy = (2\pi)\delta(k_y)$$

and the k_y integration in (D.34) sets $k_y = 0$ into the definition (D.10) of k_z so that the resulting k_z is given by (D.27). By combining the standard integral representations of the zero-order Bessel functions [1822], we obtain the representation of the Hankel function, $H_0^{(2)} = J_0 - jY_0$, for $r > 0$,

$$J_0(kr) = \frac{1}{\pi} \int_{-\infty}^{\infty} \sin(kr \cosh(u)) du$$

$$Y_0(kr) = -\frac{1}{\pi} \int_{-\infty}^{\infty} \cos(kr \cosh(u)) du \quad (D.35)$$

$$-\frac{j}{4} H_0^{(2)}(kr) = \frac{1}{4\pi} \int_{-\infty}^{\infty} e^{-jkr \cosh(u)} du$$

Changing variables from u to $y = r \sinh(u)$, we may verify Eq. (D.32),

$$-\frac{j}{4} H_0^{(2)}(kr) = \frac{1}{4\pi} \int_{-\infty}^{\infty} e^{-jkr \cosh(u)} du = \int_{-\infty}^{\infty} \frac{e^{-jk\sqrt{r^2 + y^2}}}{4\pi\sqrt{r^2 + y^2}} dy$$

E. Coordinate Systems

The definitions of cylindrical and spherical coordinates were given in Sec. 15.8. The expressions of the gradient, divergence, curl, Laplacian operators, and delta functions are given below in cartesian, cylindrical, and spherical coordinates.

[†] note that, $\partial_y G_3(x, y, z) = -\frac{y}{R} \frac{e^{-jkR}}{4\pi R} \left(jk + \frac{1}{R} \right)$, $R = \sqrt{x^2 + y^2 + z^2}$.

Cartesian Coordinates

$$\begin{aligned}\nabla\psi &= \hat{\mathbf{x}} \frac{\partial\psi}{\partial x} + \hat{\mathbf{y}} \frac{\partial\psi}{\partial y} + \hat{\mathbf{z}} \frac{\partial\psi}{\partial z} \\ \nabla^2\psi &= \frac{\partial^2\psi}{\partial x^2} + \frac{\partial^2\psi}{\partial y^2} + \frac{\partial^2\psi}{\partial z^2} \\ \nabla \cdot \mathbf{A} &= \frac{\partial A_x}{\partial x} + \frac{\partial A_y}{\partial y} + \frac{\partial A_z}{\partial z} \\ \nabla \times \mathbf{A} &= \hat{\mathbf{x}} \left(\frac{\partial A_z}{\partial y} - \frac{\partial A_y}{\partial z} \right) + \hat{\mathbf{y}} \left(\frac{\partial A_x}{\partial z} - \frac{\partial A_z}{\partial x} \right) + \hat{\mathbf{z}} \left(\frac{\partial A_y}{\partial x} - \frac{\partial A_x}{\partial y} \right) \\ &= \begin{vmatrix} \hat{\mathbf{x}} & \hat{\mathbf{y}} & \hat{\mathbf{z}} \\ \frac{\partial}{\partial x} & \frac{\partial}{\partial y} & \frac{\partial}{\partial z} \\ A_x & A_y & A_z \end{vmatrix}\end{aligned}\quad (\text{E.1})$$

$$\delta^{(3)}(\mathbf{r}-\mathbf{r}') = \delta(x-x')\delta(y-y')\delta(z-z')$$

Cylindrical Coordinates

$$\begin{aligned}\nabla\psi &= \hat{\rho} \frac{\partial\psi}{\partial\rho} + \hat{\phi} \frac{1}{\rho} \frac{\partial\psi}{\partial\phi} + \hat{\mathbf{z}} \frac{\partial\psi}{\partial z} \\ \nabla^2\psi &= \frac{1}{\rho} \frac{\partial}{\partial\rho} \left(\rho \frac{\partial\psi}{\partial\rho} \right) + \frac{1}{\rho^2} \frac{\partial^2\psi}{\partial\phi^2} + \frac{\partial^2\psi}{\partial z^2} \\ \nabla \cdot \mathbf{A} &= \frac{1}{\rho} \frac{\partial(\rho A_\rho)}{\partial\rho} + \frac{1}{\rho} \frac{\partial A_\phi}{\partial\phi} + \frac{\partial A_z}{\partial z} \\ \nabla \times \mathbf{A} &= \hat{\rho} \left(\frac{1}{\rho} \frac{\partial A_z}{\partial\phi} - \frac{\partial A_\phi}{\partial z} \right) + \hat{\phi} \left(\frac{\partial A_\rho}{\partial z} - \frac{\partial A_z}{\partial\rho} \right) + \hat{\mathbf{z}} \frac{1}{\rho} \left(\frac{\partial(\rho A_\phi)}{\partial\rho} - \frac{\partial A_\rho}{\partial\phi} \right) \\ \delta^{(3)}(\mathbf{r}-\mathbf{r}') &= \frac{1}{\rho} \delta(\rho-\rho')\delta(\phi-\phi')\delta(z-z')\end{aligned}\quad (\text{E.2a})$$

(E.2b)

(E.2c)

(E.2d)

(E.2e)

Spherical Coordinates

$$\nabla\psi = \hat{\mathbf{r}} \frac{\partial\psi}{\partial r} + \hat{\theta} \frac{1}{r} \frac{\partial\psi}{\partial\theta} + \hat{\phi} \frac{1}{r \sin\theta} \frac{\partial\psi}{\partial\phi} \quad (\text{E.3a})$$

$$\nabla^2\psi = \frac{1}{r^2} \frac{\partial}{\partial r} \left(r^2 \frac{\partial\psi}{\partial r} \right) + \frac{1}{r^2 \sin\theta} \frac{\partial}{\partial\theta} \left(\sin\theta \frac{\partial\psi}{\partial\theta} \right) + \frac{1}{r^2 \sin^2\theta} \frac{\partial^2\psi}{\partial\phi^2} \quad (\text{E.3b})$$

$$\nabla \cdot \mathbf{A} = \frac{1}{r^2} \frac{\partial(r^2 A_r)}{\partial r} + \frac{1}{r \sin\theta} \frac{\partial(\sin\theta A_\theta)}{\partial\theta} + \frac{1}{r \sin\theta} \frac{\partial A_\phi}{\partial\phi} \quad (\text{E.3c})$$

$$\begin{aligned}\nabla \times \mathbf{A} &= \hat{\mathbf{r}} \frac{1}{r \sin\theta} \left(\frac{\partial(\sin\theta A_\phi)}{\partial\theta} - \frac{\partial A_\theta}{\partial\phi} \right) + \hat{\theta} \frac{1}{r} \left(\frac{1}{\sin\theta} \frac{\partial A_r}{\partial\phi} - \frac{\partial(r A_\phi)}{\partial r} \right) \\ &\quad + \hat{\phi} \frac{1}{r} \left(\frac{\partial(r A_\theta)}{\partial r} - \frac{\partial A_r}{\partial\theta} \right)\end{aligned}\quad (\text{E.3d})$$

$$\delta^{(3)}(\mathbf{r}-\mathbf{r}') = \frac{1}{r^2 \sin\theta} \delta(r-r')\delta(\theta-\theta')\delta(\phi-\phi') \quad (\text{E.3e})$$

Transformations Between Coordinate Systems

The different coordinate conventions are summarized in Fig. E.1 below. A vector \mathbf{A} can be expressed component-wise in the three coordinate systems as:

$$\begin{aligned}\mathbf{A} &= \hat{\mathbf{x}} A_x + \hat{\mathbf{y}} A_y + \hat{\mathbf{z}} A_z \\ &= \hat{\rho} A_\rho + \hat{\phi} A_\phi + \hat{\mathbf{z}} A_z \\ &= \hat{\mathbf{r}} A_r + \hat{\theta} A_\theta + \hat{\phi} A_\phi\end{aligned}\quad (\text{E.4})$$

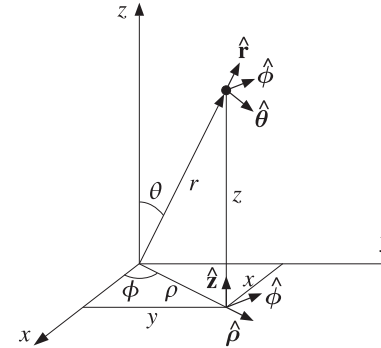


Fig. E.1 Cartesian, cylindrical, and spherical coordinate conventions.

The components in one coordinate system can be expressed in terms of the components of another by using the following relationships between the unit vectors, which were also given in Eqs. (15.8.1)–(15.8.3):

$$\begin{aligned}x &= \rho \cos\phi & \hat{\rho} &= \hat{\mathbf{x}} \cos\phi + \hat{\mathbf{y}} \sin\phi & \hat{\mathbf{x}} &= \hat{\rho} \cos\phi - \hat{\phi} \sin\phi \\ y &= \rho \sin\phi & \hat{\phi} &= -\hat{\mathbf{x}} \sin\phi + \hat{\mathbf{y}} \cos\phi & \hat{\mathbf{y}} &= \hat{\rho} \sin\phi + \hat{\phi} \cos\phi\end{aligned}\quad (\text{E.5})$$

$$\begin{aligned}\rho &= r \sin\theta & \hat{\mathbf{r}} &= \hat{\mathbf{z}} \cos\theta + \hat{\rho} \sin\theta & \hat{\mathbf{z}} &= \hat{\mathbf{r}} \cos\theta - \hat{\theta} \sin\theta \\ z &= r \cos\theta & \hat{\theta} &= -\hat{\mathbf{z}} \sin\theta + \hat{\rho} \cos\theta & \hat{\rho} &= \hat{\mathbf{r}} \sin\theta + \hat{\theta} \cos\theta\end{aligned}\quad (\text{E.6})$$

$$\begin{aligned} x &= r \sin \theta \cos \phi & \hat{\mathbf{r}} &= \hat{\mathbf{x}} \cos \phi \sin \theta + \hat{\mathbf{y}} \sin \phi \sin \theta + \hat{\mathbf{z}} \cos \theta \\ y &= r \sin \theta \sin \phi & \hat{\boldsymbol{\theta}} &= \hat{\mathbf{x}} \cos \phi \cos \theta + \hat{\mathbf{y}} \sin \phi \cos \theta - \hat{\mathbf{z}} \sin \theta \\ z &= r \cos \theta & \hat{\boldsymbol{\phi}} &= -\hat{\mathbf{x}} \sin \phi + \hat{\mathbf{y}} \cos \phi \end{aligned} \quad (\text{E.7})$$

$$\begin{aligned} \hat{\mathbf{x}} &= \hat{\mathbf{r}} \sin \theta \cos \phi + \hat{\boldsymbol{\theta}} \cos \theta \cos \phi - \hat{\boldsymbol{\phi}} \sin \phi \\ \hat{\mathbf{y}} &= \hat{\mathbf{r}} \sin \theta \sin \phi + \hat{\boldsymbol{\theta}} \cos \theta \sin \phi + \hat{\boldsymbol{\phi}} \cos \phi \\ \hat{\mathbf{z}} &= \hat{\mathbf{r}} \cos \theta - \hat{\boldsymbol{\theta}} \sin \theta \end{aligned} \quad (\text{E.8})$$

For example, to express the spherical components A_r, A_θ, A_ϕ in terms of the cartesian components, we proceed as follows:

$$\begin{aligned} A_r &= \hat{\mathbf{r}} \cdot \mathbf{A} = \hat{\mathbf{r}} \cdot (\hat{\mathbf{x}} A_x + \hat{\mathbf{y}} A_y + \hat{\mathbf{z}} A_z) = (\hat{\mathbf{r}} \cdot \hat{\mathbf{x}}) A_x + (\hat{\mathbf{r}} \cdot \hat{\mathbf{y}}) A_y + (\hat{\mathbf{r}} \cdot \hat{\mathbf{z}}) A_z \\ A_\theta &= \hat{\boldsymbol{\theta}} \cdot \mathbf{A} = \hat{\boldsymbol{\theta}} \cdot (\hat{\mathbf{x}} A_x + \hat{\mathbf{y}} A_y + \hat{\mathbf{z}} A_z) = (\hat{\boldsymbol{\theta}} \cdot \hat{\mathbf{x}}) A_x + (\hat{\boldsymbol{\theta}} \cdot \hat{\mathbf{y}}) A_y + (\hat{\boldsymbol{\theta}} \cdot \hat{\mathbf{z}}) A_z \\ A_\phi &= \hat{\boldsymbol{\phi}} \cdot \mathbf{A} = \hat{\boldsymbol{\phi}} \cdot (\hat{\mathbf{x}} A_x + \hat{\mathbf{y}} A_y + \hat{\mathbf{z}} A_z) = (\hat{\boldsymbol{\phi}} \cdot \hat{\mathbf{x}}) A_x + (\hat{\boldsymbol{\phi}} \cdot \hat{\mathbf{y}}) A_y + (\hat{\boldsymbol{\phi}} \cdot \hat{\mathbf{z}}) A_z \end{aligned}$$

The dot products can be read off Eq. (E.7), resulting in:

$$\begin{aligned} A_r &= \cos \phi \sin \theta A_x + \sin \phi \sin \theta A_y + \cos \theta A_z \\ A_\theta &= \cos \phi \cos \theta A_x + \sin \phi \cos \theta A_y - \sin \theta A_z \\ A_\phi &= -\sin \phi A_x + \cos \phi A_y \end{aligned} \quad (\text{E.9})$$

Similarly, using Eq. (E.6) the cylindrical components A_ρ, A_z can be expressed in terms of spherical components as:

$$\begin{aligned} A_\rho &= \hat{\boldsymbol{\rho}} \cdot \mathbf{A} = \hat{\boldsymbol{\rho}} \cdot (\hat{\mathbf{r}} A_r + \hat{\boldsymbol{\theta}} A_\theta + \hat{\boldsymbol{\phi}} A_\phi) = \sin \theta A_r + \cos \theta A_\theta \\ A_z &= \hat{\mathbf{z}} \cdot \mathbf{A} = \hat{\mathbf{z}} \cdot (\hat{\mathbf{r}} A_r + \hat{\boldsymbol{\theta}} A_\theta + \hat{\boldsymbol{\phi}} A_\phi) = \cos \theta A_r - \cos \theta A_\theta \end{aligned} \quad (\text{E.10})$$

F. Fresnel Integrals

The Fresnel functions $C(x)$ and $S(x)$ are defined by [1790]:

$$C(x) = \int_0^x \cos\left(\frac{\pi}{2} t^2\right) dt, \quad S(x) = \int_0^x \sin\left(\frac{\pi}{2} t^2\right) dt \quad (\text{F.1})$$

They may be combined into the complex function:

$$\mathcal{F}(x) = C(x) - jS(x) = \int_0^x e^{-j\pi t^2/2} dt \quad (\text{F.2})$$

$C(x), S(x)$, and $\mathcal{F}(x)$ are *odd* functions of x and have the asymptotic values:

$$C(\infty) = S(\infty) = \frac{1}{2}, \quad \mathcal{F}(\infty) = \frac{1-j}{2} \quad (\text{F.3})$$

At $x = 0$, we have $\mathcal{F}(0) = 0$ and $\mathcal{F}'(0) = 1$, so that the Taylor series approximation is $\mathcal{F}(x) \approx x$, for small x . The asymptotic expansions of $C(x), S(x)$, and $\mathcal{F}(x)$ are for large positive x :

$$\begin{aligned} \mathcal{F}(x) &= \frac{1-j}{2} + \frac{j}{\pi x} e^{-j\pi x^2/2} \\ C(x) &= \frac{1}{2} + \frac{1}{\pi x} \sin\left(\frac{\pi}{2} x^2\right) \\ S(x) &= \frac{1}{2} - \frac{1}{\pi x} \cos\left(\frac{\pi}{2} x^2\right) \end{aligned} \quad (\text{F.4})$$

Associated with $C(x)$ and $S(x)$ are the type-2 Fresnel integrals:

$$C_2(x) = \int_0^x \frac{\cos t}{\sqrt{2\pi t}} dt, \quad S_2(x) = \int_0^x \frac{\sin t}{\sqrt{2\pi t}} dt \quad (\text{F.5})$$

They are combined into the complex function:

$$\mathcal{F}_2(x) = C_2(x) - jS_2(x) = \int_0^x \frac{e^{-jt}}{\sqrt{2\pi t}} dt \quad (\text{F.6})$$

The two types are related by, if $x \geq 0$:

$$C(x) = C_2\left(\frac{\pi}{2} x^2\right), \quad S(x) = S_2\left(\frac{\pi}{2} x^2\right), \quad \mathcal{F}(x) = \mathcal{F}_2\left(\frac{\pi}{2} x^2\right) \quad (\text{F.7})$$

and if $x < 0$, we set $\mathcal{F}(x) = -\mathcal{F}(-x) = -\mathcal{F}_2(\pi x^2/2)$.

The Fresnel function $\mathcal{F}_2(x)$ can be evaluated numerically using Boersma's approximation [1308], which achieves a maximum error of 10^{-9} over all x . The algorithm approximates the function $\mathcal{F}_2(x)$ as follows:

$$\mathcal{F}_2(x) = \begin{cases} e^{-jx} \sqrt{\frac{x}{4}} \sum_{n=0}^{11} (a_n + jb_n) \left(\frac{x}{4}\right)^n, & \text{if } 0 \leq x \leq 4 \\ \frac{1-j}{2} + e^{-jx} \sqrt{\frac{4}{x}} \sum_{n=0}^{11} (c_n + jd_n) \left(\frac{4}{x}\right)^n, & \text{if } x > 4 \end{cases} \quad (\text{F.8})$$

where the coefficients a_n, b_n, c_n, d_n are given in [1308]. Consistency with the small- and large- x expansions of $\mathcal{F}(x)$ requires that $a_0 + jb_0 = \sqrt{8/\pi}$ and $c_0 + jd_0 = j/\sqrt{8\pi}$. We have implemented Eq. (F.8) with the MATLAB function `fcs2`:

$$F2 = \text{fcs2}(x); \quad \% \text{ Fresnel integrals } \mathcal{F}_2(x) = C_2(x) - jS_2(x)$$

The ordinary Fresnel integral $\mathcal{F}(x)$ can be computed with the help of Eq. (F.7). The MATLAB function `fcs` calculates $\mathcal{F}(x)$ for any vector of values x by calling `fcs2`:

$$F = \text{fcs}(x); \quad \% \text{ Fresnel integrals } \mathcal{F}(x) = C(x) - jS(x)$$

In calculating the radiation patterns of pyramidal horns, it is desired to calculate a Fresnel diffraction integral of the type:

$$F_0(\nu, \sigma) = \int_{-1}^1 e^{j\pi\nu\xi} e^{-j(\pi/2)\sigma^2\xi^2} d\xi \quad (\text{F.9})$$

Making the variable change $t = \sigma\xi - \nu/\sigma$, this integral can be computed in terms of the Fresnel function $\mathcal{F}(x) = C(x) - jS(x)$ as follows:

$$F_0(\nu, \sigma) = \frac{1}{\sigma} e^{j(\pi/2)(\nu^2/\sigma^2)} \left[\mathcal{F}\left(\frac{\nu}{\sigma} + \sigma\right) - \mathcal{F}\left(\frac{\nu}{\sigma} - \sigma\right) \right] \quad (F.10)$$

where we also used the oddness of $\mathcal{F}(x)$. The value of Eq. (F.9) at $\nu = 0$ is:

$$F_0(0, \sigma) = \frac{1}{\sigma} [\mathcal{F}(\sigma) - \mathcal{F}(-\sigma)] = 2 \frac{\mathcal{F}(\sigma)}{\sigma} \quad (F.11)$$

Eq. (F.10) assumes that $\sigma \neq 0$. If $\sigma = 0$, the integral (F.9) reduces to the sinc function:

$$F_0(\nu, 0) = 2 \frac{\sin(\pi\nu)}{\pi\nu} \quad (F.12)$$

From either (F.11) or (F.12), we find $F_0(0, 0) = 2$. A related integral that is also required in the theory of horns is the following:

$$F_1(\nu, \sigma) = \int_{-1}^1 \cos\left(\frac{\pi\xi}{2}\right) e^{j\pi\nu\xi} e^{-j(\pi/2)\sigma^2\xi^2} d\xi \quad (F.13)$$

Writing $\cos(\pi\xi/2) = (e^{j\pi\xi/2} + e^{-j\pi\xi/2})/2$, the integral $F_1(\nu, \sigma)$ can be expressed in terms of $F_0(\nu, \sigma)$ as follows:

$$F_1(\nu, \sigma) = \frac{1}{2} [F_0(\nu + 0.5, \sigma) + F_0(\nu - 0.5, \sigma)] \quad (F.14)$$

It can be verified easily that $F_0(0.5, \sigma) = F_0(-0.5, \sigma)$, therefore, the value of $F_1(\nu, \sigma)$ at $\nu = 0$ will be given by:

$$F_1(0, \sigma) = F_0(0.5, \sigma) = \frac{1}{\sigma} e^{j\pi/(8\sigma^2)} \left[\mathcal{F}\left(\frac{1}{2\sigma} + \sigma\right) - \mathcal{F}\left(\frac{1}{2\sigma} - \sigma\right) \right] \quad (F.15)$$

Using the asymptotic expansion (F.4), we find the expansion valid for small σ :

$$\mathcal{F}\left(\frac{1}{2\sigma} \pm \sigma\right) = \frac{1-j}{2} \mp \frac{2\sigma}{\pi} e^{-j\pi/(8\sigma^2)}, \quad \text{for small } \sigma \quad (F.16)$$

For $\sigma = 0$, the integral $F_1(\nu, \sigma)$ reduces to the double-sinc function:

$$F_1(\nu, 0) = \int_{-1}^1 \cos\left(\frac{\pi\xi}{2}\right) e^{j\pi\nu\xi} d\xi = \frac{1}{2} [F_0(\nu + 0.5, 0) + F_0(\nu - 0.5, 0)] \quad (F.17)$$

$$= \frac{\sin(\pi(\nu + 0.5))}{\pi(\nu + 0.5)} + \frac{\sin(\pi(\nu - 0.5))}{\pi(\nu - 0.5)} = \frac{4}{\pi} \frac{\cos(\pi\nu)}{1 - 4\nu^2}$$

From either Eq. (F.16) or (F.17), we find $F_1(0, 0) = 4/\pi$.

The MATLAB function `diffint` can be used to evaluate both Eq. (F.9) and (F.13) for any vector of values ν and any vector of positive numbers σ , including $\sigma = 0$. It calls `fcs` to evaluate the diffraction integral (F.9) according to Eq. (F.10). Its usage is:

```
F0 = diffint(v, sigma, 0); % diffraction integral F0(v, sigma), Eq. (F.9)
F1 = diffint(v, sigma, 1); % diffraction integral F1(v, sigma), Eq. (F.13)
```

The vectors ν, σ can be entered either as rows or columns, but the result will be a matrix of size `length(v) x length(sigma)`. The integral $F_0(\nu, \sigma)$ can also be calculated by the simplified call:

```
F0 = diffint(v, sigma); % diffraction integral F0(v, sigma), Eq. (F.9)
```

Actually, the most general syntax of `diffint` is as follows:

```
F = diffint(v, sigma, a, c1, c2); % diffraction integral F(v, sigma, a), Eq. (F.18)
```

It evaluates the more general integral:

$$F(\nu, \sigma, a) = \int_{c_1}^{c_2} \cos\left(\frac{\pi\xi a}{2}\right) e^{j\pi\nu\xi} e^{-j(\pi/2)\sigma^2\xi^2} d\xi \quad (F.18)$$

For $a = 0$, we have:

$$F(\nu, \sigma, 0) = \frac{1}{\sigma} e^{j(\pi/2)(\nu^2/\sigma^2)} \left[\mathcal{F}\left(\frac{\nu}{\sigma} - \sigma c_1\right) - \mathcal{F}\left(\frac{\nu}{\sigma} - \sigma c_2\right) \right] \quad (F.19)$$

For $a \neq 0$, we can express $F(\nu, \sigma, a)$ in terms of $F(\nu, \sigma, 0)$:

$$F(\nu, \sigma, a) = \frac{1}{2} [F(\nu + 0.5a, \sigma, 0) + F(\nu - 0.5a, \sigma, 0)] \quad (F.20)$$

For $a = 0$ and $\sigma = 0$, $F(\nu, \sigma, a)$ reduces to the complex sinc function:

$$F(\nu, 0, 0) = \frac{e^{j\pi\nu c_2} - e^{j\pi\nu c_1}}{j\pi\nu} = (c_2 - c_1) \frac{\sin(\pi(c_2 - c_1)\nu/2)}{\pi(c_2 - c_1)\nu/2} e^{j\pi(c_2+c_1)\nu/2} \quad (F.21)$$

In Sommerfeld's half-space and knife-edge diffraction problems discussed in Sections 18.14 and 18.15, the following function represents the diffraction coefficient,

$$D(\nu) = \frac{1}{1-j} \int_{-\infty}^{\nu} e^{-j\pi u^2/2} du = \frac{1}{1-j} \left[\mathcal{F}(\nu) + \frac{1-j}{2} \right] \quad (F.22)$$

It is defined for any real ν and satisfies the properties,

$$D(\nu) + D(-\nu) = 1 \quad (F.23)$$

$$D(-\infty) = 0, \quad D(0) = \frac{1}{2}, \quad D(\infty) = 1 \quad (F.24)$$

The MATLAB function `diffrr.m` calculates $D(\nu)$ at any vector of (real) values of ν . It has usage:

```
D = diffr(v); % knife-edge diffraction coefficient D(v)
```

It may also be quickly defined as an anonymous MATLAB function in terms of `fcs`,

$$\text{diffr} = @(v) (\text{fcs}(v) + (1-j)/2) / (1-j);$$

The following integral, which was originally considered by Sommerfeld in his solution of the half-space problem, can be expressed in terms of the function $D(v)$,

$$I(\phi) \equiv \frac{1}{\pi} \int_0^\infty \frac{\cos(\phi/2) \cosh(t/2)}{\cos \phi + \cosh t} e^{-jk\rho \cosh t} dt \tag{F.25}$$

$$= \text{sign}(v) \cdot e^{jk\rho \cos \phi} \cdot [1 - D(|v|)], \quad v = \sqrt{\frac{4k\rho}{\pi}} \cos\left(\frac{\phi}{2}\right)$$

where $k\rho > 0$ and ϕ is a real angle, such that $\cos(\phi/2) \neq 0$, or, $\cos \phi \neq -1$. Equivalently,

$$I(\phi) = \begin{cases} e^{jk\rho \cos \phi} \cdot [1 - D(v)] = e^{jk\rho \cos \phi} \cdot D(-v), & \text{if } v > 0 \\ -e^{jk\rho \cos \phi} \cdot [1 - D(-v)] = -e^{jk\rho \cos \phi} \cdot D(v), & \text{if } v < 0 \end{cases} \tag{F.26}$$

where we used the property (F.23). The value at $\cos(\phi/2) = 0$ is discussed below. To show Eq. (F.25), we change variables to, $s = \sinh(t/2)$, $c = \cos(\phi/2)$. Then, doubling the range of integration and using the identities,

$$\cos \phi = 2 \cos^2\left(\frac{\phi}{2}\right) - 1, \quad \cosh t = 2 \sinh^2\left(\frac{t}{2}\right) + 1$$

the integral is transformed into,

$$I(\phi) = e^{jk\rho \cos \phi} \frac{1}{2\pi} \int_{-\infty}^\infty \frac{c}{c^2 + s^2} e^{-2jk\rho(c^2+s^2)} ds \tag{F.27}$$

Following Sommerfeld [1287], we divide out the factor $e^{jk\rho \cos \phi}$, and differentiate with respect to ρ ,

$$\frac{d}{d\rho} [I(\phi, k\rho) e^{-jk\rho \cos \phi}] = \frac{-jck}{\pi} e^{-2jk\rho c^2} \int_{-\infty}^\infty e^{-2jk\rho s^2} ds = -\frac{1}{1-j} \frac{ck}{\sqrt{\pi k\rho}} e^{-2jk\rho c^2} \tag{F.28}$$

where we used the definite integral,

$$\int_{-\infty}^\infty e^{-2jk\rho s^2} ds = \frac{1-j}{2} \sqrt{\frac{\pi}{k\rho}}$$

Introducing the variable $v = |c| \sqrt{4k\rho/\pi}$, we note that, $dv/d\rho = |ck|/\sqrt{\pi k\rho}$. Noting that, $c = \text{sign}(c) |c|$, we may change variables from ρ to v and rewrite (F.28) as,

$$\frac{d}{dv} [I(\phi) e^{-jk\rho \cos \phi}] = -\text{sign}(c) \frac{1}{1-j} e^{-j\pi v^2/2} \tag{F.29}$$

Integrating with respect to v , and fixing the integration constant by requiring that $I(\phi)$ vanish as $\rho \rightarrow \infty$ or $v \rightarrow \infty$, we obtain the required result,

$$I(\phi) e^{-jk\rho \cos \phi} = 1 - \frac{1}{1-j} \int_{-\infty}^v e^{-j\pi u^2/2} du = 1 - D(v)$$

where here, $v = \sqrt{4k\rho/\pi} |\cos(\phi/2)|$. Regarding the value at $c = 0$, we may distinguish the limits as $c \rightarrow \pm 0$. Using the following limit for the delta-function,

$$\lim_{c \rightarrow \pm 0} \frac{1}{\pi} \frac{c}{c^2 + s^2} = \pm \delta(s)$$

then, Eq. (F.27) has the following limiting values, noting that $\cos \phi = 2c^2 - 1 = -1$,

$$\lim_{c \rightarrow \pm 0} I(\phi) = \lim_{c \rightarrow \pm 0} e^{jk\rho \cos \phi} \frac{1}{2\pi} \int_{-\infty}^\infty \frac{c}{c^2 + s^2} e^{-2jk\rho(c^2+s^2)} ds = \pm \frac{1}{2} e^{-jk\rho}$$

These are consistent with the limits of Eq. (F.26) since $D(0) = 1/2$.

G. Exponential, Sine, and Cosine Integrals

Several antenna calculations, such as mutual impedances and directivities, can be reduced to the exponential integral, which is defined as follows [1790]:

$$E_1(z) = \int_z^\infty \frac{e^{-u}}{u} du = e^{-z} \int_0^\infty \frac{e^{-t}}{z+t} dt \quad (\text{exponential integral}) \tag{G.1}$$

where z is a complex number with phase restricted such that $|\arg z| < \pi$. This range allows pure imaginary z 's. The built-in MATLAB function `expint` evaluates $E_1(z)$ at an array of z 's. Related to $E_1(z)$ are the sine and cosine integrals:

$$S_i(z) = \int_0^z \frac{\sin u}{u} du \quad (\text{sine integral}) \tag{G.2}$$

$$C_i(z) = \gamma + \ln z + \int_0^z \frac{\cos u - 1}{u} du \quad (\text{cosine integral})$$

where γ is the Euler constant $\gamma = 0.5772156649\dots$. A related cosine integral is:

$$C_{in}(z) = \int_0^z \frac{1 - \cos u}{u} du = \gamma + \ln z - C_i(z) \tag{G.3}$$

For $z \geq 0$, the sine and cosine integrals are related to $E_1(z)$ by [1790]:

$$S_i(z) = \frac{E_1(jz) - E_1(-jz)}{2j} + \frac{\pi}{2} = \text{Im}[E_1(jz)] + \frac{\pi}{2} \tag{G.4}$$

$$C_i(z) = -\frac{E_1(jz) + E_1(-jz)}{2} = -\text{Re}[E_1(jz)]$$

while for $z \leq 0$, we have $S_i(z) = -S_i(-z)$ and $C_i(z) = C_i(-z) + j\pi$. Conversely, we have for $z > 0$:

$$E_1(jz) = -C_i(z) + j(S_i(z) - \frac{\pi}{2}) = -\gamma - \ln(z) + C_{in}(z) + j(S_i(z) - \frac{\pi}{2}) \tag{G.5}$$

The MATLAB functions `Si`, `Ci`, `Cin` evaluate the sine and cosine integrals at any vector of z 's by using the relations (G.4) and the built-in function `expint`:

$y = \text{Si}(z);$ % sine integral, Eq. (G.2)
 $y = \text{Ci}(z);$ % sine integral, Eq. (G.2)
 $y = \text{Cin}(z);$ % sine integral, Eq. (G.3)

A related integral that appears in calculating mutual and self impedances is what may be called a “Green’s function integral”:

$$\text{Gi}(d, z_0, h, s) = \int_0^h \frac{e^{-jkR}}{R} e^{-jksz} dz, \quad R = \sqrt{d^2 + (z - z_0)^2}, \quad s = \pm 1 \quad (\text{G.6})$$

This integral can be reduced to the exponential integral by the change of variables:

$$v = jk(R + s(z - z_0)) \Rightarrow s \frac{dv}{v} = \frac{dz}{R}$$

which gives

$$\int_0^h \frac{e^{-jkR}}{R} e^{-jksz} dz = se^{-jksz_0} \int_{v_0}^{v_1} \frac{e^{-u}}{u} du, \quad \text{or,}$$

$$\text{Gi}(d, z_0, h, s) = \int_0^h \frac{e^{-jkR}}{R} e^{-jksz} dz = se^{-jksz_0} [E_1(ju_0) - E_1(ju_1)] \quad (\text{G.7})$$

where

$$v_0 = ju_0, \quad u_0 = k \left[\sqrt{d^2 + z_0^2} - sz_0 \right]$$

$$v_1 = ju_1, \quad u_1 = k \left[\sqrt{d^2 + (h - z_0)^2} + s(h - z_0) \right]$$

The function Gi evaluates Eq. (G.7), where z_0, s , and the resulting integral J , can be vectors of the same dimension. Its usage is:

$J = \text{Gi}(d, z_0, h, s);$ % Green’s function integral, Eq. (G.7)

Another integral that appears commonly in antenna work is:

$$\int_0^\pi \frac{\cos(\alpha \cos \theta) - \cos \alpha}{\sin \theta} d\theta = S_i(2\alpha) \sin \alpha - C_{\text{in}}(2\alpha) \cos \alpha \quad (\text{G.8})$$

Its proof is straightforward by first changing variables to $z = \cos \theta$, then using partial fraction expansion, and finally changing variables to $u = \alpha(1 + z)$, and using the definitions (G.2) and (G.3):

$$\int_0^\pi \frac{\cos(\alpha \cos \theta) - \cos \alpha}{\sin \theta} d\theta = \int_{-1}^1 \frac{\cos(\alpha z) - \cos \alpha}{1 - z^2} dz$$

$$= \frac{1}{2} \int_{-1}^1 \frac{\cos(\alpha z) - \cos \alpha}{1 + z} dz + \frac{1}{2} \int_{-1}^1 \frac{\cos(\alpha z) - \cos \alpha}{1 - z} dz = \int_{-1}^1 \frac{\cos(\alpha z) - \cos \alpha}{1 + z} dz$$

$$= \int_0^{2\alpha} \frac{\cos(u - \alpha) - \cos \alpha}{u} du = \sin \alpha \int_0^{2\alpha} \frac{\sin u}{u} du - \cos \alpha \int_0^{2\alpha} \frac{1 - \cos u}{u} du$$

H. Stationary Phase Approximation

The Fresnel integrals find also application in the stationary-phase approximation for evaluating integrals. We note first that Eqs. (F.2) and (F.3) imply,

$$\int_{-\infty}^{\infty} e^{\pm j\pi t^2/2} dt = 1 \pm j = \sqrt{2} e^{\pm j\pi/4} \quad (\text{H.1})$$

and by changing variables of integration, we have the following integral, for any real α ,

$$\int_{-\infty}^{\infty} e^{j\alpha x^2/2} dx = \sqrt{\frac{2\pi}{|\alpha|}} e^{j\text{sign}(\alpha)\pi/4} = \sqrt{\frac{\pi}{|\alpha|}} (1 + j\text{sign}(\alpha)) \quad (\text{H.2})$$

The *stationary-phase approximation* is a way to approximate integrals of the following form, in the limit of the positive parameter $p \rightarrow \infty$,

$$\int_{-\infty}^{\infty} f(x) e^{jp\phi(x)} dx \quad (\text{H.3})$$

where $f(x), \phi(x)$ are real-valued. To simplify the notation, we will set $p = 1$. One can always replace $\phi(x)$ by $p\phi(x)$ in what follows. The stationary-phase approximation can then be stated as follows:

$$\int_{-\infty}^{\infty} f(x) e^{j\phi(x)} dx \simeq e^{j\text{sign}(\phi''(x_0))\pi/4} \sqrt{\frac{2\pi}{|\phi''(x_0)|}} f(x_0) e^{j\phi(x_0)} \quad (\text{H.4})$$

where x_0 is a *stationary point* of the phase $\phi(x)$, that is, the solution of $\phi'(x_0) = 0$, where for simplicity we assume that there is only one such point (otherwise, one has a sum of terms like (H.4), one for each solution of $\phi'(x) = 0$). Eq. (H.4) is obtained by expanding $\phi(x)$ in Taylor series about the stationary point $x = x_0$ and keeping only up to the quadratic term:

$$\phi(x) \simeq \phi(x_0) + \phi'(x_0)(x - x_0) + \frac{1}{2}\phi''(x_0)(x - x_0)^2 = \phi(x_0) + \frac{1}{2}\phi''(x_0)(x - x_0)^2$$

Making this approximation in the integral and assuming that $f(x)$ is slowly varying in the neighborhood of x_0 , we may replace $f(x)$ by its value at x_0 :

$$\int_{-\infty}^{\infty} f(x) e^{j\phi(x)} dx \simeq \int_{-\infty}^{\infty} f(x_0) e^{j(\phi(x_0) + \phi''(x_0)(x-x_0)^2/2)} dx$$

$$= f(x_0) e^{j\phi(x_0)} \int_{-\infty}^{\infty} e^{j\phi''(x_0)(x-x_0)^2/2} dx$$

and Eq. (H.4) is obtained by applying Eq. (H.2) to the above integral. The generalization to *two dimensions* is straightforward, the objective being to evaluate double-integrals of the following form in the limit, $p \rightarrow \infty$,

$$\int_{-\infty}^{\infty} \int_{-\infty}^{\infty} f(x, y) e^{jp\phi(x, y)} dx dy$$

As before, we will set $p = 1$. The phase function $\phi(x, y)$ is now expanded about a stationary point (x_0, y_0) , at which the partial derivatives of $\phi(x, y)$ vanish,

$$\frac{\partial \phi(x_0, y_0)}{\partial x} = \frac{\partial \phi(x_0, y_0)}{\partial y} = 0 \tag{H.5}$$

The Taylor series expansion about the point (x_0, y_0) can be written as the quadratic form,

$$\begin{aligned} \phi(x, y) &\simeq \phi(x_0, y_0) + \frac{1}{2} [\alpha(x - x_0)^2 + 2\gamma(x - x_0)(y - y_0) + \beta(y - y_0)^2] \\ &= \phi(x_0, y_0) + \frac{1}{2} [x - x_0, y - y_0] \begin{bmatrix} \alpha & \gamma \\ \gamma & \beta \end{bmatrix} \begin{bmatrix} x - x_0 \\ y - y_0 \end{bmatrix} \\ &= \phi(x_0, y_0) + \frac{1}{2} X^T \Phi X, \quad \text{where } X = \begin{bmatrix} x - x_0 \\ y - y_0 \end{bmatrix}, \quad \Phi = \begin{bmatrix} \alpha & \gamma \\ \gamma & \beta \end{bmatrix} \end{aligned}$$

and α, β, γ denote the second derivatives at (x_0, y_0) , that is,

$$\alpha = \frac{\partial^2 \phi(x_0, y_0)}{\partial x^2}, \quad \gamma = \frac{\partial^2 \phi(x_0, y_0)}{\partial x \partial y}, \quad \beta = \frac{\partial^2 \phi(x_0, y_0)}{\partial y^2}$$

The stationary-phase approximation becomes then,

$$\iint_{-\infty}^{\infty} f(x, y) e^{j\phi(x, y)} dx dy \simeq f(x_0, y_0) e^{j\phi(x_0, y_0)} \iint_{-\infty}^{\infty} e^{j\frac{1}{2} X^T \Phi X} dx dy$$

The above double integral can be reduced to the product of two integrals of the form of Eq. (H.2). The resulting approximation then takes the form:

$$\boxed{\iint_{-\infty}^{\infty} f(x, y) e^{j\phi(x, y)} dx dy \simeq e^{j(\sigma+1)\tau\frac{\pi}{4}} \frac{2\pi}{\sqrt{|\det \Phi|}} f(x_0, y_0) e^{j\phi(x_0, y_0)}} \tag{H.6}$$

where σ, τ are the signs of the determinant and trace of Φ , that is,

$$\begin{aligned} \sigma &= \text{sign}(\det \Phi) = \text{sign}(\alpha\beta - \gamma^2) \\ \tau &= \text{sign}(\text{tr} \Phi) = \text{sign}(\alpha + \beta) \end{aligned} \tag{H.7}$$

In particular, the phase factor takes the following three possible values, depending on whether the stationary point (x_0, y_0) is a local minimum, a local maximum, or a saddle point of $\phi(x, y)$,

$$e^{j(\sigma+1)\tau\frac{\pi}{4}} = \begin{cases} j, & \text{if } \det \Phi > 0, \text{ tr} \Phi > 0, \text{ (minimum)} \\ -j, & \text{if } \det \Phi > 0, \text{ tr} \Phi < 0, \text{ (maximum)} \\ 1, & \text{if } \det \Phi < 0, \text{ (saddle)} \end{cases} \tag{H.8}$$

In Eq. (H.8), the conditions $\text{tr} \Phi \leq 0$ can be replaced by the equivalent conditions $\alpha \leq 0$, or by, $\beta \leq 0$. This follows from the fact that, $\alpha\beta = \gamma^2 + \det \Phi$, so that if $\det \Phi > 0$, then $\alpha\beta > 0$, and α, β must have the same sign and hence the same sign as, $\text{tr} \Phi = \alpha + \beta$. Thus, τ can be replaced by $\text{sign}(\alpha)$ in (H.6).

The evaluation of the quadratic-phase integral $\iint_{-\infty}^{\infty} e^{j\frac{1}{2} X^T \Phi X} dx dy$ can be done in two ways, leading to Eq. (H.6). First, by the method of ‘‘completing the squares’’, and second, using the eigenvalue decomposition of the matrix Φ . In the first method, we note the following quadratic form identity (assuming $\alpha \neq 0$),

$$\begin{aligned} \frac{1}{2} X^T \Phi X &= \frac{1}{2} [\alpha(x - x_0)^2 + 2\gamma(x - x_0)(y - y_0) + \beta(y - y_0)^2] \\ &= \frac{1}{2} \alpha \left(x - x_0 + \frac{\gamma}{\alpha} (y - y_0) \right)^2 + \frac{1}{2} \frac{\alpha\beta - \gamma^2}{\alpha} (y - y_0)^2 = \frac{1}{2} \alpha \xi^2 + \frac{1}{2} \frac{\det \Phi}{\alpha} \eta^2 \end{aligned}$$

$$\text{where } \xi = x - x_0 + \frac{\gamma}{\alpha} (y - y_0), \quad \eta = y - y_0$$

and $dx dy = d\xi d\eta$. Thus, using Eq. (H.2),

$$\begin{aligned} \iint_{-\infty}^{\infty} e^{j\frac{1}{2} X^T \Phi X} dx dy &= \int_{-\infty}^{\infty} e^{j\alpha \xi^2 / 2} d\xi \cdot \int_{-\infty}^{\infty} e^{j\frac{\det \Phi}{\alpha} \eta^2 / 2} d\eta \\ &= \sqrt{\frac{2\pi}{|\alpha|}} e^{j\text{sign}(\alpha)\frac{\pi}{4}} \cdot \sqrt{\frac{2\pi}{|\det \Phi|/|\alpha|}} e^{j\text{sign}(\det \Phi/\alpha)\frac{\pi}{4}} \end{aligned}$$

and noting that, $\text{sign}\left(\frac{\det \Phi}{\alpha}\right) = \text{sign}(\alpha) \cdot \text{sign}(\det \Phi) = \text{sign}(\alpha) \cdot \sigma$, we obtain,

$$\iint_{-\infty}^{\infty} e^{j\frac{1}{2} X^T \Phi X} dx dy = e^{j(\sigma+1)\text{sign}(\alpha)\frac{\pi}{4}} \frac{2\pi}{\sqrt{|\det \Phi|}}$$

which leads to an equivalent expression to (H.6). In the eigenvalue method, the real-symmetric matrix Φ is diagonalized by a real orthogonal matrix V , that is, $\Phi = V\Lambda V^T$, where $\Lambda = \text{diag}\{\lambda_+, \lambda_-\}$, with the two real eigenvalues given by,

$$\lambda_{\pm} = \frac{\alpha + \beta \pm \sqrt{(\alpha - \beta)^2 + 4\gamma^2}}{2}$$

Then, the quadratic form splits with respect to the two orthogonal directions as follows,

$$\frac{1}{2} X^T \Phi X = \frac{1}{2} X^T (V\Lambda V^T) X = \frac{1}{2} \lambda_+ u_+^2 + \frac{1}{2} \lambda_- u_-^2, \quad \text{with } \begin{bmatrix} u_+ \\ u_- \end{bmatrix} = V^T X = V^T \begin{bmatrix} x - x_0 \\ y - y_0 \end{bmatrix}$$

and the quadratic phase integral becomes the product of two single ones,

$$\iint_{-\infty}^{\infty} e^{j\frac{1}{2} X^T \Phi X} dx dy = \iint_{-\infty}^{\infty} e^{j\frac{1}{2} \lambda_+ u_+^2 + j\frac{1}{2} \lambda_- u_-^2} du_+ du_- = e^{j(\text{sign}(\lambda_+) + \text{sign}(\lambda_-))\frac{\pi}{4}} \sqrt{\frac{(2\pi)^2}{|\lambda_+ \lambda_-|}}$$

where $dx dy = du_+ du_-$, since $|\det V| = 1$. The equivalence to (H.6) follows now by recognizing that, $\det \Phi = \lambda_+ \lambda_-$, $\text{tr} \Phi = \lambda_+ + \lambda_-$, and that,

$$\text{sign}(\lambda_+) + \text{sign}(\lambda_-) = (\text{sign}(\lambda_+ \lambda_-) + 1) \cdot \text{sign}(\lambda_+ + \lambda_-) = (\sigma + 1) \cdot \tau$$

When $\det \Phi = \lambda_+ \lambda_- > 0$, there can be two cases, either, $\lambda_+ > 0$ and $\lambda_- > 0$, leading to a local minimum of $\phi(x, y)$ at the stationary point (x_0, y_0) , or, $\lambda_+ < 0$ and $\lambda_- < 0$, leading to a local maximum. Similarly, if $\det \Phi < 0$, then λ_+, λ_- must have opposite signs, corresponding to a saddle point.

For more information and subtleties of the stationary phase method, the reader may consult references [1632-1639].

I. Gauss-Legendre and Double-Exponential Quadrature

In many parts of this book it is necessary to perform numerical integration. Gauss-Legendre quadrature is one of the best integration methods, and we have implemented it with the MATLAB functions `quadr` and `quadr8`. Below, we give a brief description of the method.[†] The integral over an interval $[a, b]$ is approximated by a sum of the form:

$$\int_a^b f(x) dx \approx \sum_{i=1}^N w_i f(x_i) \tag{I.1}$$

where w_i, x_i are appropriate weights and evaluation points (nodes). This can be written in the vectorial form:

$$\int_a^b f(x) dx \approx \sum_{i=1}^N w_i f(x_i) = [w_1, w_2, \dots, w_N] \begin{bmatrix} f(x_1) \\ f(x_2) \\ \vdots \\ f(x_N) \end{bmatrix} = \mathbf{w}^T f(\mathbf{x}) \tag{I.2}$$

The function `quadr` returns the column vectors of weights \mathbf{w} and nodes \mathbf{x} , with usage:

```
[w, x] = quadr(a, b, N); % Gauss-Legendre quadrature
```

The function `quadr8` allows the splitting of the interval $[a, b]$ into subintervals, computes N weights and nodes in each subinterval, and concatenates them to form the overall weight and node vectors \mathbf{w}, \mathbf{x} :

```
[w, x] = quadr8(ab, N); % Gauss-Legendre quadrature over subintervals
```

where `ab` is an array of endpoints that define the subintervals, for example,

```
ab = [a, b],           single interval
ab = [a, c, b],       two subintervals, [a, c] and [c, b]
ab = [a, c, d, b],    three subintervals, [a, c], [c, d], and [d, b]
ab = a : c : b,       subintervals, [a, a+c, a+2c, ..., a+Mc], with a + Mc = b
```

As an example, consider the following function and its exact integral:

$$f(x) = e^x + \frac{1}{x}, \quad J = \int_1^2 f(x) dx = e^2 - e^1 + \ln 2 = 5.36392145 \tag{I.3}$$

This integral can be evaluated numerically by the MATLAB code:

```
N = 5; % number of weights and nodes
[w, x] = quadr(1, 2, N); % calculate weights and nodes for the interval [1, 2]
f = exp(x) + 1./x; % evaluate f(x) at the node vector
J = w'*f % approximate integral
```

This produces the exact value with a 4.23×10^{-7} percentage error. If the integration interval is split in two, say, $[1, 1.5]$ and $[1.5, 2]$, then the second line above can be replaced by

[†]J. Stoer and R. Burlisch, *Introduction to Numerical Analysis*, Springer, NY, (1980); and, G. H. Golub and J. H. Welsch, "Calculation of Gauss Quadrature Rules," *Math. Comput.*, 23, 221 (1969).

```
[w, x] = quadr8([1, 1.5, 2], N); % or by, [w, x] = quadr8(1:0.5:2, N);
```

which has a percentage error of 1.28×10^{-9} . Next, we discuss the theoretical basis of the method.

The interval $[a, b]$ can be replaced by the standardized interval $[-1, 1]$ with the transformation from $a \leq x \leq b$ to $-1 \leq z \leq 1$:

$$x = \left(\frac{b-a}{2}\right)z + \left(\frac{b+a}{2}\right) \tag{I.4}$$

If w_i and z_i are the weights and nodes with respect to the interval $[-1, 1]$, then those with respect to $[a, b]$ can be constructed simply as follows, for $i = 1, 2, \dots, N$:

$$x_i = \left(\frac{b-a}{2}\right)z_i + \left(\frac{b+a}{2}\right) \tag{I.5}$$

$$w_i^x = \left(\frac{b-a}{2}\right)w_i$$

where the scaling of the weights follows from the scaling of the differentials $dx = dz(b-a)/2$, so the value of the integral (I.1) is preserved by the transformation.

Gauss-Legendre quadrature is nicely tied with the theory of orthogonal polynomials over the interval $[-1, 1]$, which are the Legendre polynomials. For N -point quadrature, the nodes $z_i, i = 1, 2, \dots, N$ are the N roots of the Legendre polynomial $P_N(z)$, which all lie in the interval $[-1, 1]$. The method is justified by the following theorem:

For any polynomial $P(z)$ of degree at most $2N - 1$, the quadrature formula (I.1) is satisfied *exactly*, that is,

$$\int_{-1}^1 P(z) dz = \sum_{i=1}^N w_i P(z_i) \tag{I.6}$$

provided that the z_i are the N roots of the Legendre polynomial $P_N(z)$.

The Legendre polynomials $P_n(z)$ are obtained via the process of Gram-Schmidt orthogonalization of the non-orthogonal monomial basis $\{1, z, z^2, \dots, z^n \dots\}$. Orthogonality is defined with respect to the following inner product over the interval $[-1, 1]$:

$$(f, g) = \int_{-1}^1 f(z)g(z) dz \tag{I.7}$$

The standard definition of the Legendre polynomials is:

$$P_n(z) = \frac{1}{2^n n!} \frac{d^n}{dz^n} [(z^2 - 1)^n], \quad n = 0, 1, 2, \dots \tag{I.8}$$

The first few of them are listed below:

$$P_0(z) = 1$$

$$P_1(z) = z$$

$$P_2(z) = (3/2)[z^2 - (1/3)] \tag{I.9}$$

$$P_3(z) = (5/2)[z^3 - (3/5)z]$$

$$P_4(z) = (35/8)[z^4 - (6/7)z^2 + (3/35)]$$

They are normalized such that $P_n(1) = 1$ and are mutually orthogonal with respect to (I.7), but do not have unit norm:

$$(P_n, P_m) = \int_{-1}^1 P_n(z)P_m(z) dz = \frac{2}{2n+1} \delta_{nm} \tag{I.10}$$

Moreover, they satisfy the three-term recurrence relation:

$$zP_n(z) = \left(\frac{n}{2n+1}\right)P_{n-1}(z) + \left(\frac{n+1}{2n+1}\right)P_{n+1}(z) \tag{I.11}$$

The Gram-Schmidt orthogonalization process of the monomial basis $f_n(z) = z^n$ is the following order-recursive construction:

$$\begin{aligned} &\text{initialize } P_0(z) = f_0(z) = 1 \\ &\text{for } n = 1, 2, 3, \dots, \text{ do} \\ &P_n(z) = f_n(z) - \sum_{k=0}^{n-1} \frac{(f_n, P_k)}{(P_k, P_k)} P_k(z) \end{aligned}$$

A few steps of the construction will clarify it:

$$P_1(z) = f_1(z) - \frac{(f_1, P_0)}{(P_0, P_0)} P_0(z) = z$$

where $(f_1, P_0) = (z, 1) = \int_{-1}^1 z dz = 0$. Then, construct P_2 by:

$$P_2(z) = f_2(z) - \frac{(f_2, P_0)}{(P_0, P_0)} P_0(z) - \frac{(f_2, P_1)}{(P_1, P_1)} P_1(z)$$

where now we have $(f_2, P_1) = (z^2, z) = \int_{-1}^1 z^3 dz = 0$, and

$$(f_2, P_0) = (z^2, 1) = \int_{-1}^1 z^2 dz = \frac{2}{3}, \quad (P_0, P_0) = (1, 1) = \int_{-1}^1 dz = 2$$

Therefore,

$$P_2(z) = z^2 - \frac{2/3}{2} = z^2 - \frac{1}{3}$$

Then, normalize it such that $P_2(1) = 1$, and so on. For our discussion, we are going to renormalize the Legendre polynomials to unit norm. Because of (I.10), this amounts to multiplying the standard $P_n(z)$ by the factor $\sqrt{(2n+1)/2}$. Thus, we re-define:

$$P_n(z) = \sqrt{\frac{2n+1}{2}} \frac{1}{2^n n!} \frac{d^n}{dz^n} [(z^2 - 1)^n], \quad n = 0, 1, 2, \dots \tag{I.12}$$

Thus, (I.10) becomes $(P_n, P_m) = \delta_{nm}$. In particular, we note that now

$$P_0(z) = \frac{1}{\sqrt{2}} \tag{I.13}$$

By introducing the same scaling factors into each term of the recurrence (I.11), we find that the renormalized $P_n(z)$ satisfy:

$$zP_n(z) = \alpha_n P_{n-1}(z) + \alpha_{n+1} P_{n+1}(z), \quad \alpha_n = \frac{n}{\sqrt{4n^2 - 1}} \tag{I.14}$$

This relationship can be assumed to be valid also at $n = 0$, provided we define $P_{-1}(z) = 0$. For each order n , the Gram-Schmidt procedure replaces the non-orthogonal monomial basis by the orthonormalized Legendre basis:

$$\{1, z, z^2, \dots, z^n\} \Leftrightarrow \{P_0(z), P_1(z), P_2(z), \dots, P_n(z)\}$$

Thus, any polynomial $Q(z)$ of degree n can be expanded uniquely in either basis:

$$Q(z) = \sum_{k=0}^n q_k z^k = \sum_{k=0}^n c_k P_k(z)$$

with the expansion coefficients calculated from $c_k = (Q, P_k)$. This also implies that if $Q(z)$ has order $n - 1$ then, it will be orthogonal to $P_n(z)$.

Next, we turn to the proof of the basic Gauss-Legendre result (I.6). Given a polynomial $P(z)$ of order $2N - 1$, we can expand it uniquely in the form:

$$P(z) = P_N(z)Q(z) + R(z) \tag{I.15}$$

where $Q(z)$ and $R(z)$ are the quotient and remainder of the division by the Legendre polynomial $P_N(z)$, and both will have order $N - 1$. Then, the integral of $P(z)$ can be written in inner-product notation as follows:

$$\int_{-1}^1 P(z) dz = (P, 1) = (P_N Q + R, 1) = (P_N Q, 1) + (R, 1) = (Q, P_N) + (R, 1)$$

But $(Q, P_N) = 0$ because $Q(z)$ has order $N - 1$ and $P_N(z)$ is orthogonal to all such polynomials. Thus, the integral of $P(z)$ can be expressed only in terms of the integral of the remainder polynomial $R(z)$, which has order $N - 1$:

$$\int_{-1}^1 P(z) dz = (P, 1) = (R, 1) = \int_{-1}^1 R(z) dz \tag{I.16}$$

The right-hand side of the integration rule (I.6) can also be expressed in terms of $R(z)$:

$$\sum_{i=1}^N w_i P(z_i) = \sum_{i=1}^N w_i P_N(z_i) Q(z_i) + \sum_{i=1}^N w_i R(z_i) \tag{I.17}$$

and, because we assumed that $P_N(z_i) = 0$,

$$\sum_{i=1}^N w_i P(z_i) = \sum_{i=1}^N w_i R(z_i) \tag{I.18}$$

Thus, combining (I.16) and (I.18), we obtain the following condition, which is equivalent to Eq. (I.6),

$$\int_{-1}^1 R(z) dz = \sum_{i=1}^N w_i R(z_i) \tag{I.19}$$

Because $R(z)$ is an arbitrary polynomial of degree $N - 1$, and has only N coefficients, this condition can be satisfied with a common set of N weights w_i for all such $R(z)$. If we had not assumed initially that the z_i were the zeros of $P_N(z)$, and took them to be an arbitrary set of N distinct points in $[-1, 1]$, then (I.19) would read as

$$\int_{-1}^1 R(z) dz = \sum_{i=1}^N w_i P_N(z_i) Q(z_i) + \sum_{i=1}^N w_i R(z_i)$$

In order for this to be satisfied for all $R(z)$ and all $Q(z)$, then (I.19) must still be satisfied by setting $Q(z) = 0$, which fixes the weights w_i . Therefore, the first term in the right-hand side must be zero for all polynomials $Q(z)$ of degree $N - 1$, and one can show that this implies that $P_N(z_i) = 0$, that is, the z_i must be the zeros of $P_N(z)$.

Condition (I.19) can be used to determine the weights by expanding $R(z)$ into either the monomial basis or the Legendre basis, that is, because $R(z)$ has degree $N - 1$:

$$R(z) = \sum_{k=0}^{N-1} r_k z^k = \sum_{k=0}^{N-1} c_k P_k(z) \tag{I.20}$$

Inserting, for example, the monomial basis into (I.19) and matching the coefficients of r_k on either side, we obtain the system of N equations for the weights:

$$\sum_{i=1}^N z_i^k w_i = \int_{-1}^1 z^k dz = \frac{1 + (-1)^k}{k + 1}, \quad k = 0, 1, \dots, N - 1 \tag{I.21}$$

Defining the matrix $F_{ki} = z_i^k$ and the vector $u_k = [1 + (-1)^k] / (k + 1)$, we may write (I.21) in the compact matrix form:

$$F \mathbf{w} = \mathbf{u} \quad \Rightarrow \quad \mathbf{w} = F^{-1} \mathbf{u} \tag{I.22}$$

Alternatively, we may use the Legendre basis, which is more elegant. The left hand side of (I.19) will receive contribution only from the $k = 0$ term because P_0 is orthogonal to all the succeeding P_k . Indeed, using the definition (I.13), we have:

$$\int_{-1}^1 R(z) dz = (R, 1) = \sqrt{2} (R, P_0) = \sqrt{2} \sum_{k=0}^{N-1} c_k (P_k, P_0) = \sqrt{2} \sum_{k=0}^{N-1} c_k \delta_{k0} = \sqrt{2} c_0$$

The right-hand side of (I.19) may be written as follows. Defining the $N \times N$ matrix $P_{ki} = P_k(z_i)$, $i = 1, 2, \dots, N$, and $k = 0, 1, \dots, N - 1$, and the row vector $\mathbf{c}^T = [c_0, c_1, \dots, c_{N-1}]$ of expansion coefficients, we have,

$$\sum_{i=1}^N w_i R(z_i) = \sum_{k=0}^{N-1} \sum_{i=1}^N c_k P_k(z_i) w_i = \mathbf{c}^T P \mathbf{w}$$

Thus, (I.19) now reads, where $\mathbf{u}_0 = [1, 0, 0, \dots, 0]^T$:

$$\mathbf{c}^T P \mathbf{w} = \sqrt{2} c_0 = \sqrt{2} \mathbf{c}^T \mathbf{u}_0$$

Because the vector \mathbf{c} is arbitrary, we must have the condition:

$$P \mathbf{w} = \sqrt{2} \mathbf{u}_0 \quad \Rightarrow \quad \mathbf{w} = \sqrt{2} P^{-1} \mathbf{u}_0 \tag{I.23}$$

The matrix P has some rather interesting properties. First, it has mutually orthogonal columns. Second, these columns are the eigenvectors of a Hermitian tridiagonal matrix whose eigenvalues are the zeros z_i . Thus, the problem of finding both z_i and w_i is reduced to an eigenvalue problem.

These eigenvalue properties follow from the recursion (I.14) of the normalized Legendre polynomials. For $n = 0, 1, 2, 3$, the recursion reads explicitly:

$$\begin{aligned} z P_0(z) &= \alpha_1 P_1(z) \\ z P_1(z) &= \alpha_1 P_0(z) + \alpha_2 P_2(z) \\ z P_2(z) &= \alpha_2 P_1(z) + \alpha_3 P_3(z) \\ z P_3(z) &= \alpha_3 P_2(z) + \alpha_4 P_4(z) \end{aligned}$$

which can be written in matrix form:

$$z \begin{bmatrix} P_0(z) \\ P_1(z) \\ P_2(z) \\ P_3(z) \end{bmatrix} = \begin{bmatrix} 0 & \alpha_1 & 0 & 0 \\ \alpha_1 & 0 & \alpha_2 & 0 \\ 0 & \alpha_2 & 0 & \alpha_3 \\ 0 & 0 & \alpha_3 & 0 \end{bmatrix} \begin{bmatrix} P_0(z) \\ P_1(z) \\ P_2(z) \\ P_3(z) \end{bmatrix} + \begin{bmatrix} 0 \\ 0 \\ 0 \\ \alpha_4 P_4(z) \end{bmatrix}$$

and more generally,

$$z \begin{bmatrix} P_0(z) \\ P_1(z) \\ P_2(z) \\ \vdots \\ P_{N-2}(z) \\ P_{N-1}(z) \end{bmatrix} = \begin{bmatrix} 0 & \alpha_1 & 0 & 0 & \cdots & 0 \\ \alpha_1 & 0 & \alpha_2 & 0 & \cdots & 0 \\ 0 & \alpha_2 & 0 & \alpha_3 & \cdots & 0 \\ \vdots & \ddots & \ddots & \ddots & \ddots & \vdots \\ 0 & \cdots & 0 & \alpha_{N-2} & 0 & \alpha_{N-1} \\ 0 & \cdots & 0 & 0 & \alpha_{N-1} & 0 \end{bmatrix} \begin{bmatrix} P_0(z) \\ P_1(z) \\ P_2(z) \\ \vdots \\ P_{N-2}(z) \\ P_{N-1}(z) \end{bmatrix} + \begin{bmatrix} 0 \\ 0 \\ 0 \\ \vdots \\ 0 \\ \alpha_N P_N(z) \end{bmatrix}$$

Now, if z is replaced by the i th zero z_i of $P_N(z)$, the last column will vanish and we obtain the eigenvalue equation:

$$\begin{bmatrix} 0 & \alpha_1 & 0 & 0 & \cdots & 0 \\ \alpha_1 & 0 & \alpha_2 & 0 & \cdots & 0 \\ 0 & \alpha_2 & 0 & \alpha_3 & \cdots & 0 \\ \vdots & \ddots & \ddots & \ddots & \ddots & \vdots \\ 0 & \cdots & 0 & \alpha_{N-2} & 0 & \alpha_{N-1} \\ 0 & \cdots & 0 & 0 & \alpha_{N-1} & 0 \end{bmatrix} \begin{bmatrix} P_0(z_i) \\ P_1(z_i) \\ P_2(z_i) \\ \vdots \\ P_{N-2}(z_i) \\ P_{N-1}(z_i) \end{bmatrix} = z_i \begin{bmatrix} P_0(z_i) \\ P_1(z_i) \\ P_2(z_i) \\ \vdots \\ P_{N-2}(z_i) \\ P_{N-1}(z_i) \end{bmatrix} \tag{I.24}$$

Denoting the above tridiagonal matrix by A and the column of $P_k(z_i)$'s by \mathbf{p}_i , we may write compactly:

$$A \mathbf{p}_i = z_i \mathbf{p}_i, \quad i = 1, 2, \dots, N \tag{I.25}$$

Thus, the eigenvalues of A are the zeros z_i and the corresponding eigenvectors are the columns \mathbf{p}_i of the matrix P that we introduced in (I.23). Because the zeros z_i are distinct and A is a Hermitian matrix, its eigenvectors will be mutually orthogonal:

$$\mathbf{p}_i^T \mathbf{p}_j = d_i^2 \delta_{ij} \tag{I.26}$$

where $d_i = \|\mathbf{p}_i\|$ are the norms of the vectors \mathbf{p}_i . It follows that the orthonormalized eigenvectors of A will be $\mathbf{v}_i = \mathbf{p}_i/d_i$, and the orthogonal matrix of eigenvectors having the \mathbf{v}_i as columns will be $V = [\mathbf{v}_1, \mathbf{v}_2, \dots, \mathbf{v}_N]$, or, expressed in terms of the matrix P and the diagonal matrix $D = \text{diag}\{d_1, d_2, \dots, d_N\}$:

$$V = PD^{-1} \tag{I.27}$$

Replacing P in (I.23) by $P = VD$ and using the orthogonality $V^T V = I$ of the eigenvector matrix, or $V^{-1} = V^T$, we obtain the solution:

$$\mathbf{w} = \sqrt{2} D^{-1} V^T \mathbf{u}_0 \Rightarrow w_i = \sqrt{2} d_i^{-1} (\mathbf{v}_i^T \mathbf{u}_0) \tag{I.28}$$

The matrix D can itself be expressed in terms of V by noting that the top entry of \mathbf{p}_i is $P_0(z_i) = 1/\sqrt{2}$, and therefore, it follows from $\mathbf{v}_i = \mathbf{p}_i/d_i$ that the top entry of \mathbf{v}_i will be $\mathbf{v}_i^T \mathbf{u}_0 = 1/(\sqrt{2}d_i)$, or, $d_i^{-1} = \sqrt{2}(\mathbf{v}_i^T \mathbf{u}_0)$. It finally follows from Eq. (I.28) that

$$w_i = d_i^{-2} = 2(\mathbf{v}_i^T \mathbf{u}_0)^2 \tag{I.29}$$

In MATLAB language, $\mathbf{v}_i^T \mathbf{u}_0 = V(1, i)$, that is, the first row of V . Because the eigenvectors of the Hermitian matrix A are real-valued and unique up to a sign, Eq. (I.29) allows the unique determination of the weights from the eigenvector matrix V .

The above discussion leads to two possible implementations of the MATLAB function `quadr`. In the first, we obtain the coefficients of the Legendre polynomial $P_N(z)$, find its zeros using the built-in function `root`, and then solve the linear equation (I.22) for the weights. The second approach, implemented by the function `quadr2` and the related function `quadr2s`, determines z_i, w_i from the eigenvalue problem of the matrix A .

Tanh-Sinh Double-Exponential Quadrature

Another quadrature integration procedure is the so-called *double-exponential* or *tanh-sinh* rule.[†] It is particularly effective in handling end-point singularities. According to this rule, the integral of a function $f(x)$ over the interval $[a, b]$ is approximated by the sum,

$$\int_a^b f(x) dx \approx \sum_{i=-N}^N w_i f(x_i) \tag{I.30}$$

with weights w_i and quadrature points x_i derived from,

[†]H. Takahasi and M. Mori, "Double exponential formulas for numerical integration," *Publications Res. Inst. Math. Sci., Kyoto Univ.*, 9, 721 (1974). See also, D. H. Bailey, K. Jeyabalan, and X. S. Li, "A Comparison of Three High-Precision Quadrature Schemes," *Experimental Math.*, 14, 317 (2005), and, A. G. Polimeridis and J. R. Mosig, "Evaluation of Weakly Singular Integrals Via Generalized Cartesian Product Rules Based on the Double Exponential Formula," *IEEE Trans. Antennas Propagat.*, 58, 1980 (2010).

$$\begin{aligned} t_i &= hi, \quad -N \leq i \leq N \\ x_i &= \left(\frac{b-a}{2}\right) \tanh\left(\frac{\pi}{2} \sinh(t_i)\right) + \left(\frac{b+a}{2}\right) \\ w_i &= \left(\frac{b-a}{2}\right) \frac{h\pi}{2} \frac{\cosh(t_i)}{\cosh^2\left(\frac{\pi}{2} \sinh(t_i)\right)} \end{aligned} \tag{I.31}$$

The spacing h and number N are determined from the rules:

$$h = 2^{-M}, \quad N = 6 \cdot 2^M \tag{I.32}$$

where M is selected by the user, with typical values $M = 4-8$. The MATLAB function `quadts.m` implements Eqs. (I.31)-(I.32) and returns the column vectors of weights w_i and quadrature points x_i .

```
[w, x] = quadts(a, b, M); % tanh-sinh double-exponential quadrature
```

For the same example of Eq. (I.3), the following code segment illustrates the usage of the function,

```
M=3;
[w, x] = quadts(1, 2, M);
f = exp(x) + 1./x;
J = w'*f; % approximate integral
```

For $M = 2$ and $M = 3$, it produces the exact value with 6.87×10^{-10} and 1.66×10^{-14} percentage errors.

If the integrand has singularities at the end-points a, b of the integration interval, then replacing the interval $[a, b]$ by $[a+\epsilon, b]$ or $[a, b-\epsilon]$ often works well. This is done, for example, in the implementation of the Bethe-Bouwkamp function `BBnum.m`, described in Sec. 19.12.

J. Prolate Spheroidal Wave Functions

Prolate spheroidal wave functions (PSWF) of order zero provide an ideal basis for representing bandlimited signals that are also maximally concentrated in a finite time interval. They were extensively studied by Slepian, Pollak, and Landau in a series of papers [1643-1647] and have since been applied to a wide variety of applications, such as signal extrapolation, deconvolution, communication systems, waveform design, antennas, diffraction-limited optical systems, laser resonators, and acoustics.

In this Appendix, we summarize their properties and provide a MATLAB function for their computation. We will use them in Sec. 20.22 in our discussion of superresolution and its dual, supergain, and their relationship to superoscillations. Further details may be found in references [1643-1679].

Definition

The PSWF functions are defined with respect to two intervals: a frequency interval, $[-\omega_0, \omega_0]$ (rad/sec), over which they are bandlimited, and a time interval, $[-t_0, t_0]$ (sec), over which they are concentrated (but not limited to).

For notational convenience let us define the following three function spaces: (a) the space \mathcal{L}_∞^2 of functions $f(t)$ that are square-integrable over the real line, $-\infty < t < \infty$, (b) the space $\mathcal{L}_{t_0}^2$ of functions $f(t)$ that are square-integrable over the finite interval $[-t_0, t_0]$, and (c) the subspace \mathcal{B}_{ω_0} of \mathcal{L}_∞^2 of bandlimited functions $f(t)$ whose Fourier transform $\hat{f}(\omega)$ vanishes outside the interval $[-\omega_0, \omega_0]$, that is, $\hat{f}(\omega) = 0$ for $|\omega| > \omega_0$, so that they are representable in the form,

$$f(t) = \int_{-\omega_0}^{\omega_0} \hat{f}(\omega) e^{j\omega t} \frac{d\omega}{2\pi}, \quad \hat{f}(\omega) = \int_{-\infty}^{\infty} f(t) e^{-j\omega t} dt \tag{J.1}$$

The PSWF functions, denoted here by $\psi_n(t)$ with $n = 0, 1, 2, \dots$, belong to the subspace \mathcal{B}_{ω_0} and are defined by the following equivalent expansions in terms of Legendre polynomials or spherical Bessel functions:

$$\psi_n(t) = \sqrt{\frac{\lambda_n}{t_0}} \sum_k \beta_{nk} \sqrt{k + \frac{1}{2}} P_k\left(\frac{t}{t_0}\right) = \sqrt{\frac{c}{2\pi t_0}} \sum_k \beta_{nk} \sqrt{k + \frac{1}{2}} 2i^{k-n} j_k(\omega_0 t) \tag{J.2}$$

for $n = 0, 1, 2, \dots$, where β_{nk} are the expansion coefficients, c is the *time-bandwidth product*, $c = t_0\omega_0$, and λ_n are the positive eigenvalues (listed in decreasing order) and $\psi_n(t)$ the corresponding eigenfunctions of the following linear integral operator with the sinc-kernel:

$$\int_{-t_0}^{t_0} \frac{\sin(\omega_0(t-t'))}{\pi(t-t')} \psi_n(t') dt' = \lambda_n \psi_n(t) \quad n = 0, 1, 2, \dots, \quad \text{for all } t \tag{J.3}$$

The Legendre polynomial expansion in (J.2) is numerically accurate for $|t| \leq t_0$, whereas the spherical Bessel function expansion is valid for all t , and we use that in our MATLAB implementation. The unnormalized Legendre polynomials $P_k(x)$ were defined in Eq. (I.8) of Appendix I. The normalized Legendre polynomials are $\sqrt{k + \frac{1}{2}} P_k(x)$. The spherical Bessel functions $j_k(x)$ are defined in terms of the ordinary Bessel functions of half-integer order:

$$j_k(x) = \sqrt{\frac{\pi}{2x}} J_{k+\frac{1}{2}}(x) \tag{J.4}$$

The eigenvalues λ_n are distinct and lie in the interval, $0 < \lambda_n < 1$. Typically, they have values near unity, $\lambda_n \approx 1$, for $n = 0, 1, 2, \dots$, up to about the so-called Shannon number, $N_c = 2c/\pi$, and after that they drop rapidly towards zero. The Shannon number represents roughly the number of *degrees of freedom* for characterizing a signal of total frequency bandwidth $\Omega = 2\omega_0$ and total time duration $T = 2t_0$. If F is the total bandwidth in Hz, that is, $F = \Omega/2\pi$, then, $N_c = FT$,

$$N_c = \frac{2c}{\pi} = \frac{2\omega_0 t_0}{\pi} = \frac{2\omega_0 2t_0}{2\pi} = \frac{\Omega T}{2\pi} = FT \tag{J.5}$$

Since, $j_k(\omega_0 t) = j_k(ct/t_0)$, we note that up to a scale factor, $\psi_n(t)$ is a function of c and the scaled variable $\eta = t/t_0$. Indeed, we have, $\psi_n(t) = t_0^{-1/2} \phi_n(c, t/t_0)$, where,

$$\phi_n(c, \eta) = \sqrt{\lambda_n} \sum_k \beta_{nk} \sqrt{k + \frac{1}{2}} P_k(\eta) = \sqrt{\frac{c}{2\pi}} \sum_k \beta_{nk} \sqrt{k + \frac{1}{2}} 2i^{k-n} j_k(c\eta) \tag{J.6}$$

We will also use the following notation to indicate explicitly the dependence on the parameters t_0, ω_0 and $c = t_0\omega_0$,

$$\psi_n(t_0, \omega_0, t) = \frac{1}{\sqrt{t_0}} \phi_n\left(c, \frac{t}{t_0}\right) \tag{J.7}$$

The k -summation in (J.2) goes over $0 \leq k < \infty$. However, k takes only even values, $k = 0, 2, 4, \dots$, when n is even or zero, and only odd values, $k = 1, 3, 5, \dots$, when n is odd. This also implies that $\psi_n(t)$ is an even function of t , if n is even, and odd in t , if n is odd, so that, $\psi_n(-t) = (-1)^n \psi_n(t)$. The expansion coefficients β_{nk} are real-valued and because n, k have the same parity, i.e., $n - k$ is even, it follows that the number i^{k-n} will be real, $i^{k-n} = (-1)^{(k-n)/2}$. Therefore, all $\psi_n(t)$ are real-valued.

The k -summation can be extended to all $k \geq 0$ by redefining the expansion coefficients β_{nk} for all k by appropriately interlacing zeros as follows:

$$\beta_{nk} = \begin{cases} [\beta_{n0}, 0, \beta_{n2}, 0, \beta_{n4}, 0, \dots] & (n \text{ even}) \\ [0, \beta_{n1}, 0, \beta_{n3}, 0, \beta_{n5}, \dots] & (n \text{ odd}) \end{cases} \tag{J.8}$$

The expansion coefficients are chosen to satisfy the orthogonality property,

$$\sum_{k=0}^{\infty} \beta_{nk} \beta_{mk} = \delta_{nm} \quad n, m = 0, 1, 2, \dots \tag{J.9}$$

This particular normalization is computationally convenient and enables the orthogonality properties of the $\psi_n(t)$ functions, that is, Eqs. (J.24) and (J.26). The coefficients β_{nk} may be constructed as the orthonormal eigenvectors of a real symmetric tridiagonal matrix as we discuss below. We note also that for large t , the PSWF functions behave like sinc-functions [1643,1658],

$$\psi_n(t) \approx \sqrt{\frac{2c}{\pi\lambda_n}} \psi_n(t_0) \frac{\sin(\omega_0 t - \frac{1}{2}\pi n)}{\omega_0 t}, \quad \text{for large } |t| \tag{J.10}$$

This follows from the asymptotic expansion of the spherical Bessel functions,

$$j_k(x) \approx \frac{\sin(x - \frac{1}{2}\pi k)}{x}, \quad \text{for large } |x|$$

Fourier Transform

The bandlimited Fourier transform of $\psi_n(t)$ can be constructed as follows. First, we note that $P_k(x)$ and $j_k(x)$ satisfy the following Fourier transform relationships [1822]:

$$\int_{-1}^1 e^{j\omega t} \pi i^{-k} P_k(\omega) \frac{d\omega}{2\pi} = j_k(t), \quad \text{for all real } t$$

$$\int_{-\infty}^{\infty} e^{-j\omega t} j_k(t) dt = \pi i^{-k} P_k(\omega) \cdot \chi_1(\omega) = \begin{cases} \pi i^{-k} P_k(\omega), & |\omega| < 1 \\ 0, & |\omega| > 1 \end{cases} \quad (\text{J.11})$$

where $\chi_1(\omega)$ is the indicator function for the interval $[-1, 1]$, defined in terms of the unit-step function $u(x)$ as follows for a more general interval $[-\omega_0, \omega_0]$,[†]

$$\chi_{\omega_0}(\omega) = u(\omega_0 - |\omega|) = \begin{cases} 1, & |\omega| < \omega_0 \\ 0, & |\omega| > \omega_0 \end{cases} \quad (\text{J.12})$$

It follows that the Fourier transform $\hat{j}_k(\omega)$ of $j_k(\omega_0 t)$ is bandlimited over $[-\omega_0, \omega_0]$,

$$\hat{j}_k(\omega) = \int_{-\infty}^{\infty} e^{-j\omega t} j_k(\omega_0 t) dt = \frac{\pi}{\omega_0 i^k} P_k\left(\frac{\omega}{\omega_0}\right) \cdot \chi_{\omega_0}(\omega)$$

$$j_k(\omega_0 t) = \int_{-\omega_0}^{\omega_0} e^{j\omega t} \hat{j}_k(\omega) \frac{d\omega}{2\pi} = \int_{-\omega_0}^{\omega_0} e^{j\omega t} \frac{\pi}{\omega_0 i^k} P_k\left(\frac{\omega}{\omega_0}\right) \frac{d\omega}{2\pi} \quad (\text{J.13})$$

In fact, the functions $j_k(\omega_0 t)$, like the $\psi_n(t)$, form a *complete and orthogonal basis* of the subspace \mathcal{B}_{ω_0} , see [1678,1679]. Their mutual orthogonality follows from Parseval's identity and the orthogonality property (I.10) of the Legendre polynomials:

$$\int_{-\infty}^{\infty} j_k(\omega_0 t) j_n(\omega_0 t) dt = \int_{-\omega_0}^{\omega_0} \hat{j}_k^*(\omega) \hat{j}_n(\omega) \frac{d\omega}{2\pi} = \frac{\pi}{\omega_0} \frac{\delta_{kn}}{2k+1} \quad (\text{J.14})$$

The bandlimited Fourier transform $\hat{\psi}_n(\omega)$ of $\psi_n(t)$ can now be obtained by Fourier-transforming the spherical Bessel function expansion in (J.2), then using (J.13), and comparing the result with the Legendre expansion of (J.2), that is,

$$\hat{\psi}_n(\omega) = \sqrt{\frac{c}{2\pi t_0}} \sum_k \beta_{nk} \sqrt{k + \frac{1}{2}} 2i^{k-n} \hat{j}_k(\omega)$$

$$= \sqrt{\frac{c}{2\pi t_0}} \sum_k \beta_{nk} \sqrt{k + \frac{1}{2}} 2i^{k-n} \frac{\pi}{\omega_0 i^k} P_k\left(\frac{\omega}{\omega_0}\right) \cdot \chi_{\omega_0}(\omega)$$

$$= \frac{2\pi}{\omega_0} \frac{1}{\mu_n} \underbrace{\sqrt{\frac{\lambda_n}{t_0}} \sum_k \beta_{nk} \sqrt{k + \frac{1}{2}} P_k\left(\frac{\omega}{\omega_0}\right)}_{\psi_n(\omega t_0/\omega_0)} \cdot \chi_{\omega_0}(\omega) = \frac{2\pi}{\omega_0} \frac{1}{\mu_n} \psi_n\left(\frac{\omega t_0}{\omega_0}\right) \cdot \chi_{\omega_0}(\omega)$$

where μ_n was defined in terms of λ_n as follows:

$$\mu_n = i^n |\mu_n|, \quad |\mu_n| = \sqrt{\frac{2\pi\lambda_n}{c}} \Rightarrow \lambda_n = \frac{c}{2\pi} |\mu_n|^2 \quad (\text{J.15})$$

[†] $\chi_{\omega_0}(\omega)$ may be defined to have the value $\frac{1}{2}$ at $\omega = \pm\omega_0$ corresponding to the unit-step value $u(0) = \frac{1}{2}$.

Thus, we find that $\hat{\psi}_n(\omega)$ is a scaled version of $\psi_n(t)$ itself,

$$\hat{\psi}_n(\omega) = \int_{-\infty}^{\infty} e^{-j\omega t} \psi_n(t) dt = \frac{2\pi}{\omega_0} \frac{1}{\mu_n} \psi_n\left(\frac{\omega t_0}{\omega_0}\right) \cdot \chi_{\omega_0}(\omega) \quad (\text{J.16})$$

The inverse Fourier transform brings out more clearly the meaning of μ_n :

$$\psi_n(t) = \int_{-\omega_0}^{\omega_0} e^{j\omega t} \hat{\psi}_n(\omega) \frac{d\omega}{2\pi} \Rightarrow \int_{-\omega_0}^{\omega_0} e^{j\omega t} \psi_n\left(\frac{\omega t_0}{\omega_0}\right) \frac{d\omega}{\omega_0} = \mu_n \psi_n(t) \quad (\text{J.17})$$

for all t . By changing variables to $\omega \rightarrow t\omega_0/t_0$ and $t \rightarrow \omega t_0/\omega_0$, we also have,

$$\int_{-t_0}^{t_0} e^{j\omega t} \psi_n(t) \frac{dt}{t_0} = \mu_n \psi_n\left(\frac{\omega t_0}{\omega_0}\right) \quad \text{for all } \omega \quad (\text{J.18})$$

If (J.17) is written in terms of the scaled function $\phi_n(\eta)$ of (J.6), then μ_n is the eigenvalue and $\phi_n(\eta)$ the eigenfunction of the following integral operator with exponential kernel:

$$\int_{-1}^1 e^{j\eta\xi} \phi_n(\xi) d\xi = \mu_n \phi_n(\eta) \quad n = 0, 1, 2, \dots, \quad \text{and all } \eta \quad (\text{J.19})$$

Similarly, (J.3) reads as follows with respect to $\phi_n(\eta)$,

$$\int_{-1}^1 \frac{\sin(c(\eta - \xi))}{\pi(\eta - \xi)} \phi_n(\xi) d\xi = \lambda_n \phi_n(\eta) \quad \text{for all } \eta \quad (\text{J.20})$$

Eqs. (J.3) and (J.15) can be derived from Eqs. (J.17) and (J.18). Indeed, multiplying both sides of (J.17) by μ_n^* and taking the complex conjugate of (J.18), we have,

$$|\mu_n|^2 \psi_n(t) = \int_{-\omega_0}^{\omega_0} \mu_n^* \psi_n\left(\frac{\omega t_0}{\omega_0}\right) e^{j\omega t} \frac{d\omega}{\omega_0} = \int_{-\omega_0}^{\omega_0} \left[\int_{-t_0}^{t_0} e^{-j\omega t'} \psi_n(t') \frac{dt'}{t_0} \right] e^{j\omega t} \frac{d\omega}{\omega_0}$$

$$= \frac{2\pi}{t_0 \omega_0} \int_{-t_0}^{t_0} \left[\int_{-\omega_0}^{\omega_0} e^{j\omega(t-t')} \frac{d\omega}{2\pi} \right] \psi_n(t') dt' = \frac{2\pi}{c} \int_{-t_0}^{t_0} \frac{\sin(\omega_0(t-t'))}{\pi(t-t')} \psi_n(t') dt'$$

where we used the sinc-function transform,

$$\frac{\sin(\omega_0 t)}{\pi t} = \int_{-\infty}^{\infty} \chi_{\omega_0}(\omega) e^{j\omega t} \frac{d\omega}{2\pi} = \int_{-\omega_0}^{\omega_0} e^{j\omega t} \frac{d\omega}{2\pi} \quad (\text{J.21})$$

Eq. (J.3) follows now by multiplying both sides by $c/2\pi$ and using the definition (J.15). Any function $f(t)$ in \mathcal{B}_{ω_0} with a bandlimited Fourier transform $\hat{f}(\omega)$ over $[-\omega_0, \omega_0]$ satisfies a similar sinc-kernel integral equation, but over the infinite time interval, $-\infty < t < \infty$. Indeed, using the convolution theorem of Fourier transforms and (J.21), we have,

$$f(t) = \int_{-\omega_0}^{\omega_0} \hat{f}(\omega) e^{j\omega t} \frac{d\omega}{2\pi} = \int_{-\infty}^{\infty} \chi_{\omega_0}(\omega) \hat{f}(\omega) e^{j\omega t} \frac{d\omega}{2\pi} = \int_{-\infty}^{\infty} \frac{\sin(\omega_0(t-t'))}{\pi(t-t')} f(t') dt'$$

that is, for $f(t) \in \mathcal{B}_{\omega_0}$ and for all t ,

$$f(t) = \int_{-\infty}^{\infty} \frac{\sin(\omega_0(t-t'))}{\pi(t-t')} f(t') dt' \quad (J.22)$$

Thus, because they lie in \mathcal{B}_{ω_0} , all $\psi_n(t)$ satisfy a similar condition,

$$\int_{-\infty}^{\infty} \frac{\sin(\omega_0(t-t'))}{\pi(t-t')} \psi_n(t') dt' = \psi_n(t), \quad \text{for all } t \quad (J.23)$$

Orthogonality and Completeness Properties

The PSWF functions $\psi_n(t)$ satisfy *dual* orthogonality and completeness properties, that is, the $\psi_n(t)$ functions form an orthogonal and complete basis for both $\mathcal{L}_{t_0}^2$ and \mathcal{B}_{ω_0} . With respect to the space $\mathcal{L}_{t_0}^2$, we have,

$$\boxed{\int_{-t_0}^{t_0} \psi_n(t) \psi_m(t) dt = \lambda_n \delta_{nm}} \quad (\text{orthogonality}) \quad (J.24)$$

$$\boxed{\sum_{n=0}^{\infty} \frac{1}{\lambda_n} \psi_n(t) \psi_n(t') = \delta(t-t')} \quad (\text{completeness}) \quad (J.25)$$

for $t, t' \in [-t_0, t_0]$. And, with respect to the subspace \mathcal{B}_{ω_0} , we have for the infinite time interval, $-\infty < t < \infty$,

$$\boxed{\int_{-\infty}^{\infty} \psi_n(t) \psi_m(t) dt = \delta_{nm}} \quad (J.26)$$

$$\boxed{\sum_{n=0}^{\infty} \psi_n(t) \psi_n(t') = \frac{\sin(\omega_0(t-t'))}{\pi(t-t')}} \quad \text{for all } t, t' \quad (J.27)$$

Eq. (J.24) can be derived from the Legendre expansion in (J.2) as a consequence of the normalization condition (J.9) and the Legendre polynomial orthogonality (I.10). Similarly, (J.26) can be derived from the spherical Bessel function expansion and (J.14).

The sinc-kernel in (J.27) plays the role of the identity operator for functions in \mathcal{B}_{ω_0} , as implied by (J.22). Taking the limit $t' \rightarrow t$ on both sides of (J.27), we obtain the following relationship, valid for all t ,

$$\sum_{n=0}^{\infty} \psi_n^2(t) = \frac{\omega_0}{\pi} \quad (J.28)$$

Integrating this over $[-t_0, t_0]$ and using (J.24) for $n = m$, we obtain the sums,

$$\sum_{n=0}^{\infty} \lambda_n = \frac{2c}{\pi} = N_c \quad \Rightarrow \quad \sum_{n=0}^{\infty} |\mu_n|^2 = 4 \quad (J.29)$$

Another identity can be derived from (J.27) by taking Fourier transforms of both sides with respect to the variable t' and using the delay theorem of Fourier transforms on the right-hand-side, resulting in,

$$e^{-j\omega t} \cdot \chi_{\omega_0}(\omega) = \sum_{n=0}^{\infty} \psi_n(t) \hat{\psi}_n(\omega) = \frac{2\pi}{\omega_0} \chi_{\omega_0}(\omega) \sum_{n=0}^{\infty} \frac{1}{\mu_n} \psi_n(t) \psi_n\left(\frac{\omega t_0}{\omega_0}\right), \quad \text{or,}$$

$$\frac{2\pi}{\omega_0} \sum_{n=0}^{\infty} \frac{1}{\mu_n} \psi_n(t) \psi_n\left(\frac{\omega t_0}{\omega_0}\right) = e^{-j\omega t}, \quad \text{for all } t \text{ and } |\omega| < \omega_0 \quad (J.30)$$

and in particular, setting $\omega = 0$, we have for all t ,

$$\frac{2\pi}{\omega_0} \sum_{n=0}^{\infty} \frac{1}{\mu_n} \psi_n(0) \psi_n(t) = 1 \quad (J.31)$$

Eqs. (J.27)–(J.31) are demonstrated in Examples J.1–J.2. The completeness property (J.25) can also be derived by complex-conjugating both sides of (J.30) and taking Fourier transforms with respect to the variable t , denoting the corresponding frequency by ω' , with $|\omega'| < \omega_0$,

$$\frac{2\pi}{\omega_0} \sum_{n=0}^{\infty} \frac{1}{\mu_n^*} \hat{\psi}_n(\omega') \psi_n\left(\frac{\omega t_0}{\omega_0}\right) = 2\pi \delta(\omega - \omega'), \quad \text{or,}$$

$$\frac{(2\pi)^2}{\omega_0^2} \sum_{n=0}^{\infty} \frac{1}{|\mu_n|^2} \psi_n\left(\frac{\omega t_0}{\omega_0}\right) \psi_n\left(\frac{\omega' t_0}{\omega_0}\right) = 2\pi \delta(\omega - \omega')$$

or, using the relationship, $|\mu_n|^2 = 2\pi\lambda_n/c$,

$$\sum_{n=0}^{\infty} \frac{1}{\lambda_n} \psi_n\left(\frac{\omega t_0}{\omega_0}\right) \psi_n\left(\frac{\omega' t_0}{\omega_0}\right) = \delta\left(\frac{\omega t_0}{\omega_0} - \frac{\omega' t_0}{\omega_0}\right) \quad (J.32)$$

for $\omega, \omega' \in [-\omega_0, \omega_0]$. This becomes equivalent to Eq. (J.25) after replacing, $\omega t_0/\omega_0 \rightarrow t$ and $\omega' t_0/\omega_0 \rightarrow t'$, with $t, t' \in [-t_0, t_0]$. In a similar fashion, Eq. (J.24) can be derived by applying Parseval's identity to (J.26).

Signal Restoration

Another application is in *signal restoration*, such as image restoration through a finite-aperture diffraction-limited optical system, involving the inversion of the sinc-kernel over the finite interval $[-t_0, t_0]$, that is, finding a kernel function, say, $K(t, t')$, that performs the inverse operation,

$$g(t) = \int_{t_0}^{t_0} \frac{\sin(\omega_0(t-t'))}{\pi(t-t')} f(t') dt' \quad \Rightarrow \quad f(t) = \int_{-t_0}^{t_0} K(t, t') g(t') dt' \quad (J.33)$$

for $|t| \leq t_0$. It is easily verified that $K(t, t')$ is given formally by [1569],[†]

$$K(t, t') = \sum_n \frac{1}{\lambda_n^2} \psi_n(t) \psi_n(t'), \quad \text{for } t, t' \in [-t_0, t_0] \quad (J.34)$$

[†]A more precise meaning may be given to (J.34) by the regularized versions discussed below.

The operation of $K(t, t')$ on the sinc-kernel generates the identity kernel, that is,

$$\int_{-t_0}^{t_0} K(t, t'') \frac{\sin(\omega_0(t'' - t'))}{\pi(t'' - t')} dt'' = \delta(t - t'), \quad \text{for } t, t' \in [-t_0, t_0] \quad (\text{J.35})$$

Indeed, using (J.24), (J.25), (J.27), and (J.34), we have,

$$\begin{aligned} & \int_{-t_0}^{t_0} K(t, t'') \frac{\sin(\omega_0(t'' - t'))}{\pi(t'' - t')} dt'' = \\ &= \int_{-t_0}^{t_0} \left[\sum_n \frac{1}{\lambda_n^2} \psi_n(t) \psi_n(t'') \right] \left[\sum_m \psi_m(t'') \psi_m(t') \right] dt'' \\ &= \sum_n \sum_m \frac{1}{\lambda_n^2} \psi_n(t) \underbrace{\left[\int_{-t_0}^{t_0} \psi_n(t'') \psi_m(t'') dt'' \right]}_{\lambda_n \delta_{nm}} \psi_m(t') \\ &= \sum_n \frac{1}{\lambda_n} \psi_n(t) \psi_n(t') = \delta(t - t'), \quad \text{for } t, t' \in [-t_0, t_0] \end{aligned}$$

Such inversion method will most surely fail in practice if there is even a tiny amount of noise in the observed data. Suppose, for example, that we add a small noise component $v(t)$ to Eq. (J.33),

$$g(t) = \int_{t_0}^{t_0} \frac{\sin(\omega_0(t - t'))}{\pi(t - t')} f(t') dt' + v(t) \quad (\text{J.36})$$

then, the restored signal will be,

$$f_{\text{rest}}(t) = \int_{-t_0}^{t_0} K(t, t') g(t') dt' = f(t) + \int_{-t_0}^{t_0} K(t, t') v(t') dt' \equiv f(t) + u(t)$$

where the noise $v(t)$ and its inverse-filtered version $u(t)$ can be expanded in the following forms over $[-t_0, t_0]$,

$$v(t) = \sum_n v_n \psi_n(t) \quad \Rightarrow \quad u(t) = \int_{-t_0}^{t_0} K(t, t') v(t') dt' = \sum_n \frac{v_n}{\lambda_n} \psi_n(t)$$

Thus, even if all the v_n were tiny, the ratios v_n/λ_n can become very large, because the λ_n tend to zero for large n , and the filtered noise $u(t)$ will be amplified and may completely mask the desired signal component $f(t)$.

A way out of this, which provides only an approximation to the inverse kernel, is to limit the summation over n to those eigenvalues λ_n that are large and near unity, that is, for n less than about the Shannon number N_c . For example, using $M + 1$ terms, with M near N_c , we have the following approximation to $K(t, t')$ and to the delta function in (J.35), for t, t' in $[-t_0, t_0]$,

$$\hat{K}(t, t') = \sum_{n=0}^M \frac{1}{\lambda_n^2} \psi_n(t) \psi_n(t') \quad (\text{J.37})$$

$$\hat{\delta}(t, t') = \int_{-t_0}^{t_0} \hat{K}(t, t'') \frac{\sin(\omega_0(t'' - t'))}{\pi(t'' - t')} dt'' = \sum_{n=0}^M \frac{1}{\lambda_n} \psi_n(t) \psi_n(t') \quad (\text{J.38})$$

where $\hat{\delta}(t, t')$ approximates $\delta(t - t')$, for $t, t' \in [-t_0, t_0]$. With $f(t)$ expanded as,

$$f(t) = \sum_{n=0}^{\infty} f_n \psi_n(t), \quad |t| \leq t_0 \quad (\text{J.39})$$

it follows that the restoration approximations correspond to the finite sums,

$$f_{\text{rest}}(t) = \hat{f}(t) + \hat{u}(t) = \sum_{n=0}^M f_n \psi_n(t) + \sum_{n=0}^M \frac{v_n}{\lambda_n} \psi_n(t) \quad (\text{J.40})$$

Keeping only a finite number of terms is a form of *regularization* of the inverse filtering operation. Other regularization schemes are possible, for example, the Tikhonov-type regularization approximating $\delta(t - t')$ over $[-t_0, t_0]$,

$$\hat{\delta}(t, t') = \sum_{n=0}^{\infty} \frac{\lambda_n}{\lambda_n^2 + \varepsilon^2} \psi_n(t) \psi_n(t') \quad (\text{J.41})$$

where ε small regularization parameter, $\varepsilon^2 \ll 1$. The summation in (J.41) effectively cuts off as soon as $\lambda_n \approx \varepsilon$, while it behaves like (J.38) for $1 \geq \lambda_n \gg \varepsilon$.

Setting $t' = 0$ in Eqs. (J.25), (J.38), and (J.41), we obtain the following bandlimited approximations to a delta function $\delta(t)$, over the finite interval $[-t_0, t_0]$,

$$\delta(t) = \sum_{n=0}^{\infty} \frac{1}{\lambda_n} \psi_n(0) \psi_n(t), \quad -t_0 \leq t \leq t_0 \quad (\text{J.42})$$

$$\hat{\delta}(t) = \sum_{n=0}^M \frac{1}{\lambda_n} \psi_n(0) \psi_n(t), \quad -t_0 \leq t \leq t_0 \quad (\text{J.43})$$

$$\hat{\delta}(t) = \sum_{n=0}^{\infty} \frac{\lambda_n}{\lambda_n^2 + \varepsilon^2} \psi_n(0) \psi_n(t), \quad -t_0 \leq t \leq t_0 \quad (\text{J.44})$$

Given that $\delta(t)$ has a flat spectrum extending over $-\infty < \omega < \infty$, referring to a “bandlimited” delta function is an oxymoron. However, the above expressions approximate $\delta(t)$ only over the finite interval, $-t_0 \leq t \leq t_0$, while they have bandlimited spectrum over $-\omega_0 < \omega < \omega_0$. Outside the $[-t_0, t_0]$ interval, they result in extremely large values. In fact, these expressions provide the ultimate example of *superoscillations* [1619-1631], which are bandlimited signals that, over a finite time interval, appear to oscillate faster than their highest frequency, but typically, exhibit much higher values outside that interval. Indeed, the above $\delta(t)$ is the fastest varying signal in $[-t_0, t_0]$ while at the same time it remains bandlimited.

Example J.3 explores the approximation of Eq. (J.43). We will use it in Sec. 20.22 in the design of superresolving pupil masks for achieving highly focused fields, and in the design of supergain aperture antennas for achieving very high directivity.

Representation and Extrapolation of Bandlimited Functions

If a function $f(t)$ is *bandlimited* over $[-\omega_0, \omega_0]$, then the completeness of the $\psi_n(t)$ basis implies that $f(t)$ can be expanded in the following form, for all t ,

$$f(t) = \sum_n c_n \psi_n(t), \quad \text{with} \quad c_n = \int_{-\infty}^{\infty} \psi_n(t) f(t) dt \quad (J.45)$$

Using the expansion (J.45) and the orthogonality property (J.24), we may obtain an alternative way of calculating the coefficients c_n that involves knowledge of $f(t)$ only over the finite interval $[-t_0, t_0]$,

$$c_n = \frac{1}{\lambda_n} \int_{-t_0}^{t_0} \psi_n(t) f(t) dt \quad (J.46)$$

Thus, once c_n are determined, $f(t)$ can be extrapolated outside $[-t_0, t_0]$ using (J.45). The validity of this procedure rests on the assumption that $f(t)$ is a bandlimited function in \mathcal{B}_{ω_0} and a segment of it is known over the interval $[-t_0, t_0]$.

If $f(t)$ is an arbitrary function in $\mathcal{L}_{t_0}^2$, but is not necessarily a segment of a bandlimited function in \mathcal{B}_{ω_0} , then the orthogonality and completeness properties (J.24) and (J.25) still allow an expansion in the following form, but valid only for $|t| \leq t_0$,

$$f(t) = \sum_n c_n \psi_n(t), \quad \text{with} \quad c_n = \frac{1}{\lambda_n} \int_{-t_0}^{t_0} \psi_n(t) f(t) dt \quad (J.47)$$

The attempt to extrapolate $f(t)$ beyond $[-t_0, t_0]$ using (J.47) could diverge and lead to extremely large values for $f(t)$ outside the $[-t_0, t_0]$ interval. This, again, is an example of superoscillations.

The representation (J.45) of a bandlimited function $f(t)$ in the $\psi_n(t)$ basis is convenient, but is not the only one. One could also expand $f(t)$ in the spherical Bessel function basis $j_n(\omega_0 t)$, or in the familiar sinc-function basis that appears in the sampling theorem. We summarize these expansions and their Fourier transforms below.

The expansion coefficients c_n can be expressed either in the time domain or in the frequency domain. Let $f(t)$ be in \mathcal{B}_{ω_0} with a bandlimited Fourier transform $\hat{f}(\omega)$, then, in the $\psi_n(t)$ basis,

$$\begin{aligned} f(t) &= \sum_n c_n \psi_n(t) \\ \hat{f}(\omega) &= \sum_n c_n \frac{2\pi}{\omega_0} \frac{1}{\mu_n} \psi_n\left(\frac{\omega t_0}{\omega_0}\right) \cdot \chi_{\omega_0}(\omega) \end{aligned} \quad (J.48)$$

with,

$$c_n = \int_{-\infty}^{\infty} \psi_n(t) f(t) dt = \frac{1}{\lambda_n} \int_{-t_0}^{t_0} \psi_n(t) f(t) dt = \frac{1}{\mu_n^*} \int_{-\omega_0}^{\omega_0} \psi_n\left(\frac{\omega t_0}{\omega_0}\right) \hat{f}(\omega) \frac{d\omega}{\omega} \quad (J.49)$$

Similarly, in the $j_n(\omega_0 t)$ basis, with Legendre polynomial Fourier transform,

$$\begin{aligned} f(t) &= \sum_n c_n j_n(\omega_0 t) \\ \hat{f}(\omega) &= \sum_n c_n \frac{\pi}{\omega_0 i^n} P_n\left(\frac{\omega}{\omega_0}\right) \cdot \chi_{\omega_0}(\omega) \end{aligned} \quad (J.50)$$

with,

$$c_n = \frac{(2n+1)\omega_0}{\pi} \int_{-\infty}^{\infty} j_n(\omega_0 t) f(t) dt = \frac{i^n (2n+1)}{2\pi} \int_{-\omega_0}^{\omega_0} \hat{f}(\omega) P_n\left(\frac{\omega}{\omega_0}\right) d\omega \quad (J.51)$$

and in the sinc-function basis, with $T_s = \pi/\omega_0$ denoting the sampling time interval,

$$\begin{aligned} f(t) &= \sum_n c_n \frac{\sin(\omega_0(t - nT_s))}{\pi(t - nT_s)} = T_s \sum_n f(nT_s) \frac{\sin(\omega_0(t - nT_s))}{\pi(t - nT_s)} \\ \hat{f}(\omega) &= \sum_n c_n e^{-j\omega nT_s} \cdot \chi_{\omega_0}(\omega) = T_s \sum_n f(nT_s) e^{-j\omega nT_s} \cdot \chi_{\omega_0}(\omega) \end{aligned} \quad (J.52)$$

with,

$$c_n = T_s f(nT_s) = T_s \int_{-\omega_0}^{\omega_0} \hat{f}(\omega) e^{j\omega nT_s} \frac{d\omega}{2\pi} \quad (J.53)$$

Note that the sinc-basis satisfies the orthogonality condition:

$$\int_{-\infty}^{\infty} \frac{\sin(\omega_0(t - nT_s))}{\pi(t - nT_s)} \frac{\sin(\omega_0(t - mT_s))}{\pi(t - mT_s)} dt = \frac{1}{T_s} \delta_{nm} \quad (J.54)$$

The result, $c_n = T_s f(nT_s)$, follows from (J.54) by applying (J.22) at $t = nT_s$, indeed,

$$\begin{aligned} f(nT_s) &= \int_{-\infty}^{\infty} \frac{\sin(\omega_0(t - nT_s))}{\pi(t - nT_s)} f(t) dt \\ &= \int_{-\infty}^{\infty} \frac{\sin(\omega_0(t - nT_s))}{\pi(t - nT_s)} \left[\sum_m c_m \frac{\sin(\omega_0(t - mT_s))}{\pi(t - mT_s)} \right] dt \\ &= \sum_m c_m \int_{-\infty}^{\infty} \frac{\sin(\omega_0(t - nT_s))}{\pi(t - nT_s)} \frac{\sin(\omega_0(t - mT_s))}{\pi(t - mT_s)} dt \\ &= \sum_m c_m \frac{1}{T_s} \delta_{nm} = \frac{c_n}{T_s} \Rightarrow c_n = T_s f(nT_s) \end{aligned}$$

Up to the factor T_s , the c_n are the time samples of $f(t)$, and $\hat{f}(\omega)$ in (J.52) is recognized as the central Nyquist replica of the DTFT of the discrete-time signal $f(nT_s)$. Moreover, Eq. (J.53) is the inverse DTFT of $\hat{f}(\omega)$ integrated over the Nyquist interval.

The Shannon number can be understood with the help of (J.52). In this context, we are assuming that the bandlimited function $f(t)$ is sampled at its Nyquist rate, which is $2\omega_0$ in units of radians/sec, or, $f_s = 2\omega_0/2\pi = \omega_0/\pi$ in samples/sec, so that the sampling time interval is $T_s = 1/f_s = \pi/\omega_0$ in seconds. Thus, the sampling rate f_s plays the role of F in (J.5).

Because $f(t)$ is frequency-limited, it cannot be time-limited. However, if we assume that the *most significant* time samples of $f(t)$ are contained within a total time interval T , say, $0 \leq nT_s \leq T$, then the maximum time index, and hence the number of significant time samples will be, $n_{\max}T_s = T$, or, $n_{\max} = T/T_s = f_s T$, that is, the Shannon number.

Energy Concentration Properties

Consider a bandlimited signal $f(t)$ in \mathcal{B}_{ω_0} with an expansion of the form (J.48),

$$f(t) = \sum_n c_n \psi_n(t), \quad \text{with } c_n = \int_{-\infty}^{\infty} \psi_n(t) f(t) dt = \frac{1}{\lambda_n} \int_{-t_0}^{t_0} \psi_n(t) f(t) dt \quad (\text{J.55})$$

Then, its energy contained in $[-t_0, t_0]$ and in the infinite interval are given by the norms,

$$\int_{-t_0}^{t_0} f^2(t) dt = \sum_{n=0}^{\infty} \lambda_n c_n^2, \quad \int_{-\infty}^{\infty} f^2(t) dt = \sum_{n=0}^{\infty} c_n^2 \quad (\text{J.56})$$

The proportion of the total energy contained in the interval $[-t_0, t_0]$ is the ratio,

$$\mathcal{R}(f) = \frac{\int_{-t_0}^{t_0} f^2(t) dt}{\int_{-\infty}^{\infty} f^2(t) dt} = \frac{\sum_{n=0}^{\infty} \lambda_n c_n^2}{\sum_{n=0}^{\infty} c_n^2} \quad (\text{J.57})$$

In the context of designing apodization functions in Sec. 20.12, it is known as the ‘‘encircled energy’’ ratio, while in the context of superdirective antennas, its inverse is known as Taylor’s supergain or superdirectivity ratio [1602].

The following extremal properties of the PSWF functions can be derived from (J.57). Because the eigenvalues λ_n are in decreasing order, $1 > \lambda_0 > \lambda_1 > \lambda_2 > \dots > 0$, it is easily seen that $\mathcal{R}(f)$ is maximized when $c_0 \neq 0$, and $c_n = 0$, for $n \geq 1$, that is, when $f(t) = \psi_0(t)$, and the maximized value is $\mathcal{R}(\psi_0) = \lambda_0$. This follows from the inequality,

$$\lambda_0 - \mathcal{R}(f) = \frac{\sum_{n=1}^{\infty} (\lambda_0 - \lambda_n) c_n^2}{\sum_{n=0}^{\infty} c_n^2} \geq 0$$

with equality realized when $c_n = 0$ for all $n \geq 1$. Similarly, among all the functions in \mathcal{B}_{ω_0} that are orthogonal to $\psi_0(t)$, the energy ratio $\mathcal{R}(f)$ is maximized when $f(t) = \psi_1(t)$, with maximum value $\mathcal{R}(\psi_1) = \lambda_1$. In this case the c_0 term is absent because of the orthogonality to ψ_0 , and $\mathcal{R}(f)$ becomes,

$$\mathcal{R}(f) = \frac{\sum_{n=1}^{\infty} \lambda_n c_n^2}{\sum_{n=1}^{\infty} c_n^2} \Rightarrow \lambda_1 - \mathcal{R}(f) = \frac{\sum_{n=2}^{\infty} (\lambda_1 - \lambda_n) c_n^2}{\sum_{n=1}^{\infty} c_n^2} \geq 0$$

More generally, among all the functions in \mathcal{B}_{ω_0} that are simultaneously orthogonal to $\psi_0(t), \psi_1(t), \dots, \psi_{n-1}(t)$, the function $f(t) = \psi_n(t)$ maximizes $\mathcal{R}(f)$ with maximum value $\mathcal{R}(\psi_n) = \lambda_n$.

If $f(t)$ is not necessarily bandlimited in \mathcal{B}_{ω_0} then, as we mentioned earlier, its values outside the interval $[-t_0, t_0]$ could become very large causing the energy concentration ratio $\mathcal{R}(f)$ to become very small.

Thus, a related optimization problem is to find that function $g(t)$ in \mathcal{B}_{ω_0} that has a prescribed value of the energy ratio, say, $\mathcal{R}(g) = \mathcal{R}_0 < 1$, and provides the best approximation to a given $f(t)$ within the $[-t_0, t_0]$ interval. Using a mean-square criterion, the problem can be stated as finding $g(t) \in \mathcal{B}_{\omega_0}$ that minimizes the following performance index subject to the energy ratio constraint,

$$\mathcal{J} = \int_{-t_0}^{t_0} (f(t) - g(t))^2 dt = \min, \quad \text{subject to } \mathcal{R}_0 = \frac{\int_{-t_0}^{t_0} g^2(t) dt}{\int_{-\infty}^{\infty} g^2(t) dt} \quad (\text{J.58})$$

or equivalently, we may introduce a Lagrange multiplier μ for the constraint,

$$\mathcal{J} = \int_{-t_0}^{t_0} (f(t) - g(t))^2 dt + \mu \left(\mathcal{R}_0 \int_{-\infty}^{\infty} g^2(t) dt - \int_{-t_0}^{t_0} g^2(t) dt \right) = \min \quad (\text{J.59})$$

Expand $f(t)$ and $g(t)$ in the $\psi_n(t)$ basis,

$$\begin{aligned} f(t) &= \sum_n f_n \psi_n(t), \quad \text{for } |t| \leq t_0 \\ g(t) &= \sum_n g_n \psi_n(t), \quad \text{for all } t \end{aligned} \quad (\text{J.60})$$

where f_n may be assumed to be known since $f(t)$ is given. Then, (J.59) becomes,

$$\mathcal{J} = \sum_n \lambda_n (g_n - f_n)^2 + \mu \left(\mathcal{R}_0 \sum_n g_n^2 - \sum_n \lambda_n g_n^2 \right) = \min \quad (\text{J.61})$$

The minimization condition with respect to g_n gives,

$$\frac{\partial \mathcal{J}}{\partial g_n} = 0 \Rightarrow \lambda_n (g_n - f_n) + \mu (\mathcal{R}_0 - \lambda_n) g_n = 0, \quad \text{or,}$$

$$g_n = \frac{\lambda_n f_n}{\lambda_n + \mu (\mathcal{R}_0 - \lambda_n)} \quad (\text{J.62})$$

with the Lagrange multiplier μ determined by solving the constraint equation,

$$\begin{aligned} \mathcal{R}_0 \sum_n g_n^2 - \sum_n \lambda_n g_n^2 &= \sum_n (\mathcal{R}_0 - \lambda_n) g_n^2 = 0, \quad \text{or,} \\ \sum_n (\mathcal{R}_0 - \lambda_n) \left[\frac{\lambda_n f_n}{\lambda_n + \mu (\mathcal{R}_0 - \lambda_n)} \right]^2 &= 0 \end{aligned} \quad (\text{J.63})$$

Computation

The numerical computation of $\psi_n(t)$ is based on keeping only a finite number of terms in the summation of Eq. (J.2), e.g., $0 \leq k \leq K - 1$,

$$\psi_n(t) = \sqrt{\frac{\lambda_n}{t_0}} \sum_{k=0}^{K-1} \beta_{nk} \sqrt{k + \frac{1}{2}} P_k\left(\frac{t}{t_0}\right) = \sqrt{\frac{c}{2\pi t_0}} \sum_{k=0}^{K-1} \beta_{nk} \sqrt{k + \frac{1}{2}} 2t^{k-n} j_k(\omega_0 t) \quad (J.64)$$

where K is chosen to be sufficiently large. In practice, the choice, $K = 2N + 30$, is adequate [1670], where $N = M + 1$ is the number of PSWF functions to be calculated, that is, $\psi_n(t)$, $n = 0, 1, 2, \dots, M$.

The computation of β_{nk} is based on the observation [1643] that the PSWF functions $\psi_n(t)$ are also the eigenfunctions of the following Sturm-Liouville differential operator eigenproblem, that arises in solving the Helmholtz equation in spheroidal coordinates,

$$\left[(t^2 - t_0^2) \frac{d^2}{dt^2} + 2t \frac{d}{dt} + \omega_0^2 t^2 \right] \psi_n(t) = \chi_n \psi_n(t), \quad n = 0, 1, 2, \dots \quad (J.65)$$

The eigenvalues χ_n are real and positive and when listed in increasing order, they match the eigenvalues λ_n of Eq. (J.3) listed in decreasing order, that is, we have the correspondence,

$$\begin{aligned} 0 < \chi_0 < \chi_1 < \chi_2 < \dots, \\ 1 > \lambda_0 > \lambda_1 > \lambda_2 > \dots, \end{aligned}$$

There is extensive literature on the computation of the PSWF solutions of (J.65), including its generalization to higher order PSWFs, with implementations in FORTRAN, MATLAB, and Mathematica [1654-1677].

Our MATLAB implementation is based on Rhodes [1658] who gives normalization-independent expressions, Hodge [1660] who was the first to suggest using a tridiagonal eigenvalue problem for calculating the coefficients β_{nk} , Kozin et al. [1662] who applied Hodge's method specifically to order-zero PSWFs, and Xiao et al [1664] and Boyd [1670] for some more recent implementations. Accurate computation of the eigenvalues λ_n and eigenfunctions $\psi_n(t)$ is very demanding for large values of c and large values of n because the λ_n quickly get smaller than the machine epsilon, even using double precision as in MATLAB.

If one inserts the Legendre polynomial expansion of Eq. (J.2) into (J.65), one finds that the coefficients β_{nk} satisfy the following recursion formula, for $k \geq 0$,

$$A_{k,k-2} \beta_{n,k-2} + A_{k,k} \beta_{nk} + A_{k,k+2} \beta_{n,k+2} = \chi_n \beta_{nk} \quad (J.66)$$

where the first term is present only for $k \geq 2$, and,

$$\begin{aligned} A_{k,k} &= k(k+1) + c^2 \cdot \frac{2k(k+1)-1}{(2k+3)(2k-1)}, & k \geq 0 \\ A_{k,k+2} &= c^2 \cdot \frac{(k+2)(k+1)}{(2k+3)\sqrt{(2k+1)(2k+5)}}, & k \geq 0 \\ A_{k,k-2} &= A_{k-2,k} = c^2 \cdot \frac{k(k-1)}{(2k-1)\sqrt{(2k-3)(2k+1)}}, & k \geq 2 \end{aligned} \quad (J.67)$$

If a finite number of coefficients is kept, such as, $K = 2N + 30$, then, we may define a $K \times K$ symmetric tridiagonal matrix A whose main diagonal is $A_{k,k}$, for $k = 0, 1, \dots, K - 1$, and whose upper and lower second diagonals are given by $A_{k,k+2}$, for $k = 0, 1, \dots, K - 3$. For example, if $K = 8$, the matrix will have the following structure,

$$A = \begin{bmatrix} A_{00} & 0 & A_{02} & 0 & 0 & 0 & 0 & 0 \\ 0 & A_{11} & 0 & A_{13} & 0 & 0 & 0 & 0 \\ A_{02} & 0 & A_{22} & 0 & A_{24} & 0 & 0 & 0 \\ 0 & A_{13} & 0 & A_{33} & 0 & A_{35} & 0 & 0 \\ 0 & 0 & A_{24} & 0 & A_{44} & 0 & A_{46} & 0 \\ 0 & 0 & 0 & A_{35} & 0 & A_{55} & 0 & A_{57} \\ 0 & 0 & 0 & 0 & A_{46} & 0 & A_{66} & 0 \\ 0 & 0 & 0 & 0 & 0 & A_{57} & 0 & A_{77} \end{bmatrix}$$

The difference equation (J.65) is equivalent then to the following eigenvalue equation, where the coefficients $\beta_{n,k}$ are arranged into the corresponding eigenvectors,

$$A \boldsymbol{\beta}_n = \chi_n \boldsymbol{\beta}_n, \quad \boldsymbol{\beta}_n = \begin{bmatrix} \beta_{n,0} \\ \beta_{n,1} \\ \vdots \\ \beta_{n,K-1} \end{bmatrix} \quad (J.68)$$

Because A is real and symmetric, its eigenvectors may be chosen to be real-valued and orthonormal, that is, satisfying Eq. (J.9). And because of the particular structure of A , having only a nonzero second upper/lower subdiagonal, every other element of the eigenvectors may be set to zero, that is, $\beta_{n,k} = 0$, if $n - k$ is odd. For example, if $K = 8$, the eigenvectors, will have the following structure,

$$\boldsymbol{\beta}_{n,\text{even}} = \begin{bmatrix} \beta_{n0} \\ 0 \\ \beta_{n2} \\ 0 \\ \beta_{n4} \\ 0 \\ \beta_{n6} \\ 0 \end{bmatrix}, \quad \boldsymbol{\beta}_{n,\text{odd}} = \begin{bmatrix} 0 \\ \beta_{n1} \\ 0 \\ \beta_{n3} \\ 0 \\ \beta_{n5} \\ 0 \\ \beta_{n7} \end{bmatrix}$$

$n=0,2,4,6$ $n=1,3,5,7$

MATLAB can very efficiently and accurately solve the above tridiagonal eigenvalue problem using the built-in function `eig`, and obtain all K eigenvectors $\boldsymbol{\beta}_n$ and eigenvalues χ_n (even for very large values of c, K , e.g., $c = 100, K = 1000$).

Once the $K \times K$ eigenvalue problem (J.68) is solved, we may retain the first $M + 1$ eigenvectors $\boldsymbol{\beta}_n$, for $n = 0, 1, \dots, M$, that are needed in the computation of $\psi_n(t)$. One still has the task of determining the corresponding eigenvalues λ_n of the eigenproblem (J.3). Since λ_n appears in (J.2), we may solve for it by evaluating both sides of (J.64) at a particular value of t . It's simpler to solve for μ_n and then calculate λ_n from (J.15). Multiplying both sides of (J.64) by $i^n \sqrt{2\pi t_0}/c$, we obtain the relationship:

$$i^n \sqrt{\frac{2\pi t_0}{c}} \psi_n(t) = \mu_n \sum_{k=0}^{K-1} \beta_{nk} \sqrt{k + \frac{1}{2}} P_k\left(\frac{t}{t_0}\right) = \sum_{k=0}^{K-1} \beta_{nk} \sqrt{k + \frac{1}{2}} 2t^k j_k(\omega_0 t) \quad (J.69)$$

One obvious choice is to set $t = t_0$, and since $P_n(1) = 1$, we may solve for μ_n ,

$$\mu_n = \frac{\sum_{k=0}^{K-1} \beta_{nk} \sqrt{k + \frac{1}{2}} 2i^k j_k(c)}{\sum_{k=0}^{K-1} \beta_{nk} \sqrt{k + \frac{1}{2}}} \quad n = 0, 1, \dots, M \quad (J.70)$$

Another choice is to set $t = 0$, resulting in

$$\mu_n \sum_{k=0}^{K-1} \beta_{nk} \sqrt{k + \frac{1}{2}} P_k(0) = \sum_{k=0}^{K-1} \beta_{nk} \sqrt{k + \frac{1}{2}} 2i^k j_k(0) \quad (J.71)$$

However, this works only for n even, because if n and k are odd, both $P_k(0)$ and $j_k(0)$ are zero. In this case, one may work with the time derivative of both sides of (J.64),

$$\mu_n \sum_{k=0}^{K-1} \beta_{nk} \sqrt{k + \frac{1}{2}} \frac{1}{t_0} P'_k\left(\frac{t}{t_0}\right) = \sum_{k=0}^{K-1} \beta_{nk} \sqrt{k + \frac{1}{2}} 2i^k \omega_0 j'_k(\omega_0 t), \quad \text{or,}$$

$$\mu_n \sum_{k=0}^{K-1} \beta_{nk} \sqrt{k + \frac{1}{2}} P'_k\left(\frac{t}{t_0}\right) = \sum_{k=0}^{K-1} \beta_{nk} \sqrt{k + \frac{1}{2}} 2i^k c j'_k(\omega_0 t)$$

Evaluating this at $t = 0$ will work for n odd, but not for n even,

$$\mu_n \sum_{k=0}^{K-1} \beta_{nk} \sqrt{k + \frac{1}{2}} P'_k(0) = \sum_{k=0}^{K-1} \beta_{nk} \sqrt{k + \frac{1}{2}} 2i^k c j'_k(0) \quad (J.72)$$

We may add (J.71) and (J.72) together to get a combined formula that works for all n , even or odd, and solve for μ_n ,

$$\mu_n = \frac{\sum_{k=0}^{K-1} \beta_{nk} \sqrt{k + \frac{1}{2}} 2i^k [j_k(0) + c j'_k(0)]}{\sum_{k=0}^{K-1} \beta_{nk} \sqrt{k + \frac{1}{2}} [P_k(0) + P'_k(0)]} \quad n = 0, 1, \dots, M \quad (J.73)$$

The spherical Bessel functions $j_k(x)$ for $k \geq 0$ have the following limiting behavior,

$$j_k(x) \xrightarrow{x \rightarrow 0} \frac{x^k}{1 \cdot 3 \cdot 5 \cdots (2k + 1)} \Rightarrow j_k(0) = \delta_k = \begin{cases} 1, & k = 0 \\ 0, & k \neq 0 \end{cases} \quad (J.74)$$

The derivative, $j'_k(x)$, can be computed from the recursion:

$$j'_k(x) = \frac{k j_{k-1}(x) - (k + 1) j_{k+1}(x)}{2k + 1} \quad (J.75)$$

and using the result (J.74),

$$j'_k(0) = \frac{k \delta_{k-1} - (k + 1) \delta_{k+1}}{2k + 1} = \frac{1}{3} \delta_{k-1} \quad (J.76)$$

Using (J.74) and (J.76), the numerator in (J.73) simplifies to the $k = 0$ and $k = 1$ terms,

$$\mu_n = \frac{\sqrt{2} \beta_{n0} + \sqrt{\frac{2}{3}} i c \beta_{n1}}{\sum_{k=0}^{K-1} \beta_{nk} \sqrt{k + \frac{1}{2}} [P_k(0) + P'_k(0)]} \quad n = 0, 1, \dots, M \quad (J.77)$$

The quantities, $P_k(0), P'_k(0)$, can be calculated in terms of gamma-functions,

$$P_k(0) = \frac{\sqrt{\pi}}{\Gamma\left(\frac{k}{2} + 1\right) \Gamma\left(\frac{1}{2} - \frac{k}{2}\right)}, \quad P'_k(0) = k P_{k-1}(0) = \frac{-2\sqrt{\pi}}{\Gamma\left(\frac{k}{2} + \frac{1}{2}\right) \Gamma\left(-\frac{k}{2}\right)} \quad (J.78)$$

These are valid for all $k \geq 0$ and give $P_k(0) = 0$, for odd k , and $P'_k(0) = 0$, for even k . Moreover, they can be implemented as vectorized functions in MATLAB. For a given n , either the left or the right terms will be non-zero in the numerator and denominator of (J.77). We have found that the choice (J.77) produces more accurate results than (J.70) for moderate values of c, M , up to about, $c = 50, M = 50$.

The following MATLAB function, `pswf.m`, implements the above computational steps. It also computes the derivatives $\psi'_n(t)$. It has usage:

```
[Psi,La,dPsi,Chi,B] = pswf(t0,w0,M,t); % prolate spheroidal wave functions
[Psi,La,dPsi,Chi,B] = pswf(t0,w0,M,t,K);
```

t_0 = time limit, $[-t_0, t_0]$, (sec)
 w_0 = freq limit, $[-w_0, w_0]$, (rad/sec)
 M = max order computed, evaluating $\psi_n(t)$, $n = 0, 1, \dots, M$
 t = length- L vector of time instants (sec), e.g., $t = [t_1, t_2, \dots, t_L]$

Ψ = $(M+1) \times L$ matrix of prolate function values
 La = $(M+1) \times 1$ vector of eigenvalues
 $d\Psi$ = $(M+1) \times L$ matrix of derivatives of prolate functions
 Chi = $(M+1) \times 1$ vector of eigenvalues of spheroidal differential operator
 B = $(M+1) \times K$ matrix of expansion coefficients
 K = number of expansion terms (default, $K = 2 * N + 30, N = M + 1$)

For a given maximum order M and time vector $t = [t_1, t_2, \dots, t_L]$, the output matrix Ψ contains the computed values $\psi_n(t_i)$, arranged into an $(M + 1) \times L$ matrix,

$$\Psi = \begin{bmatrix} \psi_0(t_1) & \psi_0(t_2) & \psi_0(t_3) & \cdots & \psi_0(t_L) \\ \psi_1(t_1) & \psi_1(t_2) & \psi_1(t_3) & \cdots & \psi_1(t_L) \\ \psi_2(t_1) & \psi_2(t_2) & \psi_2(t_3) & \cdots & \psi_2(t_L) \\ \vdots & \vdots & \vdots & \cdots & \vdots \\ \psi_M(t_1) & \psi_M(t_2) & \psi_M(t_3) & \cdots & \psi_M(t_L) \end{bmatrix}$$

The output $d\Psi$ contains the derivatives $\psi'_n(t_i)$ arranged in a similar fashion. The outputs La, Chi are column vectors containing the eigenvalues $\lambda_n, \chi_n, n = 0, 1, \dots, M$.

The $(M + 1) \times K$ matrix B contains the expansion coefficients, $B_{nk} = \beta_{nk}$, in its rows, with the appropriate interlacing of zeros for even or odd n , that is,

$$B = \begin{bmatrix} \beta_{0,0} & 0 & \beta_{0,2} & 0 & \beta_{0,4} & 0 & \cdots & \beta_{0,K-1} \\ 0 & \beta_{1,1} & 0 & \beta_{1,3} & 0 & \beta_{1,5} & \cdots & \beta_{1,K-1} \\ \beta_{2,0} & 0 & \beta_{2,2} & 0 & \beta_{2,4} & 0 & \cdots & \beta_{2,K-1} \\ 0 & \beta_{3,1} & 0 & \beta_{3,3} & 0 & \beta_{3,5} & \cdots & \beta_{3,K-1} \\ \vdots & \vdots & \vdots & \vdots & \vdots & \vdots & \cdots & \vdots \end{bmatrix}$$

The eigenvector matrix is actually the transposed, $B^T = [\beta_0, \beta_1, \dots, \beta_M]$, which satisfies the eigenvalue equation, $AB^T = B^T\mathcal{X}$, where $\mathcal{X} = \text{diag}\{\chi_0, \chi_1, \dots, \chi_M\}$, and the orthonormality property,

$$BB^T = I_{M+1} \Rightarrow \sum_{k=0}^{K-1} \beta_{nk}\beta_{mk} = \delta_{nm}, \quad n, m = 0, 1, \dots, M$$

The required spherical Bessel function computations are implemented by the MATLAB function, `spherj.m`, which also computes the derivatives using the recursion (J.75). It arranges its output similarly to `pswf`, and has usage:

```
[J, dJ] = spherj(k, x); % spherical Bessel functions and derivatives
```

The derivatives, $\psi'_n(t)$, are computed using the expansion,

$$\psi'_n(t) = \sqrt{\frac{c}{2\pi t_0}} \sum_{k=0}^{K-1} \beta_{nk} \sqrt{k + \frac{1}{2}} 2i^{k-n} \omega_0 j'_k(\omega_0 t) \quad (J.79)$$

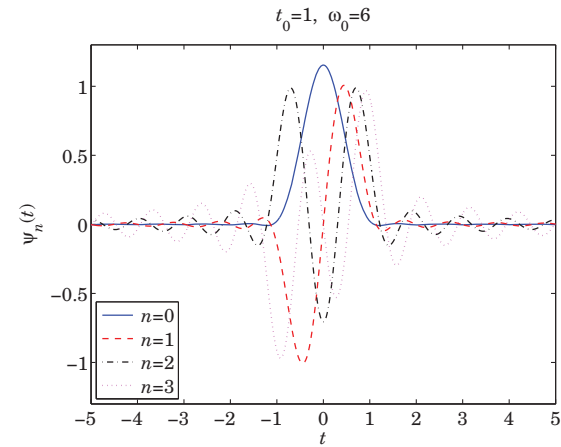
The functions `pswf` and `spherj` are included in the EWA-toolbox of this book, and work well for parameter values up to about $c = 50$ and $M = 50$. A related function that evaluates Legendre polynomials and can be used in the Legendre expansion of Eq. (J.2) is the function `legpol` with usage:

```
P = legpol(N, x); % evaluates Legendre polynomials of orders n=0:N
```

Example J.1: The following MATLAB code illustrates the usage of the `pswf` function and reproduces the data tables and plots from Rhodes [1658] for the case $c = 6$.

```
t0=1; w0=6; c=t0*w0; M=13;
t = linspace(-5, 5, 501);
[Psi, La, dPsi, Chi] = pswf(t0, w0, M, t); % calculate the first 14 PSWFs
figure; plot(t, Psi(1:4, :)); % plot first four PSWFs
```

The following graph plots the first four PSWFs, $\psi_n(t)$, $n = 0, 1, 2, 3$.



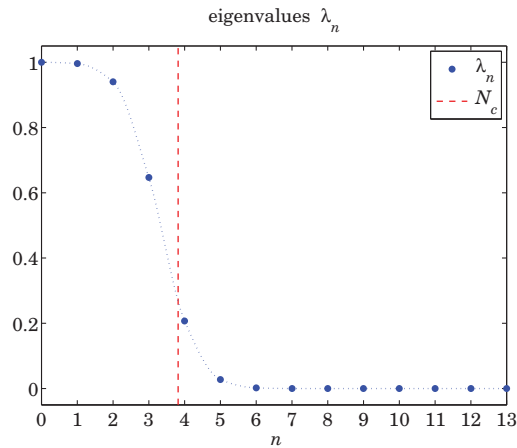
The following table contains the values of the quantities χ_n, μ_n, λ_n for $n = 0, 1, \dots, 13$, as well as the values of the sum, $\psi_n(0) + \psi'_n(0)$, which represents either $\psi_n(0)$ if n is even, or $\psi'_n(0)$ if n is odd. They agree with those in [1658].

n	chi_n	mu_n	psi_n(0)+psi_n'(0)	lambda_n
0	5.208269160e+00	1.023276504e+00	1.631136822e-03	9.999018826e-01
1	1.600044275e+01	1.021309607e+00	-5.777995494e-02	9.960616433e-01
2	2.535647864e+01	9.922435547e-01	3.539393687e-02	9.401733902e-01
3	3.320419949e+01	8.229938914e-01	4.428586710e-01	6.467919492e-01
4	4.072019427e+01	4.659781027e-01	-3.045590356e-01	2.073492169e-01
5	4.977371213e+01	1.693510361e-01	-7.517787765e-01	2.738716624e-02
6	6.118075690e+01	4.524678973e-02	7.141707743e-01	1.955000734e-03
7	7.485286653e+01	9.966212672e-03	5.750889706e-01	9.484876556e-05
8	9.065115937e+01	1.897100693e-03	-1.117460330e+00	3.436783286e-06
9	1.085154453e+02	3.192404741e-04	3.163806610e-02	9.732115989e-08
10	1.284188799e+02	4.820488557e-05	1.196006265e+00	2.218980545e-09
11	1.503474435e+02	6.605196410e-06	-9.118593645e-01	4.166226284e-11
12	1.742930029e+02	8.286721621e-07	-5.384541132e-01	6.557478591e-13
13	2.002505133e+02	9.588946460e-08	1.423257002e+00	8.780377122e-15

The table was generated by the MATLAB code,

```
n = (0:M)';
Mu = sqrt(2*pi/c*La); % calculate |mu_n| from la_n
P = Psi(:,1) + dPsi(:,1); % interlace psi_n(0) and its derivative psi_n'(0)
fprintf(' n chi_n |mu_n| psi_n(0)+psi_n''(0) lambda_n\n')
fprintf('-----\n')
fprintf('%3d %1.9e %1.9e % 1.9e % 1.9e\n', [n, Chi, Mu, P, La])
```

The Shannon number is $N_c = 2c/\pi = 3.8194$. We observe in the above table how quickly the eigenvalues λ_n decay towards zero for $n > N_c$. The following figure plots λ_n and the dividing line at N_c (the eigenvalues have been joined by a smooth curve to guide the eye).



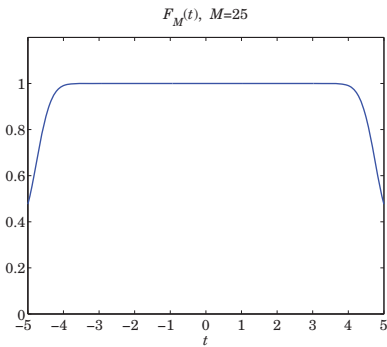
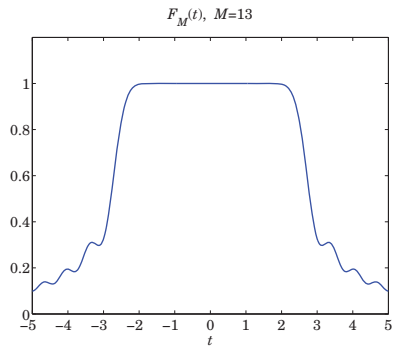
The following MATLAB code tests the relationships (J.28) and (J.29) for $M = 13$ and $M = 25$. The graphs plot the quantity,

$$F_M(t) = \frac{\pi}{\omega_0} \sum_{n=0}^M \psi_n^2(t) \tag{J.80}$$

which should tend to unity as M increases and more terms are included in the sum.

```
F = sum(Psi.^2) * pi/w0; % test: pi/w0 * \sum_n psi_n(t)^2 = 1
figure; plot(t,F,'b-') % gets better as M is increased

Nc = 2*c/pi; % Nc = 3.8197, Shannon number
Err = abs(sum(La)-Nc); % Err = 1.3323e-15, for M=13
```



Example J.2: This example tests the relationships (J.27) and (J.31). Setting $t' = 0$ in (J.27), we obtain the limit,

$$\lim_{M \rightarrow \infty} F_M(t) = \frac{\sin(\omega_0 t)}{\pi t}, \quad \text{where } F_M(t) = \sum_{n=0}^M \psi_n(0) \psi_n(t)$$

Similarly we have the limit of (J.31),

$$\lim_{M \rightarrow \infty} G_M(t) = 1, \quad \text{where } G_M(t) = \frac{2\pi}{\omega_0} \sum_{n=0}^M \frac{1}{\mu_n} \psi_n(0) \psi_n(t)$$

The following MATLAB code computes and plots $F_M(t)$, $G_M(t)$ for $M = 4$ and $M = 20$ for the case $t_0 = 1$, $\omega_0 = 6$,

```
t0 = 1; w0 = 6; c = t0*w0;
t = linspace(-4,4,801);

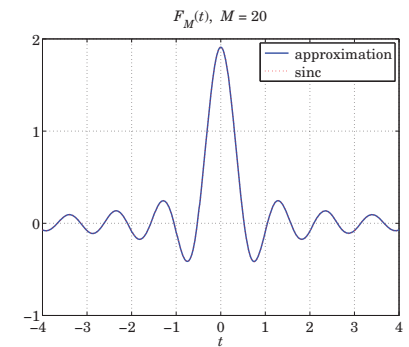
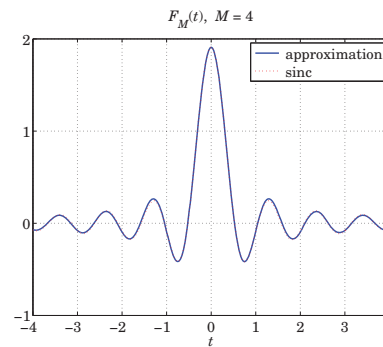
for M = [4,20]
    [Psi,La] = pswf(t0,w0,M,t);
    Psi0 = Psi(:,t==0);

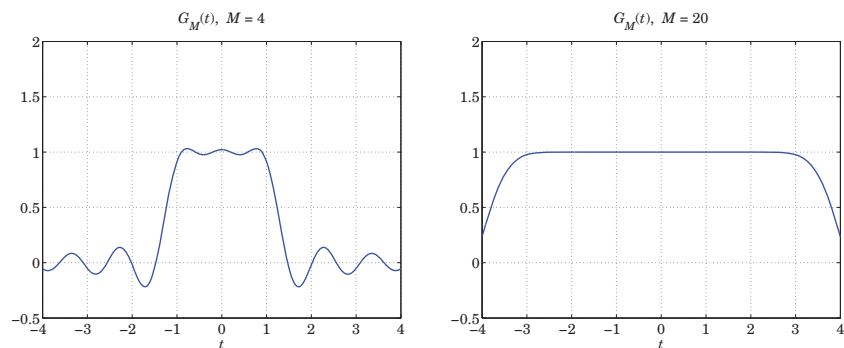
    F = Psi0' * Psi;

    figure; plot(t,F,'b-', t,sinc(w0*t/pi)*w0/pi,'r:');

    n = (0:M)';
    Mu = i.^n .* sqrt(2*pi*La/c);
    G = (2*pi/w0) * Psi0' * diag(1./Mu) * Psi;

    figure; plot(t,G,'b-');
end
```





The convergence of $F_M(t)$ is very quick and one can barely distinguish the approximation from the exact sinc function on the graphs (see the color graphs in the PDF book file). □

Example J.3: Here we explore the bandlimited approximation (J.43) of a delta function over a limited time interval. Let us denote the approximation by,

$$\delta_M(t) = \sum_{n=0}^M \frac{1}{\lambda_n} \psi_n(0) \psi_n(t) \tag{J.81}$$

The following MATLAB code segment evaluates and plots $\delta_M(t)$ for the following values of the parameters: $t_0 = 1$, $\omega_0 = 4\pi$, and the cases, $M = 20$ and $M = 30$.

```
t0 = 1; w0 = 4*pi;
t = linspace(-2,2,401);

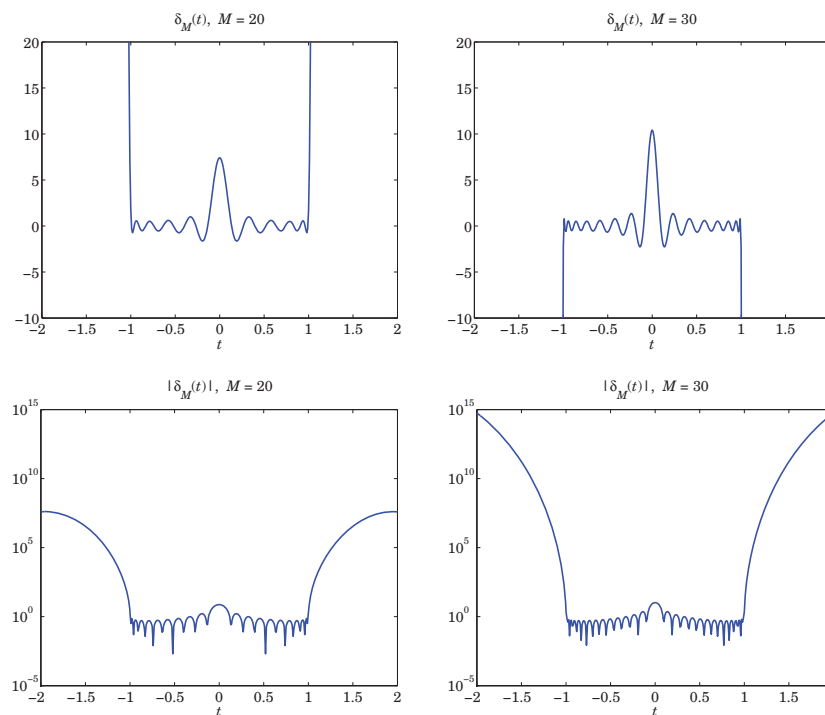
for M = [20,30]
    [Psi,La] = pswf(t0,w0,M,t);
    Psi0 = Psi(:,t==0);

    F = Psi0' * diag(1./La) * Psi;          % the summation in (J.81)

    figure; plot(t,F, 'b-', 'linewidth',2);
    axis([-2,2,-10,20]); xlabel('\itt');
end
```

Because $\psi_n(t) = (-1)^n \psi_n(-t)$, it follows that $\psi_n(0) = 0$ for odd n and the summation in (J.81) can be restricted to even n 's. However, in the MATLAB implementation above it is much simpler to keep all terms. The following graphs plot $\delta_M(t)$ versus t , over the interval $-2t_0 \leq t \leq 2t_0$.

To display the incredibly large values outside the interval, $[-t_0, t_0]$, we have also plotted the absolute values $|\delta_M(t)|$ using a semi-log scale. Within the $[-t_0, t_0]$ interval, the peak around $t = 0$ approximating $\delta(t)$ becomes narrower with increasing M .



We note that since the maximum frequency is $f_0 = \omega_0 / (2\pi) = 2$ in cycles per unit time, the approximation $\delta_M(t)$ clearly oscillates several times faster than f_0 over the $[-t_0, t_0]$ interval, exhibiting a superoscillatory behavior [1619-1631].

The bandlimited Fourier transform of the approximation (J.81) is obtained from the Fourier transform of $\psi_n(t)$,

$$\Delta_M(\omega) = \int_{-\infty}^{\infty} e^{-j\omega t} \delta_M(t) dt = \sum_{n=0}^M \frac{1}{\lambda_n} \psi_n(0) \hat{\psi}_n(\omega)$$

or, using (J.16),

$$\begin{aligned} \Delta_M(\omega) &= \sum_{n=0}^M \frac{2\pi}{\omega_0 \lambda_n \mu_n} \psi_n(0) \psi_n\left(\frac{\omega t_0}{\omega_0}\right) \cdot \chi_{\omega_0}(\omega) \\ &= \sqrt{\frac{2\pi t_0}{\omega_0}} \sum_{n=0}^M \frac{1}{i^n \lambda_n^{3/2}} \psi_n(0) \psi_n\left(\frac{\omega t_0}{\omega_0}\right) \cdot \chi_{\omega_0}(\omega) \end{aligned} \tag{J.82}$$

The following MATLAB code computes and plots $\Delta_M(\omega)$ over $[-\omega_0, \omega_0]$ for the same parameter values, $t_0 = 1$, $\omega_0 = 4\pi$, and $M = 20, 30$.

```
t0 = 1; w0 = 4*pi;
w = linspace(-1,1,401);          % normalized frequency, w = omega/omega_0
```

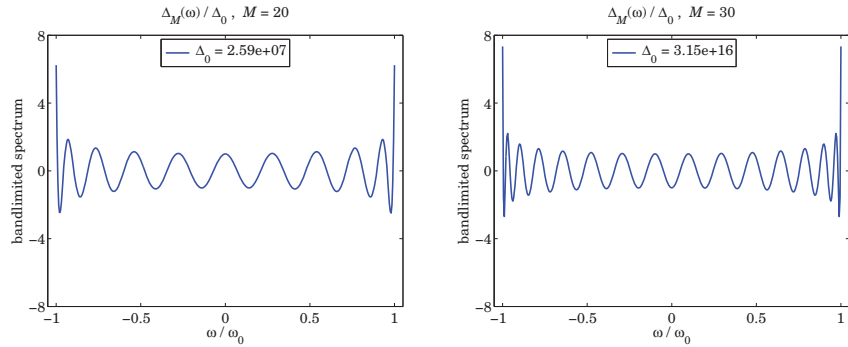
```

for M = [20,30]
    [Psi,La] = pswf(t0,w0,M,w*t0);
    Psi0 = Psi(:,w==0);
    n = (0:M)';

    D = sqrt(2*pi*t0/w0) * Psi0' * diag(1./i.^n./La.^(3/2)) * Psi;

    D0 = abs(D(w==0));

    figure; plot(w,D/D0, 'b-', 'linewidth', 2);
    axis([-1.05, 1.05, -8, 8]);
end
    
```



For plotting purposes, the spectrum is normalized to its magnitude at $\omega = 0$, that is, the quantity $\Delta_M(\omega)/\Delta_0$ is plotted, where $\Delta_0 = |\Delta_M(0)|$. The computed values of Δ_0 and hence the values of $\Delta_M(\omega)$ in absolute scales are huge, indeed, we have, $\Delta_0 = 2.5897 \times 10^7$ and $\Delta_0 = 3.1503 \times 10^{16}$ for the two cases of $M = 20$ and $M = 30$, respectively.

We will revisit this type of example in Sec. 20.22 in our discussion of superresolving optical systems and the design of superdirective aperture antennas.

In the optics context, we must map the variables (t, ω) to the spatial variables (x, k_x) , with the optical system introducing bandlimiting in the wavenumber domain k_x . The sharp focusing of the delta-function approximation $\delta_M(x)$ is accompanied by huge values outside a specified “field-of-view” interval $[-x_0, x_0]$ which plays the role of $[-t_0, t_0]$. Such huge values can be blocked with additional aperture stops provided the object fits within this field of view.

In the context of aperture-limited antennas, we must remap the variables (t, ω) onto the spatial variables (k_x, x) , so that $\delta_M(t)$ maps into $\delta_M(k_x)$ and becomes the radiation pattern of the antenna as a function of the wavenumber k_x . The Fourier spectrum $\Delta_M(\omega)$ maps onto the aperture-limited field distribution $\Delta_M(x)$ as a function of distance x along the finite antenna, limited to an interval $-a \leq x \leq a$, where $2a$ is the length of the antenna.

Although in principle one can design an aperture antenna that has high directivity, approximating $\delta(k_x)$, the extremely large values of the aperture distribution $\Delta_M(x)$, make such designs effectively unrealizable in practice.

The role of the bandwidth interval $[-\omega_0, \omega_0]$ is played by the space interval $[-a, a]$, while the role of $[-t_0, t_0]$ is played by the visible region of the wavenumber interval, $[-k_0, k_0]$, where k_0 is the free-space wavenumber, $k_0 = 2\pi/\lambda$. Although the visible radiation pattern

is limited to $|k_x| \leq k_0$, and emulates a sharp radiation pattern $\delta_M(k_x)$, the rest of the pattern over the invisible region $|k_x| > k_0$ takes on very large values as we saw in this example. These are associated with very large reactive power stored in the vicinity of the antenna.

Further discussion of these issues is presented in Sec. 20.22. We note also that the super-resolution examples of Barnes [1569] can be reproduced by changing the parameters to $\omega_0 = 4$ and $M = [2, 4, 6, 8]$ in the above MATLAB segments, while the supergain design example of Kritikos [1616] is reproduced by the choice, $t_0 = 1, \omega_0 = 6, M = 8$. □

K. Lorentz Transformations

According to Einstein’s special theory of relativity [474], Lorentz transformations describe the transformation between the space-time coordinates of two coordinate systems moving relative to each other at constant velocity. Maxwell’s equations remain invariant under Lorentz transformations. This is demonstrated below.

Let the two coordinate frames be S and S' . By convention, we may think of S as the “fixed” laboratory frame with respect to which the frame S' is moving at a constant velocity \mathbf{v} . For example, if \mathbf{v} is in the z -direction, the space-time coordinates $\{t, x, y, z\}$ of S are related to the coordinates $\{t', x', y', z'\}$ of S' by the Lorentz transformation:

$$\begin{cases} t' = \gamma(t - \frac{v}{c^2}z) \\ z' = \gamma(z - vt) \\ x' = x \\ y' = y \end{cases}, \quad \text{where } \gamma = \frac{1}{\sqrt{1 - v^2/c^2}}$$

where c is the speed of light in vacuum. Defining the scaled quantities $\tau = ct$ and $\beta = v/c$, the above transformation and its inverse, obtained by replacing β by $-\beta$, may be written as follows:

$$\begin{cases} \tau' = \gamma(\tau - \beta z) \\ z' = \gamma(z - \beta\tau) \\ x' = x \\ y' = y \end{cases} \Leftrightarrow \begin{cases} \tau = \gamma(\tau' + \beta z') \\ z = \gamma(z' + \beta\tau') \\ x = x' \\ y = y' \end{cases} \quad (\text{K.1})$$

These transformations are also referred to as *Lorentz boosts* to indicate the fact that one frame is boosted to move relative to the other. Interchanging the roles of z and x , or z and y , one obtains the Lorentz transformations for motion along the x or y directions, respectively. Eqs. (K.1) may be expressed more compactly in matrix form:

$$\boxed{x' = Lx}, \quad \text{where } x = \begin{bmatrix} \tau \\ x \\ y \\ z \end{bmatrix}, \quad x' = \begin{bmatrix} \tau' \\ x' \\ y' \\ z' \end{bmatrix}, \quad L = \begin{bmatrix} \gamma & 0 & 0 & -\gamma\beta \\ 0 & 1 & 0 & 0 \\ 0 & 0 & 1 & 0 \\ -\gamma\beta & 0 & 0 & \gamma \end{bmatrix} \quad (\text{K.2})$$

Such transformations leave the quadratic form $(c^2t^2 - x^2 - y^2 - z^2)$ invariant, that is,

$$c^2t'^2 - x'^2 - y'^2 - z'^2 = c^2t^2 - x^2 - y^2 - z^2 \tag{K.3}$$

Introducing the diagonal metric matrix $G = \text{diag}(1, -1, -1, -1)$, we may write the quadratic form as follows, where x^T denotes the transposed vector, that is, the row vector $x^T = [\tau, x, y, z]$:

$$x^T G x = \tau^2 - x^2 - y^2 - z^2 = c^2 t^2 - x^2 - y^2 - z^2 \tag{K.4}$$

More generally, a Lorentz transformation is defined as any linear transformation $x' = Lx$ that leaves the quadratic form $x^T G x$ invariant. The invariance condition requires that: $x'^T G x' = x^T L^T G L x = x^T G x$, or

$$\boxed{L^T G L = G} \tag{K.5}$$

In addition to the Lorentz boosts of Eq. (K.1), the more general transformations satisfying (K.5) include rotations of the three spatial coordinates, as well as time or space reflections. For example, a rotation has the form:

$$L = \left[\begin{array}{c|ccc} 1 & 0 & 0 & 0 \\ \hline 0 & & & \\ 0 & & & R \\ 0 & & & \end{array} \right]$$

where R is a 3×3 orthogonal rotation matrix, that is, $R^T R = I$, where I is the 3×3 identity matrix. The most general Lorentz boost corresponding to arbitrary velocity $\mathbf{v} = [v_x, v_y, v_z]^T$ is given by:

$$L = \left[\begin{array}{c|c} \gamma & -\gamma \boldsymbol{\beta}^T \\ \hline -\gamma \boldsymbol{\beta} & I + \frac{\gamma^2}{\gamma + 1} \boldsymbol{\beta} \boldsymbol{\beta}^T \end{array} \right], \text{ where } \boldsymbol{\beta} = \frac{\mathbf{v}}{c}, \quad \gamma = \frac{1}{\sqrt{1 - \boldsymbol{\beta}^T \boldsymbol{\beta}}} \tag{K.6}$$

When $\mathbf{v} = [0, 0, v]^T$, or $\boldsymbol{\beta} = [0, 0, \beta]^T$, Eq. (K.6) reduces to (K.1). Defining $\beta = |\boldsymbol{\beta}| = \sqrt{\boldsymbol{\beta}^T \boldsymbol{\beta}}$ and the unit vector $\hat{\boldsymbol{\beta}} = \boldsymbol{\beta} / \beta$, and using the relationship $\gamma^2 \beta^2 = \gamma^2 - 1$, it can be verified that the spatial part of the matrix L can be written in the form:

$$I + \frac{\gamma^2}{\gamma + 1} \boldsymbol{\beta} \boldsymbol{\beta}^T = I + (\gamma - 1) \hat{\boldsymbol{\beta}} \hat{\boldsymbol{\beta}}^T \tag{K.7}$$

The set of matrices L satisfying Eq. (K.5) forms a group called the *Lorentz group*. In particular, the z-directed boosts of Eq. (K.2) form a commutative subgroup. Denoting these boosts by $L(\beta)$, the application of two successive boosts by velocity factors $\beta_1 = v_1/c$ and $\beta_2 = v_2/c$ leads to the combined boost $L(\beta) = L(\beta_1)L(\beta_2)$, where:

$$\boxed{\beta = \frac{\beta_1 + \beta_2}{1 + \beta_1 \beta_2}} \Leftrightarrow \boxed{v = \frac{v_1 + v_2}{1 + v_1 v_2 / c^2}} \tag{K.8}$$

with $\beta = v/c$. Eq. (K.8) is Einstein's relativistic velocity addition theorem. The same group property implies also that $L^{-1}(\beta) = L(-\beta)$. The proof of Eq. (K.8) follows from the following condition, where $\gamma_1 = 1/\sqrt{1 - \beta_1^2}$ and $\gamma_2 = 1/\sqrt{1 - \beta_2^2}$:

$$\begin{bmatrix} \gamma & 0 & 0 & -\gamma\beta \\ 0 & 1 & 0 & 0 \\ 0 & 0 & 1 & 0 \\ -\gamma\beta & 0 & 0 & \gamma \end{bmatrix} = \begin{bmatrix} \gamma_1 & 0 & 0 & -\gamma_1\beta_1 \\ 0 & 1 & 0 & 0 \\ 0 & 0 & 1 & 0 \\ -\gamma_1\beta_1 & 0 & 0 & \gamma_1 \end{bmatrix} \begin{bmatrix} \gamma_2 & 0 & 0 & -\gamma_2\beta_2 \\ 0 & 1 & 0 & 0 \\ 0 & 0 & 1 & 0 \\ -\gamma_2\beta_2 & 0 & 0 & \gamma_2 \end{bmatrix}$$

A *four-vector* is a four-dimensional vector that transforms like the vector x under Lorentz transformations, that is, its components with respect to the two moving frames S and S' are related by:

$$\boxed{a' = La}, \text{ where } a = \begin{bmatrix} a_0 \\ a_x \\ a_y \\ a_z \end{bmatrix}, \quad a' = \begin{bmatrix} a'_0 \\ a'_x \\ a'_y \\ a'_z \end{bmatrix} \tag{K.9}$$

For example, under the z-directed boost of Eq. (K.1), the four-vector a will transform as:

$$\boxed{\begin{matrix} a'_0 = \gamma(a_0 - \beta a_z) \\ a'_z = \gamma(a_z - \beta a_0) \\ a'_x = a_x \\ a'_y = a_y \end{matrix}} \Leftrightarrow \boxed{\begin{matrix} a_0 = \gamma(a'_0 + \beta a'_z) \\ a_z = \gamma(a'_z + \beta a'_0) \\ a_x = a'_x \\ a_y = a'_y \end{matrix}} \tag{K.10}$$

Four-vectors transforming according to Eq. (K.9) are referred to as *contravariant*. Under the general Lorentz boost of Eq. (K.6), the spatial components of a that are *transverse* to the direction of the velocity vector \mathbf{v} remain *unchanged*, whereas the *parallel* component transforms as in Eq. (K.10), that is, the most general Lorentz boost transformation for a four-vector takes the form:

$$\boxed{\begin{matrix} a'_0 = \gamma(a_0 - \beta a_{\parallel}) \\ a'_{\parallel} = \gamma(a_{\parallel} - \beta a_0) \\ a'_{\perp} = a_{\perp} \end{matrix}} \quad \gamma = \frac{1}{\sqrt{1 - \beta^2}}, \quad \beta = |\boldsymbol{\beta}|, \quad \boldsymbol{\beta} = \frac{\mathbf{v}}{c} \tag{K.11}$$

where $a_{\parallel} = \hat{\boldsymbol{\beta}}^T \mathbf{a}$ and $\mathbf{a} = [a_x, a_y, a_z]^T$ is the spatial part of a . Then,

$$\mathbf{a}_{\parallel} = \hat{\boldsymbol{\beta}} \mathbf{a}_{\parallel} = \hat{\boldsymbol{\beta}} (\hat{\boldsymbol{\beta}}^T \mathbf{a}) \quad \text{and} \quad \mathbf{a}_{\perp} = \mathbf{a} - \mathbf{a}_{\parallel} = \mathbf{a} - \hat{\boldsymbol{\beta}} \mathbf{a}_{\parallel}$$

Setting $\boldsymbol{\beta} = \beta \hat{\boldsymbol{\beta}}$ and using Eq. (K.7), the Lorentz transformation (K.6) gives:

$$\begin{bmatrix} a'_0 \\ \mathbf{a}' \end{bmatrix} = \begin{bmatrix} \gamma & -\gamma \boldsymbol{\beta}^T \\ -\gamma \boldsymbol{\beta} & I + (\gamma - 1) \hat{\boldsymbol{\beta}} \hat{\boldsymbol{\beta}}^T \end{bmatrix} \begin{bmatrix} a_0 \\ \mathbf{a} \end{bmatrix} = \begin{bmatrix} \gamma(a_0 - \beta a_{\parallel}) \\ \mathbf{a} - \hat{\boldsymbol{\beta}} \mathbf{a}_{\parallel} + \hat{\boldsymbol{\beta}} \gamma (a_{\parallel} - \beta a_0) \end{bmatrix}$$

from which Eq. (K.11) follows.

For any two four-vectors a, b , the quadratic form $a^T G b$ remains invariant under Lorentz transformations, that is, $a'^T G b' = a^T G b$, or,

$$a'_0 b'_0 - \mathbf{a}' \cdot \mathbf{b}' = a_0 b_0 - \mathbf{a} \cdot \mathbf{b}, \quad \text{where } a = \begin{bmatrix} a_0 \\ \mathbf{a} \end{bmatrix}, \quad b = \begin{bmatrix} b_0 \\ \mathbf{b} \end{bmatrix} \tag{K.12}$$

Some examples of four-vectors are given in the following table:

four-vector	a_0	a_x	a_y	a_z
time and space	ct	x	y	z
frequency and wavenumber	ω/c	k_x	k_y	k_z
energy and momentum	E/c	p_x	p_y	p_z
charge and current densities	$c\rho$	J_x	J_y	J_z
scalar and vector potentials	φ	cA_x	cA_y	cA_z

(K.13)

For example, under the z-directed boost of Eq. (K.1), the frequency-wavenumber transformation will be as follows:

$$\begin{array}{|l}
 \omega' = \gamma(\omega - \beta ck_z) \\
 k'_z = \gamma(k_z - \frac{\beta}{c}\omega) \\
 k'_x = k_x \\
 k'_y = k_y
 \end{array}
 \Leftrightarrow
 \begin{array}{|l}
 \omega = \gamma(\omega' + \beta ck'_z) \\
 k_z = \gamma(k'_z + \frac{\beta}{c}\omega') \\
 k_x = k'_x \\
 k_y = k'_y
 \end{array},
 \quad \beta c = v, \quad \frac{\beta}{c} = \frac{v}{c^2} \quad (K.14)$$

where we rewrote the first equations in terms of ω instead of ω/c . The change in frequency due to motion is the basis of the Doppler effect. The invariance property (K.12) applied to the space-time and frequency-wavenumber four-vectors reads:

$$\omega' t' - \mathbf{k}' \cdot \mathbf{r}' = \omega t - \mathbf{k} \cdot \mathbf{r} \quad (K.15)$$

This implies that a uniform plane wave remains a uniform plane wave in all reference frames moving at a constant velocity relative to each other. Similarly, the charge and current densities transform as follows:

$$\begin{array}{|l}
 c\rho' = \gamma(c\rho - \beta J_z) \\
 J'_z = \gamma(J_z - \beta c\rho) \\
 J'_x = J_x \\
 J'_y = J_y
 \end{array}
 \Leftrightarrow
 \begin{array}{|l}
 c\rho = \gamma(c\rho' + \beta J'_z) \\
 J_z = \gamma(J'_z + \beta c\rho') \\
 J_x = J'_x \\
 J_y = J'_y
 \end{array} \quad (K.16)$$

Because Eq. (K.5) implies that $L^{-T} = GLG$, we are led to define four-vectors that transform according to L^{-T} . Such four-vectors are referred to as being *covariant*. Given any contravariant 4-vector a , we define its covariant version by $\bar{a} = Ga$. This operation simply reverses the sign of the spatial part of a :

$$\bar{a} = Ga = \begin{bmatrix} 1 & 0 \\ 0 & -I \end{bmatrix} \begin{bmatrix} a_0 \\ \mathbf{a} \end{bmatrix} = \begin{bmatrix} a_0 \\ -\mathbf{a} \end{bmatrix} \quad (K.17)$$

The vector \bar{a} transforms as follows:

$$\bar{a}' = Ga' = GLa = (GLG)(Ga) = L^{-T}\bar{a} \quad (K.18)$$

where we used the property that $G^2 = I_4$, the 4×4 identity matrix. The most important covariant vector is the four-dimensional gradient:

$$\partial_x = \begin{bmatrix} \partial_\tau \\ \partial_x \\ \partial_y \\ \partial_z \end{bmatrix} = \begin{bmatrix} \partial_\tau \\ \nabla \end{bmatrix} \quad (K.19)$$

Because $x' = Lx$, it follows that $\partial_{x'} = L^{-T}\partial_x$. Indeed, we have component-wise:

$$\frac{\partial}{\partial x'_i} = \sum_j \frac{\partial x'_j}{\partial x_i} \frac{\partial}{\partial x'_j} = \sum_j L_{ji} \frac{\partial}{\partial x'_j} \Rightarrow \partial_x = L^T \partial_{x'} \Rightarrow \partial_{x'} = L^{-T} \partial_x$$

For the z-directed boost of Eq. (K.1), we have $L^{-T} = L^{-1}$, which gives:

$$\begin{array}{|l}
 \partial_{\tau'} = \gamma(\partial_\tau + \beta \partial_z) \\
 \partial_{z'} = \gamma(\partial_z + \beta \partial_\tau) \\
 \partial_{x'} = \partial_x \\
 \partial_{y'} = \partial_y
 \end{array}
 \Leftrightarrow
 \begin{array}{|l}
 \partial_\tau = \gamma(\partial_{\tau'} - \beta \partial_{z'}) \\
 \partial_z = \gamma(\partial_{z'} - \beta \partial_{\tau'}) \\
 \partial_x = \partial_{x'} \\
 \partial_y = \partial_{y'}
 \end{array} \quad (K.20)$$

The four-dimensional divergence of a four-vector is a Lorentz scalar. For example, denoting the current density four-vector by $J = [c\rho, J_x, J_y, J_z]^T$, the charge conservation law involves the four-dimensional divergence:

$$\partial_t \rho + \nabla \cdot \mathbf{J} = [\partial_\tau, \partial_x, \partial_y, \partial_z] \begin{bmatrix} c\rho \\ J_x \\ J_y \\ J_z \end{bmatrix} = \partial_x^T J \quad (K.21)$$

Under a Lorentz transformation, this remains invariant, and therefore, if it is zero in one frame it will remain zero in all frames. Using $\partial_x^T = \partial_{x'}^T L$, we have:

$$\partial_t \rho + \nabla \cdot \mathbf{J} = \partial_{x'}^T J = \partial_{x'}^T L J = \partial_{x'} J' = \partial_{t'} \rho' + \nabla' \cdot \mathbf{J}' \quad (K.22)$$

Although many quantities in electromagnetism transform like four-vectors, such as the space-time or the frequency-wavenumber vectors, the actual electromagnetic fields do not. Rather, they transform like six-vectors or rank-2 antisymmetric tensors.

A rank-2 tensor is represented by a 4×4 matrix, say F . Its Lorentz transformation properties are the same as the transformation of the product of a column and a row four-vector, that is, F transforms like the quantity ab^T , where a, b are column four-vectors. This product transforms like $a'b'^T = L(ab^T)L^T$. Thus, a general second-rank tensor transforms as follows:

$$F' = LFL^T \quad (K.23)$$

An *antisymmetric* rank-2 tensor F defines, and is completely defined by, two three-dimensional vectors, say $\mathbf{a} = [a_x, a_y, a_z]^T$ and $\mathbf{b} = [b_x, b_y, b_z]^T$. Its matrix form is:

$$F = \begin{bmatrix} 0 & -a_x & -a_y & -a_z \\ a_x & 0 & -b_z & b_y \\ a_y & b_z & 0 & -b_x \\ a_z & -b_y & b_x & 0 \end{bmatrix} \quad (K.24)$$

Given the tensor F , one may define its *covariant* version through $\tilde{F} = GFG$, and its *dual*, denoted by \tilde{F} and obtained by the replacements $\mathbf{a} \rightarrow \mathbf{b}$ and $\mathbf{b} \rightarrow -\mathbf{a}$, that is,

$$\tilde{F} = \begin{bmatrix} 0 & a_x & a_y & a_z \\ -a_x & 0 & -b_z & b_y \\ -a_y & b_z & 0 & -b_x \\ -a_z & -b_y & b_x & 0 \end{bmatrix}, \quad \tilde{F} = \begin{bmatrix} 0 & -b_x & -b_y & -b_z \\ b_x & 0 & a_z & -a_y \\ b_y & -a_z & 0 & a_x \\ b_z & a_y & -a_x & 0 \end{bmatrix} \quad (\text{K.25})$$

Thus, \tilde{F} corresponds to the pair $(-\mathbf{a}, \mathbf{b})$, and \tilde{F} to $(\mathbf{b}, -\mathbf{a})$. Their Lorentz transformation properties are:

$$\tilde{F}' = L^{-T} \tilde{F} L^{-1}, \quad \tilde{F}' = L \tilde{F} L^T \quad (\text{K.26})$$

Thus, the dual \tilde{F} transforms like F itself. For the z-directed boost of Eq. (K.1), it follows from (K.23) that the two vectors \mathbf{a}, \mathbf{b} transform as follows:

$$\begin{array}{ll} a'_x = \gamma(a_x - \beta b_y) & b'_x = \gamma(b_x + \beta a_y) \\ a'_y = \gamma(a_y + \beta b_x) & b'_y = \gamma(b_y - \beta a_x) \\ a'_z = a_z & b'_z = b_z \end{array} \quad (\text{K.27})$$

These are obtained by equating the expressions:

$$\begin{bmatrix} 0 & -a'_x & -a'_y & -a'_z \\ a'_x & 0 & -b'_z & b'_y \\ a'_y & b'_z & 0 & -b'_x \\ a'_z & -b'_y & b'_x & 0 \end{bmatrix} = \begin{bmatrix} \gamma & 0 & 0 & -\gamma\beta \\ 0 & 1 & 0 & 0 \\ 0 & 0 & 1 & 0 \\ -\gamma\beta & 0 & 0 & \gamma \end{bmatrix} \begin{bmatrix} 0 & -a_x & -a_y & -a_z \\ a_x & 0 & -b_z & b_y \\ a_y & b_z & 0 & -b_x \\ a_z & -b_y & b_x & 0 \end{bmatrix} \begin{bmatrix} \gamma & 0 & 0 & -\gamma\beta \\ 0 & 1 & 0 & 0 \\ 0 & 0 & 1 & 0 \\ -\gamma\beta & 0 & 0 & \gamma \end{bmatrix}$$

More generally, under the boost transformation (K.6), it can be verified that the components of \mathbf{a}, \mathbf{b} parallel and perpendicular to \mathbf{v} transform as follows:

$$\begin{array}{l} a'_\perp = \gamma(\mathbf{a}_\perp + \boldsymbol{\beta} \times \mathbf{b}_\perp) \\ b'_\perp = \gamma(\mathbf{b}_\perp - \boldsymbol{\beta} \times \mathbf{a}_\perp) \\ a'_\parallel = a_\parallel \\ b'_\parallel = b_\parallel \end{array} \quad \gamma = \frac{1}{\sqrt{1 - \beta^2}}, \quad \beta = |\boldsymbol{\beta}|, \quad \boldsymbol{\beta} = \frac{\mathbf{v}}{c} \quad (\text{K.28})$$

Thus, in contrast to Eq. (K.11) for a four-vector, the parallel components remain unchanged while the transverse components change. A pair of three-dimensional vectors (\mathbf{a}, \mathbf{b}) transforming like Eq. (K.28) is referred to as a *six-vector*.

It is evident also that Eqs. (K.28) remain invariant under the duality transformation $\mathbf{a} \rightarrow \mathbf{b}$ and $\mathbf{b} \rightarrow -\mathbf{a}$, which justifies Eq. (K.26). Some examples of (\mathbf{a}, \mathbf{b}) six-vector pairs defining an antisymmetric rank-2 tensor are as follows:

$$\begin{array}{cc} \mathbf{a} & \mathbf{b} \\ \hline E & c\mathbf{B} \\ c\mathbf{D} & \mathbf{H} \\ c\mathbf{P} & -\mathbf{M} \end{array} \quad (\text{K.29})$$

where \mathbf{P}, \mathbf{M} are the polarization and magnetization densities defined through the relationships $\mathbf{D} = \epsilon_0 \mathbf{E} + \mathbf{P}$ and $\mathbf{B} = \mu_0 (\mathbf{H} + \mathbf{M})$. Thus, the (\mathbf{E}, \mathbf{B}) and (\mathbf{D}, \mathbf{H}) fields have the following Lorentz transformation properties:

$$\begin{array}{ll} E'_\perp = \gamma(E_\perp + c\boldsymbol{\beta} \times \mathbf{B}_\perp) & H'_\perp = \gamma(H_\perp - c\boldsymbol{\beta} \times \mathbf{D}_\perp) \\ B'_\perp = \gamma(B_\perp - \frac{1}{c}\boldsymbol{\beta} \times \mathbf{E}_\perp) & D'_\perp = \gamma(D_\perp + \frac{1}{c}\boldsymbol{\beta} \times \mathbf{H}_\perp) \\ E'_\parallel = E_\parallel & H'_\parallel = H_\parallel \\ B'_\parallel = B_\parallel & D'_\parallel = D_\parallel \end{array} \quad (\text{K.30})$$

where we may replace $c\boldsymbol{\beta} = \mathbf{v}$ and $\boldsymbol{\beta}/c = \mathbf{v}/c^2$. Note that the two groups of equations transform into each other under the usual duality transformations: $\mathbf{E} \rightarrow \mathbf{H}, \mathbf{H} \rightarrow -\mathbf{E}, \mathbf{D} \rightarrow \mathbf{B}, \mathbf{B} \rightarrow -\mathbf{D}$. For the z-directed boost of Eq. (K.1), we have from Eq. (K.30):

$$\begin{array}{ll} E'_x = \gamma(E_x - c\beta B_y) & H'_x = \gamma(H_x + c\beta D_y) \\ E'_y = \gamma(E_y + c\beta B_x) & H'_y = \gamma(H_y - c\beta D_x) \\ B'_x = \gamma(B_x + \frac{1}{c}\beta E_y) & D'_x = \gamma(D_x - \frac{1}{c}\beta H_y) \\ B'_y = \gamma(B_y - \frac{1}{c}\beta E_x) & D'_y = \gamma(D_y + \frac{1}{c}\beta H_x) \\ E'_z = E_z & H'_z = H_z \\ B'_z = B_z & D'_z = D_z \end{array} \quad (\text{K.31})$$

Associated with a six-vector (\mathbf{a}, \mathbf{b}) , there are two scalar invariants: the quantities $(\mathbf{a} \cdot \mathbf{b})$ and $(\mathbf{a} \cdot \mathbf{a} - \mathbf{b} \cdot \mathbf{b})$. Their invariance follows from Eq. (K.28). Thus, the scalars $(\mathbf{E} \cdot \mathbf{B}), (\mathbf{E} \cdot \mathbf{E} - c^2 \mathbf{B} \cdot \mathbf{B}), (\mathbf{D} \cdot \mathbf{H}), (c^2 \mathbf{D} \cdot \mathbf{D} - \mathbf{H} \cdot \mathbf{H})$ remain invariant under Lorentz transformations. In addition, it follows from (K.30) that the quantity $(\mathbf{E} \cdot \mathbf{D} - \mathbf{B} \cdot \mathbf{H})$ is invariant.

Given a six-vector (\mathbf{a}, \mathbf{b}) and its dual $(\mathbf{b}, -\mathbf{a})$, we may define the following four-dimensional ‘‘current’’ vectors that are dual to each other:

$$\mathbf{J} = \begin{bmatrix} \nabla \cdot \mathbf{a} \\ \nabla \times \mathbf{b} - \partial_\tau \mathbf{a} \end{bmatrix}, \quad \tilde{\mathbf{J}} = \begin{bmatrix} \nabla \cdot \mathbf{b} \\ -\nabla \times \mathbf{a} - \partial_\tau \mathbf{b} \end{bmatrix} \quad (\text{K.32})$$

It can be shown that both \mathbf{J} and $\tilde{\mathbf{J}}$ transform as four-vectors under Lorentz transformations, that is, $\mathbf{J}' = L\mathbf{J}$ and $\tilde{\mathbf{J}}' = L\tilde{\mathbf{J}}$, where $\mathbf{J}', \tilde{\mathbf{J}}'$ are defined with respect to the

coordinates of the S' frame:

$$J' = \begin{bmatrix} \nabla' \cdot \mathbf{a}' \\ \nabla' \times \mathbf{b}' - \partial_{\tau'} \mathbf{a}' \end{bmatrix}, \quad \tilde{J}' = \begin{bmatrix} \nabla' \cdot \mathbf{b}' \\ -\nabla' \times \mathbf{a}' - \partial_{\tau'} \mathbf{b}' \end{bmatrix} \quad (\text{K.33})$$

The calculation is straightforward but tedious. For example, for the z-directed boost (K.1), we may use Eqs. (K.20) and (K.27) and the identity $\gamma^2(1 - \beta^2) = 1$ to show:

$$\begin{aligned} J'_x &= (\nabla' \times \mathbf{b}' - \partial_{\tau'} \mathbf{a}')_x = \partial_{y'} b'_z - \partial_{z'} b'_y - \partial_{\tau'} a'_x \\ &= \partial_y b_z - \gamma^2(\partial_z + \beta \partial_\tau)(b_y - \beta a_x) - \gamma^2(\partial_\tau + \beta \partial_z)(a_x - \beta b_y) \\ &= \partial_y b_z - \partial_z b_y - \partial_\tau a_x = (\nabla \times \mathbf{b} - \partial_\tau \mathbf{a})_x = J_x \end{aligned}$$

Similarly, we have:

$$\begin{aligned} J'_0 &= \nabla' \cdot \mathbf{a}' = \partial_{x'} a'_x + \partial_{y'} a'_y + \partial_{z'} a'_z \\ &= \gamma \partial_x (a_x - \beta b_y) + \gamma \partial_y (a_y + \beta b_x) + \gamma (\partial_z + \beta \partial_\tau) a_z \\ &= \gamma [(\partial_x a_x + \partial_y a_y + \partial_z a_z) - \beta (\partial_x b_y - \partial_y b_x - \partial_\tau a_z)] = \gamma (J_0 - \beta J_z) \end{aligned}$$

In this fashion, one can show that J and \tilde{J} satisfy the Lorentz transformation equations (K.10) for a four-vector. To see the significance of this result, we rewrite Maxwell's equations, with magnetic charge and current densities ρ_m, \mathbf{J}_m included, in the four-dimensional forms:

$$\begin{bmatrix} \nabla \cdot c\mathbf{D} \\ \nabla \times \mathbf{H} - \partial_\tau c\mathbf{D} \end{bmatrix} = \begin{bmatrix} c\rho \\ \mathbf{J} \end{bmatrix}, \quad \begin{bmatrix} \nabla \cdot c\mathbf{B} \\ -\nabla \times \mathbf{E} - \partial_\tau c\mathbf{B} \end{bmatrix} = \begin{bmatrix} c\rho_m \\ \mathbf{J}_m \end{bmatrix} \quad (\text{K.34})$$

Thus, applying the above result to the six-vector $(c\mathbf{D}, \mathbf{H})$ and to the dual of $(\mathbf{E}, c\mathbf{B})$ and assuming that the electric and magnetic current densities transform like four-vectors, it follows that Maxwell's equations remain invariant under Lorentz transformations, that is, they retain their form in the moving system:

$$\begin{bmatrix} \nabla' \cdot c\mathbf{D}' \\ \nabla' \times \mathbf{H}' - \partial_{\tau'} c\mathbf{D}' \end{bmatrix} = \begin{bmatrix} c\rho' \\ \mathbf{J}' \end{bmatrix}, \quad \begin{bmatrix} \nabla' \cdot c\mathbf{B}' \\ -\nabla' \times \mathbf{E}' - \partial_{\tau'} c\mathbf{B}' \end{bmatrix} = \begin{bmatrix} c\rho'_m \\ \mathbf{J}'_m \end{bmatrix} \quad (\text{K.35})$$

The Lorentz transformation properties of the electromagnetic fields allow one to solve problems involving moving media, such as the Doppler effect, reflection and transmission from moving boundaries, and so on. The main technique for solving such problems is to transform to the frame (here, S') in which the boundary is at rest, solve the reflection problem in that frame, and transform the results back to the laboratory frame by using the inverse of Eq. (K.30).

This procedure was discussed by Einstein in his 1905 paper on special relativity in connection to the Doppler effect from a moving mirror. To quote [474]: "All problems in the optics of moving bodies can be solved by the method here employed. What is essential is that the electric and magnetic force of the light which is influenced by a moving body, be transformed into a system of co-ordinates at rest relatively to the body. By this means all problems in the optics of moving bodies will be reduced to a series of problems in the optics of stationary bodies."

L. MATLAB Functions

The MATLAB functions are grouped by category. They are available from the web page: www.ece.rutgers.edu/~orfanidi/ewa.

Multilayer Dielectric Structures

brewster	- calculates Brewster and critical angles
fresnel	- Fresnel reflection coefficients for isotropic or birefringent media
n2r	- refractive indices to reflection coefficients of M-layer structure
r2n	- reflection coefficients to refractive indices of M-layer structure

multidie1	- reflection response of isotropic or birefringent multilayer structures
multidie11	- simplified version of multidie1 for isotropic layers
multidie12	- reflection response of lossy isotropic multilayer dielectric structures
omniband	- bandwidth of omnidirectional mirrors and Brewster polarizers
omniband2	- bandwidth of birefringent multilayer mirrors

snel	- calculates refraction angles from Snell's law for birefringent media
------	--

Quarter-Wavelength Transformers

bkwrec	- order-decreasing backward layer recursion - from a,b to r
frwrec	- order-increasing forward layer recursion - from r to A,B

chebtr	- Chebyshev broadband reflectionless quarter-wave transformer
chebtr2	- Chebyshev broadband reflectionless quarter-wave transformer
chebtr3	- Chebyshev broadband reflectionless quarter-wave transformer

Dielectric Waveguides

dguide	- TE modes in dielectric slab waveguide
dslab	- solves for the TE-mode cutoff wavenumbers in a dielectric slab
dguide3	- TE and TM modes in asymmetric 3-slab dielectric waveguide

Plasmonic Waveguides

drude	- Drude-Lorentz model for Silver, Gold, Copper, Aluminum
dmda	- asymmetric DMD plasmonic waveguide - iterative solution
dmds	- symmetric DMD plasmonic waveguide - iterative solution
dmdcut	- cutoff width for asymmetric DMD guides
pwg	- plasmonic waveguide solution for symmetric guides
pwga	- plasmonic waveguide solution for asymmetric guides
pwgpower	- transmitted power in plasmonic waveguide

Sommerfeld and Goubau Wires

sommer	- solve characteristic equation for Sommerfeld wire
goubau	- solve characteristic equation of Goubau line
goubatt	- Goubau line attenuation
gcut	- cutoff function for Goubau line
attw	- characteristic equation of Attwood surface waveguide
attwatt	- attenuation of Attwood surface waveguide
J01	- J0(z)/J1(z) approximation for large imag(z)

Transmission Lines

g2z	- reflection coefficient to impedance transformation
z2g	- impedance to reflection coefficient transformation
lmin	- find locations of voltage minima and maxima
mstripa	- microstrip analysis (calculates Z _{eff} from w/h)
mstripr	- microstrip synthesis with refinement (calculates w/h from Z)
mstrips	- microstrip synthesis (calculates w/h from Z)
multiline	- reflection response of multi-segment transmission line
swr	- standing wave ratio
tsection	- T-section equivalent of a length-l transmission line segment
gprop	- reflection coefficient propagation
vprop	- wave impedance propagation
zprop	- wave impedance propagation

Impedance Matching

qwt1	- quarter wavelength transformer with series segment
qwt2	- quarter wavelength transformer with 1/8-wavelength shunt stub
qwt3	- quarter wavelength transformer with shunt stub of adjustable length
dualband	- two-section dual-band Chebyshev impedance transformer
dualbw	- two-section dual-band transformer bandwidths
stub1	- single-stub matching
stub2	- double-stub matching
stub3	- triple-stub matching
onesect	- one-section impedance transformer
twosect	- two-section impedance transformer
pi2t	- Pi to T transformation
t2pi	- Pi to T transformation
lmatch	- L-section reactive conjugate matching network
pmatch	- Pi-section reactive conjugate matching network

S-Parameters

gin	- input reflection coefficient in terms of S-parameters
gout	- output reflection coefficient in terms of S-parameters
nfcirc	- constant noise figure circle
nfig	- noise figure of two-port
sgain	- transducer, available, and operating power gains of two-port
sgcirc	- stability and gain circles
smat	- S-parameters to S-matrix
smatch	- simultaneous conjugate match of a two-port
smith	- draw basic Smith chart
smithcir	- add stability and constant gain circles on Smith chart
sparam	- stability parameters of two-port
circint	- circle intersection on Gamma-plane
circtan	- point of tangency between the two circles

Linear Antenna Functions

dipdir	- dipole directivity
dmax	- computes directivity and beam solid angle of g(th) gain
dipole	- gain of center-fed linear dipole of length L
traveling	- gain of traveling-wave antenna of length L
vee	- gain of traveling-wave vee antenna
rhomboh	- gain of traveling-wave rhombic antenna
king	- King's 3-term sinusoidal approximation
kingeval	- evaluate King's 3-term sinusoidal current approximation
kingfit	- fits a sampled current to King's 2-term sinusoidal approximation
kingprime	- converts King's 3-term coefficients from unprimed to primed form
hbasis	- basis functions for Hallen equation
hdelta	- solve Hallen's equation with delta-gap input
hfield	- solve Hallen's equation with arbitrary incident E-field
hmat	- Hallen impedance matrix with method of moments and point-matching
hwrap	- wraps a Toeplitz impedance matrix to half its size
kernel	- thin-wire kernel computation for Hallen equation
pfield	- solve Pocklington's equation with arbitrary incident E-field
pmat	- Pocklington impedance matrix with method of moments and point-matching
hcoupled	- solve Hallen's equation for 2D array of non-identical parallel dipoles
hcoupled2	- solve Hallen's equation for 2D array of identical parallel dipoles
gain2d	- normalized gain of 2D array of parallel dipoles with Hallen currents
gain2s	- normalized gain of 2D array of parallel dipoles with sinusoidal currents
imped	- mutual impedance between two parallel standing-wave dipoles
imped2	- mutual impedance between two parallel standing-wave dipoles
impedmat	- mutual impedance matrix of array of parallel dipole antennas
resonant	- calculates the length of a resonant dipole antenna
yagi	- simplified Yagi-Uda array design

Aperture Antenna Functions

BBnum	- computation of fields in Bethe-Bouwkamp model
BBfar	- far fields in Bethe-Bouwkamp model
BBnear	- near fields in Bethe-Bouwkamp model
diffint	- generalized Fresnel diffraction integral
diffr	- knife-edge diffraction coefficient
dsinc	- the double-sinc function $\cos(\pi*x)/(1-4*x^2)$
fcs	- Fresnel integrals C(x) and S(x)
fcs2	- type-2 Fresnel integrals C2(x) and S2(x)
jinc	- jinc and "shifted" jinc function
talbot	- Gauss sums for fractional Talbot effect
tbw	- Taylor's one-parameter window
tnb1	- Taylor's n-bar window (1-D)
tnb2	- Taylor's n-bar window (2-D)
hband	- horn antenna 3-dB width
heff	- aperture efficiency of horn antenna
hgain	- horn antenna H-plane and E-plane gains
hopt	- optimum horn antenna design

hsigma - optimum sigma parameter for horn antenna

Antenna Array Functions

gain1d - normalized gain computation for 1D equally-spaced isotropic array
 bwidth - beamwidth mapping from psi-space to phi-space
 binomial - binomial array weights
 dolph - Dolph-Chebyshev array weights
 dolph2 - Riblet-Pritchard version of Dolph-Chebyshev
 dolph3 - DuHamel version of endfire Dolph-Chebyshev
 multibeam - multibeam array design
 pro1 - prolate array design
 pro1mat - prolate matrix
 scan - scan array with given scanning phase
 sector - sector beam array design
 steer - steer array towards given angle
 taylornb - Taylor n-bar line source array design
 taylor1p - Taylor 1-parameter array design
 taylorbw - Taylor B-parameter and beamwidth
 uniform - uniform array weights
 woodward - Woodward-Lawson-Butler beams
 ville - Villeneuve array design

chebarray - Bresler's Chebyshev array design method (written by P. Simon)

Gain Plotting Functions

abp - polar gain plot in absolute units
 abz - azimuthal gain plot in absolute units
 ab2p - polar gain plot in absolute units - 2π angle range
 abz2 - azimuthal gain plot in absolute units - 2π angle range
 dbp - polar gain plot in dB
 dbz - azimuthal gain plot in dB
 dbp2 - polar gain plot in dB - 2π angle range
 dbz2 - azimuthal gain plot in dB - 2π angle range
 abadd - add gain in absolute units
 abadd2 - add gain in absolute units - 2π angle range
 dbadd - add gain in dB
 dbadd2 - add gain in dB - 2π angle range
 addbwp - add 3-dB angle beamwidth in polar plots
 addbwz - add 3-dB angle beamwidth in azimuthal plots
 addcirc - add grid circle in polar or azimuthal plots
 addline - add grid ray line in azimuthal or polar plots
 addray - add ray in azimuthal or polar plots

Miscellaneous Utility Functions

ab - dB to absolute power units
 db - absolute power to dB units
 c2p - complex number to phasor form
 p2c - phasor form to complex number
 d2r - degrees to radians

r2d - radians to degrees

dtft - DTFT of a signal x at a frequency vector w
 I0 - modified Bessel function of 1st kind and 0th order
 ellipse - polarization ellipse parameters
 etac - eta and c
 wavenum - calculate wavenumber and characteristic impedance
 poly2 - specialized version of poly with increased accuracy

quadr - Gauss-Legendre quadrature weights and evaluation points
 quadrs - quadrature weights and evaluation points on subintervals
 quadr2 - Gauss-Legendre quadrature weights and evaluation points
 quadrs2 - quadrature weights and evaluation points on subintervals
 quadts - tanh-sinh, double-exponential, quadrature

Ci - cosine integral Ci(z)
 Cin - cosine integral Cin(z)
 Si - sine integral Si(z)
 Gi - Green's function integral

pswf - prolate spheroidal wave functions
 spherj - spherical Bessel functions
 legpol - evaluate Legendre polynomials

sinhc - hyperbolic sinc function
 asinhc - inverse hyperbolic sinc function
 sqrts - evanescent SQRT for waves problems

flip - flip a column, a row, or both
 blockmat - manipulate block matrices
 upulse - generates trapezoidal, rectangular, triangular pulses, or a unit-step
 ustep - unit-step or rising unit-step function

dnv - dn elliptic function at a vector of moduli
 snv - sn elliptic function at a vector of moduli
 ellipK - complete elliptic integral of first kind at a vector of moduli
 ellipE - complete elliptic integral of second kind at a vector of moduli
 landenv - Landen transformations of a vector of elliptic moduli

MATLAB Movies

grvmovie1 - pulse propagation with slow and negative group velocity ($v_g < 0$)
 grvmovie2 - pulse propagation with slow and fast group velocity ($v_g > c$)
 pulsemovie - step and pulse propagation on terminated transmission lines
 pulse2movie - step propagation on two cascaded lines
 RLcmovie - step getting reflected off a reactive termination
 TDRmovie - fault location by time-domain reflectometry
 xtalkmovie - crosstalk signals on coupled transmission lines
 dipmovie - electric field pattern of radiating Hertzian dipole